

Molecular Mechanism of Hairpin Formation and Passenger Secretion in the Inverse Autotransporter Intimin

Sai Priya Sarma Kandanur



The Department of Biosciences
The faculty of Mathematics and Natural Sciences

UNIVERSITY OF OSLO

June 2019

© Author: Sai Priya Sarma Kandanur

Year: 2019

Title: Molecular Mechanisms of Hairpin Formation and Passenger Secretion in the Inverse Autotransporter Intimin

Sai Priya Sarma Kandanur

<http://www.duo.uio.no/>

Print: Representeren, University of Oslo

Acknowledgements

I would like to thank Dr. Jack Leo and Prof. Dirk Linke for giving me the opportunity to work in their group. I sincerely thank Dr. Jack Leo for his immense support and patience throughout this work. I would also like to thank the entire Linke and Leo groups, especially Kenneth and Athanasios for patiently answering all my naive questions and Daniel and Thomas for being my stress busters during the course of this project.

I thank Dr. Monika Schütz for organising my trip to Tübingen and letting me work in her lab. I also thank her group for being very warm and helpful during my stay.

Ina Meuskens, your addition to this group has been the best thing that has happened. I want to specially thank you for always explaining the basic background details related to my project with a constant smile on your face.

Lastly, I would like to thank my friends and family for always being there.

Table of Contents

Abstract	XI
1. Introduction.....	1
1.1 Review of the literature.....	1
1.1.1 Gram-negative bacteria.....	1
1.1.2 Protein secretion systems in Gram-negative bacteria	2
1.1.2.1 Protein translocation across the IM	2
1.1.2.1.1 The general secretion (Sec) system.....	2
1.1.2.1.2 The YidC insertase	3
1.1.2.1.3 The twin arginine translocase (Tat) system	3
1.1.2.2 Protein translocation across the OM	4
1.2 The type V secretion system (T5SS)	5
1.2.1 The type Va secretion system: classical autotransport (T5aSS)	6
1.2.2 The type Vb secretion system: two-partner secretion (TPS) system (T5bSS)	8
1.2.3 The type Vc secretion system (T5cSS): trimeric autotransporter adhesins (TAAs)	9
1.2.4 The type Vd secretion system: fused two-partner secretion system (T5dSS)	10
1.2.5 The type Ve secretion system: the inverse autotransporter (IAT) system (T5eSS).....	10
1.3 Intimin: an adhesion protein of EPEC.....	11
1.3.1 Function of Intimin	11
1.3.2 Structure of Intimin	12
1.3.2.1 The signal peptide	13
1.3.2.2 The periplasmic domain	13
1.3.2.3 The translocator: the β -barrel and the linker.....	14
1.3.2.4 The passenger.....	14
1.3.3 Intimin dimerization	15
1.3.4 Findings on the inverse autotransport process of Intimin	16
1.3.5 Biogenesis of Intimin	17
2. Aim.....	18
2.1 Questions.....	18
2.2 Overall Strategy	19
3. Materials and Methods	20
3.1 Genetics.....	20

3.1.1	Primers	20
3.1.2	Plasmids.....	20
3.1.3	Polymerase chain reaction (PCR)	21
3.1.3.1	PCR using Q5 polymerase.....	21
3.1.4	Cloning by gibson assembly.....	22
3.1.5	Colony PCR.....	23
3.1.6	Agarose gel electrophoresis for DNA separation	24
3.1.7	Site-directed mutagenesis by PCR.....	24
3.1.8	Plasmid extraction	24
3.1.9	Sequencing	25
3.2	Microbiology.....	25
3.2.1	Bacterial strains	25
3.2.2	Media and growth conditions for bacterial strains	25
3.2.3	Antibiotics.....	25
3.2.4	Transformation of chemically competent <i>E. coli</i> cells.....	26
3.2.4.1	Transformation using CaCl ₂ competent cells	26
3.2.4.2	Transformation using Transformation and storage solution (TSS) competent cells.....	26
3.3	Expression and assembly of Intimin mutants.....	27
3.3.1	Overexpression of Intimin by auto-induction	27
3.3.2	Outer membrane protein (OMP) isolation.....	27
3.3.3	Heat modifiability assays.....	28
3.3.4	Membrane integration assays by urea extraction	28
3.4	SDS-Polyacrylamide gel electrophoresis	28
3.5	Western blotting	28
3.6	Immunofluorescence microscopy	29
3.7	Whole-cell ELISAs	29
3.8	Statistics.....	30
3.9	Bioinformatics	30
3.10	Adhesion assays with pre-infected HeLa cells.....	30
3.11	Plasmid stability.....	31
4.	Results	32
4.1	Designing mutations in the β -barrel of Intimin	32
4.1.1	Mutations in the α -helical turn on the periplasmic side of the β -barrel.....	32

4.1.2	Mutations in the linker connecting the β -barrel to the passenger and interacting residues facing the lumen of the β -barrel.....	32
4.1.3	Mutations in the small β -sheet formed between the linker and two loops of the β -barrel on the extracellular surface	33
4.2	Conserved regions within the β -barrels of IATs	38
4.3	Expression and assembly of Intimin mutants.....	41
4.3.1	Heat modifiability assays.....	41
4.3.2	Membrane integration assays.....	44
4.4	Immunofluorescence microscopy	47
4.5	Whole-cell ELISAs	50
4.6	Adhesion assays.....	57
4.7	Plasmid stability.....	60
5.	Discussion.....	62
5.1	<i>E. coli</i> , Intimin and Pathogenesis.....	62
5.2	The β -strand present at the C-terminus of the linker is important for hairpin formation and passenger secretion	62
5.3	Proposed models for the biogenesis of IATs	66
6.	Conclusion and future goals	69
	References.....	71
	Appendix 1 Abbreviations	81
	Appendix 2 Primer Sequences.....	84
	Appendix 3 Buffers and Chemicals.....	87
	Supplementary	92

Abstract

Gram-negative bacteria use different protein secretion systems, ranging from type I through type IX, to invade the host and cause infections. Proteins of the type V secretion system, called autotransporters, can autonomously transport a part of their own polypeptide chain to the bacterial cell surface through an outer membrane-embedded β -barrel domain. The transported part of the protein is called the passenger. Thus, autotransporters can be considered self-contained secretion systems, with several described subclasses.

Intimin, an adhesin of enteropathogenic *Escherichia coli*, is a prototypical member of the Type Ve secretion system or inverse autotransporter pathway. Intimin has been proposed to export its passenger through the β -barrel domain via a hairpin intermediate. During studies on Intimin autotransport, a double HA tag was inserted into the N-terminus of the passenger resulting in a stalled secretion intermediate caught in the hairpin conformation.

In this project, to study the molecular details of hairpin formation and passenger secretion, I have made mutations in three regions of the β -barrel of Intimin. The mutations were made both in wild-type Intimin and the stalled variant to see the effect on passenger secretion and hairpin formation, respectively. All mutant proteins, except the mutation where a β -strand on the extracellular side of the β -barrel was deleted, were produced, correctly folded and inserted into the membrane. Using the stalled variant, the formation of the hairpin was studied by exposure of the HA tag at the cell surface. Using the mutant proteins in the secretion-competent background, the exposure of the C-terminus of Intimin was studied.

After introducing mutations in the three regions of the barrel, a region with a β -strand on the extracellular side of the β -barrel was observed to be important for hairpin formation and successful passenger secretion. This β -strand is a part of a β -sheet formed with the β -strands located on extracellular loop 4 and 5 of the β -barrel. The β -strand is present at the very C-terminus of the linker. The β -barrel forms a pore in the outer membrane of the bacteria through which the passenger is translocated. In this study, I propose two alternative models: one, where the sequence forming the β -strand directs the linker into the OM pore formed by the β -barrel, stabilizes the hairpin and promotes passenger secretion and the other, where the hairpin is formed by unknown means and the β -strand interacts with the extracellular loops locking the hairpin in its configuration thereby promoting passenger translocation.

1. Introduction

Bacteria have evolved many methods to invade the host and cause disease. Of these, secretion of proteins is an important, but not universal, mechanism followed by bacteria to cause the disease. The mechanisms that bacteria use for protein secretion varies with different classes of bacteria and depends on whether the proteins are secreted across a single phospholipid membrane (Gram-positive bacteria), two membranes (Gram-negative bacteria) or even three membranes (where two are bacterial membranes and one is the host cell membrane). The protein secretion systems in Gram-negative bacteria are divided into different classes ranging from Type I to Type IX based on their structure, function and specificity (Green and Mecsas, 2016). In this project, I study the structure and functions of the adhesion protein Intimin (Section 1.3), a virulence factor of enteropathogenic *Escherichia coli* (EPEC) and a Type V protein secretion system (Section 1.2.5) that mediates adherence to the host intestinal epithelial cells, which ultimately leads to diarrhea.

1.1 Review of the literature

1.1.1 Gram-negative bacteria

Gram-negative bacteria such as *E. coli*, *Pseudomonas aeruginosa*, *Neisseria gonorrhoea*, *Chlamydia trachomatis*, *Salmonella enterica* and *Yersinia enterocolitica* are causative agents for many commonly occurring bacterial infections. The unique characteristic of these Gram-negative bacteria is the architecture of their cell envelope.

The cell envelope of Gram-negative bacteria, is composed of different layers. In order for the proteins to be secreted, they must cross two membranes: the inner membrane (IM) and the outer membrane (OM). The IM and OM are separated by a space called the periplasm that contains highly cross-linked glycopolymers called the peptidoglycan. The periplasm contains binding proteins for amino acids, sugars, vitamins, iron, and enzymes essential for bacterial nutrition and can act as a reservoir for some pilins, S-layer proteins and virulence factors (Beveridge, 1999). The periplasm allows for sequestration of enzymes that can be toxic in the cytoplasm, can harbor important signaling functions and regulation of cell division. Additionally, the periplasm provides the cell with structural systems that jointly work with the OM, such as, the peptidoglycan, multidrug efflux systems and specific solutes that provides ionic potential across the OM (Miller and Salama, 2018). The IM of Gram-negative bacteria is composed of phospholipids and proteins that are either integrated into the membrane or peripherally attached. The inner leaflet of the OM is made of phospholipids facing the periplasm and the outer leaflet is made of lipopolysaccharides (LPS) that face the external environment. The LPS is a large molecule comprised of lipids and a polysaccharide composed of the O-antigen; an outer core and inner core. The structure of the O-antigen in LPS is specific to each strain of bacteria while the outer and inner core are similar within bacterial

species. The LPS is highly charged in nature, conferring an overall negative charge to the Gram-negative cell surface.

The OM of Gram-negative bacteria makes them impervious to antibiotics like penicillin and confers resistance to lysozyme. Some enzymes present in the periplasmic space degrade or alter the antibiotics that manage to permeate through the OM and the LPS provides structural stability and protection from harmful compounds. Due to the aforementioned factors and with rise in resistance to antibiotics, treating infections caused by Gram-negative bacteria has become very challenging and alternative strategies are required to combat diseases caused by them. For this reason, understanding molecular details of the processes required for infection may help in developing a way to disarm the bacteria and prevent them from causing infections (Calvert et al., 2018).

1.1.2 Protein secretion systems in Gram-negative bacteria

1.1.2.1 Protein translocation across the IM

E. coli membrane proteins can either be integral proteins which are integrated into the membrane or proteins that are peripherally attached to the membrane. The proteins that are destined for the periplasm cross the IM by employing the general secretion (Sec) system, or the twin-arginine translocase (Tat) system. The YidC insertase system is used for insertion of proteins into the IM. In addition to translocating proteins across the IM, the Sec system allows for insertion of integral proteins into the membrane.

1.1.2.1.1 The general secretion (Sec) system

The Sec system is present in all bacteria, archaea and the endoplasmic reticulum membrane of eukaryotic cells. In Gram-negative bacteria, this system either transports secretory proteins across the IM or inserts membrane proteins into the IM. The Sec system interacts with cytosolic proteins like SecA or a ribonucleoprotein (protein-RNA complex) like the Signal Recognition Particle (SRP) and recognizes signal sequence-containing proteins to initiate membrane targeting (Koch et al., 2003). The proteins are targeted to the IM or the periplasm by their respective hydrophobic transmembrane segments (TMS) or signal sequences, respectively. Signal sequences, also referred to as signal peptides, are short amino acid sequences, usually 16-20 amino acids long, present at the N-terminus of newly synthesized proteins. The signal sequence directs the newly synthesized protein to the SecYEG protein conducting channel (SecYEG translocon) present in the plasma membrane. The SecYEG translocon, embedded in the IM of Gram-negative bacteria, is a highly conserved protein complex (~75kDa), in which the SecY, the largest subunit, forms a channel across the IM, while the smaller subunits SecE and SecG are integral membrane proteins peripherally attached to SecY. The SecYEG translocon is involved in two different targeting pathways mediating translocation across the IM by signal sequences. One pathway targets the integral

IM proteins co-translationally by the SRP and the other targets the secretory proteins to the periplasm post-translationally by the SecA/SecB pathway (Kudva et al., 2013).

In the co-translational pathway, as soon as the N-terminal signal sequence is translated from the ribosome, the SRP and trigger factor (TF; a ribosome-associated molecular chaperone that is the first extra-ribosomal protein to interact with nascent polypeptides) compete to bind to the nascent chain. The stop-transfer sequences (~ 8-14 amino acid residues that follows the signal sequence, known to halt translocation) of the IM proteins then interact with the TMS that are tightly bound to SRPs. This interaction slows down elongation of the nascent chain allowing SRP to bind to its membrane receptor FtsY. Once bound, the nascent chain is transferred to the SecYEG translocon, after which translation continues initiating membrane protein insertion (Lycklama A Nijeholt and Driessen, 2012).

In the post-translational pathway, the nascent secretory proteins are bound by TF and the translation is not slowed down. After elongation, SecB takes over the activity of TF keeping the nascent protein unfolded and directs it to the motor protein SecA. SecA then binds to SecYEG translocon and subsequently ATP binds to SecA, which initiates translocation. SecA uses ATP as an energy source and transports the unfolded polypeptide across the IM. The SecDF complex pulls the translocated peptide across the channel and into the periplasm in a PMF (Proton-motive Force) dependent manner (Lycklama A Nijeholt and Driessen, 2012).

1.1.2.1.2 The YidC insertase

Some IM proteins use the YidC insertase as an alternative pathway for insertion into the IM. This is to compensate for the fact that the SecYEG becomes less accessible to secretory proteins when it is occupied by translating ribosomes. This system was first described for phage proteins (Samuelson et al., 2000) and later for endogenous *E. coli* proteins (Dalbey et al., 2011). The membrane proteins are first recognized by the SRP and then targeted to the SecYEG translocon or to the YidC insertase. For the membrane proteins that are inserted solely by YidC, the targeting pathway is not known. Recently, crosslinking experiments on the cytoplasmic coiled-coil (C1) domain of YidC was shown to use the SRP pathway in order to integrate proteins into the IM (Petriman et al., 2018). However, the role played by this domain is not clear.

1.1.2.1.3 The twin arginine translocase (Tat) system

Unlike the Sec translocase and the YidC insertase systems that transport unfolded proteins, the Tat system is involved in transporting specific folded proteins harboring a characteristic twin-arginine pair in their signal sequences, across the IM. The Tat system is present in the cytoplasmic membranes of most bacterial species but absent in mitochondria. It requires a transmembrane PMF for protein translocation. In *E. coli*, protein translocation is achieved by

the use of three small membrane proteins, namely TatA, TatB and TatC. TatB and TatC form an integral membrane complex while TatA is present as “dispersed promoters” (Berks, 2015). The TatBC complex binds to the signal peptide of the protein when TatC recognizes the twin arginine motif of the Tat-specific signal peptide. This is an energy-independent step. TatBC closes in on the signal peptide making it less accessible from the cytoplasm leaving the amino-terminus cytoplasmically exposed. TatBC then recruits TatA promoters, which polymerize around the substrate to form an active TatABC translocation complex. This step is dependent on PMF. The protein then crosses the lipid bilayer, mediated by the polymerized TatA while the signal peptide remains bound to the TatBC complex. Once the protein moves across the IM, the signal peptide is proteolytically cleaved. Then, TatA disassociates from TatBC back to its original form (Berks, 2015; Palmer and Berks, 2012).

1.1.2.2 Protein translocation across the OM

For transport across the OM, the secretion systems vary based on whether they extend across both the IM and OM or whether they extend only across the OM. These secretion systems, numbered from Type I through Type IX (T1SS to T9SS), plus the chaperone-usher (CU) pathway used for pilus assembly on the cell surface, are dependent on β -barrel channels in the OM and transport a specific subset of proteins. The secretion systems that extend across the IM, periplasm and OM are the T1SS, T2SS, T3SS, T4SS and T6SS, while the T5SS and CU pathway extend only across the OM (Costa et al., 2015). Some of these secretion systems depend on the Sec machinery for IM transit whereas some do not.

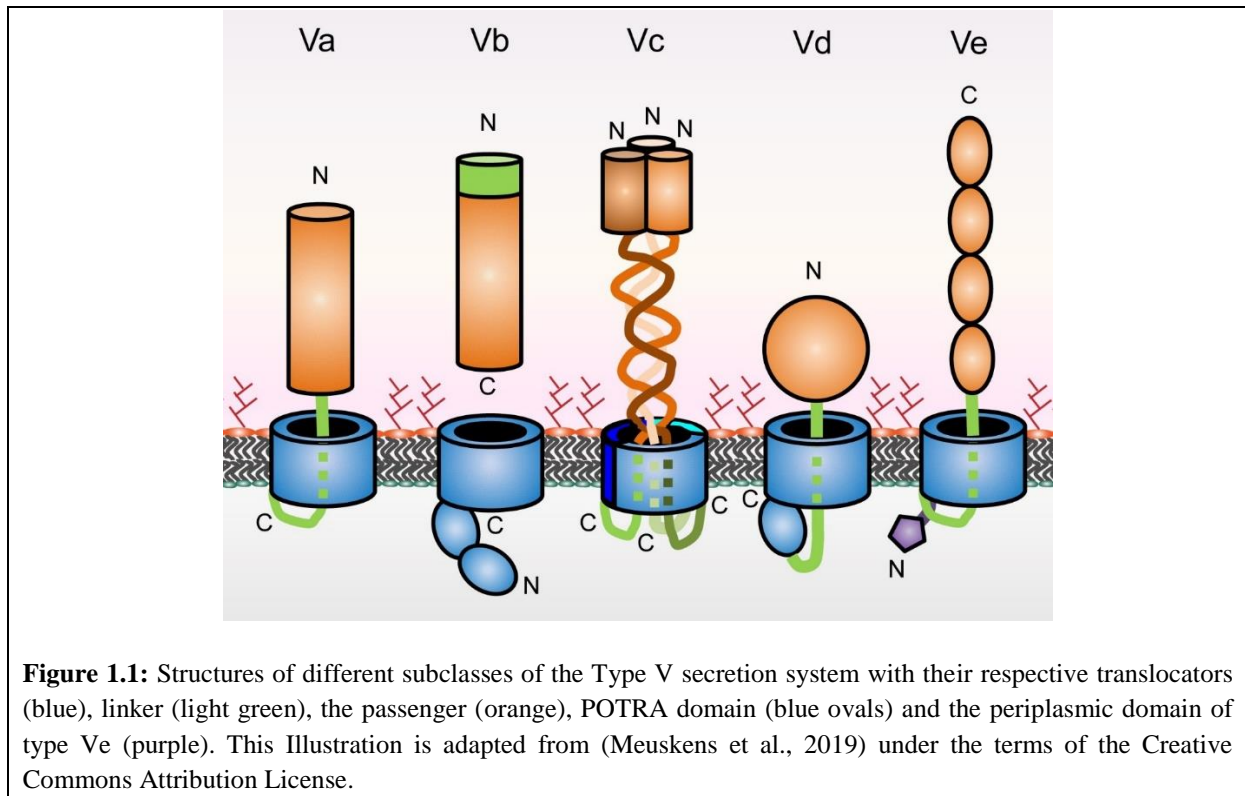
The T1SS is a Sec-independent system that enables secretion of proteins of different sizes and functions from the cytoplasm to the external environment bypassing the periplasm. The protein secretion takes place with the help of a translocator that spans the cell envelope. The translocator is composed three proteins: an Outer Membrane Protein (OMP), the cytoplasmic ATP-binding cassette and the periplasmically located membrane fusion or adaptor protein (MFP) (Morgan et al., 2017). The Sec-dependent T2SS (Cianciotto and White, 2017) and the Sec-independent T3SS (Deng et al., 2017) and T4SS (Christie et al., 2014) are complex systems that form pilus-like structures on the cell surface, which transport proteins either into the extracellular environment (T2SS) or directly from the bacterial cytoplasm into the host cell (T3SS and T4SS). T5SS is discussed in detail in Section 1.2. The Sec-independent T6SS comprises a harpoon-like structure related to bacteriophage contractile tails that punctures the lipid bilayer of target cells contributing to virulence development of various pathogens (Gallique et al., 2017). In addition, the T6SS is also involved in bacterial competition. The T6SS is activated upon contact with the target cell (Bönemann et al., 2010). Some Gram-positive bacteria, like *Mycobacteria*, *Actinobacteria*, *Firmicutes* and *Corynebacteria*, contain a lipid-rich cell wall called the mycomembrane that acts as a barrier against environmental stresses and antimicrobial compounds. These bacteria utilize the T7SS for transport of proteins across the IM and the mycomembrane (Freudl, 2013). The T8SS, also known as the extracellular nucleation/precipitation pathway, is involved in the production of extracellular protein fibers, called Curli, by many enteric bacteria like *E. coli* and *Salmonella enterica*.

Curli are an important proteinaceous component playing a vital role in biofilm formation and interactions with host immune responses (Evans and Chapman, 2014). Recently, a new type of protein secretion system, called the T9SS, was discovered in the *Bacteroidetes* phylum. This system can either act in gliding motility for non-pathogenic bacteria or as a weapon for pathogens (Lasica et al., 2017).

1.2 The type V secretion system (T5SS)

The proteins secreted via the T5SS, called autotransporters, have the ability to transit across the OM autonomously. These autotransporters are mainly virulence factors participating in cell-to-cell adhesion and biofilm formation (Leo et al., 2012), but can also have other functions (Meuskens et al., 2019). The process of autotransport was first described by Johannes Pohlner and colleagues, whose studies on the Immunoglobulin A (IgA) protease from *Neisseria gonorrhoea* suggested that the carboxy terminus of the enzyme formed a pore through which the remaining part of the enzyme was translocated across the OM (Pohlner et al., 1987b).

The T5SS is sub-classified into monomeric or classical autotransporters (Type Va), two-partner secretion systems (Type Vb), trimeric autotransporters (Type Vc), fused two-partner secretion system (Type Vd) and the inverse autotransporters (Type Ve) (Figure 1.1). All autotransporters have a common structural organization and mechanism of passenger transport and are dependent on the Sec machinery for translocation across the IM. The common structure of autotransporters includes an amino-terminal signal peptide that facilitates translocation across the IM to the periplasm, a secreted mature protein (the passenger) that harbors the specific activity of the autotransporter, and a translocator domain (β -barrel) embedded in the OM. In classical autotransporters, this β -barrel contains a α -helical linker that is connected to the passenger facilitating its export across the OM (Konieczny et al., 2001).



1.2.1 The type Va secretion system: classical autotransport (T5aSS)

The proteins secreted by the T5aSS, called classical autotransporters, were the first class of autotransporters to be studied in detail. Classical autotransporters can function either as extracellular proteases or lipases, or as adhesins. Examples include IgA protease from *Neisseria meningitidis* (Pohlner et al., 1987a), Adhesin Involved in Diffuse Adherence (AIDA)-I from *Escherichia coli* (Benz and Schmidt, 1989) and Pertactin from *Bordetella pertussis* (Leininger et al., 1991). Some classical autotransporters possess enzymatic activities that proteolytically cleave the passenger after it is transported to the external environment. Conserved residues present in the barrel and a conserved cleavage site at the C-terminus of the passenger facilitates this autoproteolysis (Provence and Curtiss, 1994).

Many models explaining the mechanism of classical autotransport have been described. The first model was described for *Neisseria* IgA protease (Pohlner et al., 1987a) and the first crystal structure of the translocator domain was shown for *Neisseria* Na1P (Oomen et al., 2004). This structure supported the findings of the original model that explained the C-terminus of the protein forming a pore in the OM through which the linker forms a hairpin leading to passenger export.

The classical autotransport process entails the production of proteins as a single polypeptide containing an N-terminal signal sequence. These proteins transit the IM into the periplasm via the Sec machinery in an unfolded state. There are several steps during the transport process that ensure the protein remains unfolded. For example, Hbp, the hemoglobin protease of *E.*

coli, uses the SRP pathway for translocation through the Sec machinery to ensure that the protein does not fold in the cytosol (Sijbrandi et al., 2003). Depletion of YidC showed periplasmic aggregates of Hbp indicating that YidC helps in keeping Hbp unfolded (Jong et al., 2010). Many classical autotransporters, like Hbp, contain extended signal peptides (52 amino acid residues long in the case of Hbp) that differentiates them from other Sec-dependent proteins. Experimental analysis of these signal peptides showed that they lead to slowing down of IM translocation giving time for the C-terminus of the protein to prepare for OM transport while the signal peptide is still attached to the Sec machinery (Szabady et al., 2005). Several studies also demonstrated that the interactions of periplasmic chaperones with unfolded autotransporters inhibits premature folding or misfolding. For example, EspP, an extracellular serine protease from enterohemorrhagic *E. coli* (EHEC), interacts with periplasmic chaperones SurA, Skp, the protease DegP, and the peptidyl-prolyl cis/trans isomerase FkpA, and Hbp interacts with SurA (Ieva and Bernstein, 2009; Ruiz-Perez et al., 2009; Ruiz-Perez et al., 2010; Sauri et al., 2009). DegP is a periplasmic protease involved in quality control which degrades misfolded proteins in the periplasm as shown for Hbp after depletion of YidC (Jong et al., 2010).

After crossing the periplasm, the unfolded autotransporters must then integrate into the OM. They do so with the help of the β -barrel assembly machinery (BAM) complex. The BAM complex is composed of five subunits, BamA-BamE, with BamA being a 16-stranded β -barrel protein belonging to the Omp85 superfamily and the rest being lipoproteins (Noinaj et al., 2013). BamA and BamD are the most essential subunits and cannot be knocked out while the other subunits are not essential though their knockout leads to growth defects. BamA has five periplasmic polypeptide transport-associated (POTRA) domains which plays a vital role along with BamD in cell viability. The other Bam components are needed for the full folding activity of OMPs. BamA forms a dome-like structure in the OM, and contains a very narrow hydrophobic stretch on one side. The connection between β -strand 1 and β -strand 16 of BamA is unstable which allows integration of the fully folded β -barrel OMPs into the OM. The POTRA domains and lipoprotein subunits form a ring like shape at the base of BamA. It has been proposed that, by the rotation of the basal ring complex, BamA opens laterally allowing insertion of β -barrel proteins into the membrane in a stepwise manner. The mechanism by which the integration takes place is not clearly understood (Hussain and Bernstein, 2018; Zhang and Han, 2016). However, alternative models have been proposed using molecular dynamics simulations (Fleming et al., 2016; Noinaj et al., 2013) and other studies (Sinnige et al., 2014) which suggests that the BamA causes thinning of the adjacent membrane thereby catalyzing OMP assembly.

The C-terminal 12-stranded β -barrel is recognized by the Bam complex in the OM which then inserts the β -barrel into the membrane forming a molecular pore. After insertion, the linker that connects the passenger to the barrel forms a hairpin initiating the C-terminal passenger export through the pore proceeding in the C-to-N terminal direction, i.e. export starts at the C-terminus and the N-terminus is secreted last (Junker et al., 2009). The exported part of the protein folds which then, sequentially, leads to the complete transport of the passenger to the external environment (Peterson et al., 2010). In most cases, the C-terminal passenger is

thought to have greater thermostability than the remaining protein. This difference in energy mediates vectorial folding of the passenger leading to its secretion (Peterson et al., 2010; Renn et al., 2012). Once several passengers from their cognate β -barrels are exported, they are proteolytically cleaved and released from the cell surface (Dautin and Bernstein, 2007).

With emerging insights on OMP biogenesis and new experimental evidence, Harris D. Bernstein proposed a synthetic model for classical autotransport (Bernstein, 2019). According to this model, based on the finding that the EspP linker is protected from proteolysis and chemical changes before passenger export (Ieva et al., 2008), it was suggested that the β -barrel begins folding in the periplasm (Saurí et al., 2011). Then, the β -barrel migrates towards BamA and integrates partially into the OM (Pavlova et al., 2013; Soprova et al., 2010). At this point, the β -barrel and BamA are in a hybrid conformation. The passenger segment of the T5aSS protein sequentially moves from the periplasmic chaperone SurA to the first POTRA domain of the Bam complex and then to the membrane-proximal POTRA domain and finally to the BamA transport channel (Pavlova et al., 2013). Once the hairpin forms and the passenger is translocated, surface exposure of a large polar residue present in a few subset of classical autotransporters facilitates closing of the β -barrel (Peterson et al., 2018). Finally, the β -barrel is separated from the Bam complex and the passenger is proteolytically cleaved.

1.2.2 The type Vb secretion system: two-partner secretion (TPS) system (T5bSS)

The proteins of the TPS system follow the same process of translocation across the OM as that of the T5aSS. However, the passenger and the β -barrel of TPS are translated as two separate protein chains, referred to as TpsA and TpsB, respectively (Figure 1.1) and the proteins are expressed from the same operon (Jacob-Dubuisson et al., 2013). Examples include the filamentous hemagglutinin (FHA) from *Bordetella pertussis* (Willems et al., 1994), the hemolytic Sh1AB system of *Serratia marcescens* (Braun et al., 1993), HpmAB of *Proteus mirabilis* and the high molecular weight adhesins HMW1 and HMW2 from *Haemophilus influenzae* (St. Geme and Yeo, 2009). The TpsA secretory passenger proteins are large β -helical structures that contain an extended signal sequence and a TPS domain at the N-terminus. The TPS domain is recognized by its TpsB transporter, which is a 16-stranded β -barrel homologous to BamA (Clantin et al., 2007). The specificity of the TpsB β -barrel to TpsA passenger varies with different systems and some TpsBs are known to secrete more than one TpsA (Julio and Cotter, 2005).

The first characterized TPSS, the filamentous hemagglutinin (FHA) of *Bordetella pertussis* and the Ca^{2+} -independent haemolysins of *Serratia marcescens* and *Proteus mirabilis* was found to secrete effector proteins like cytolysins or adhesins in pathogenic bacteria (Jacob-Dubuisson et al., 2004; Jacob-Dubuisson et al., 2001). Later, the TPS system was also found to be involved in “contact-dependent growth inhibition” (CDI) systems between closely related bacterial species recognized by molecular interactions (Aoki et al., 2010; Aoki et al., 2005; Willett et al., 2015).

The mechanism for TPS involves the synthesis of the TpsA preprotein in the cytoplasm, which then transits the IM via the Sec machinery. Similar to EspP in classical autotransport, the long N-terminal signal peptide slows down IM translocation and delays signal peptide cleavage increasing the efficiency of TpsA secretion (Chevalier et al., 2004; Guérin et al., 2017). In the case of FHA, periplasmic chaperones like DegP facilitate periplasmic transit of TpsA and TpsB to the OM. TpsB with its two periplasmic POTRA domains forms the OM pore. The N-terminal TPS domain of TpsA binds to the TpsB POTRA domain and directs the TpsA for translocation across the OM in a C- to N-terminal direction (Guérin et al., 2017). A model for FHA suggested by Mazar & Cotter showed that the N-terminus of the TpsA passenger remains attached to its TpsB while the remainder of the protein is secreted via protein folding. It is likely that secretion and folding occur simultaneously. Once the TpsA protein is exposed extracellularly, it begins to fold into a β -helix and the difference in energies of the extended and folded arms is presumed to be the driving force for passenger secretion (Jacob-Dubuisson et al., 2004).

1.2.3 The type Vc secretion system (T5cSS): trimeric autotransporter adhesins (TAAs)

TAAs form a rigid rod-like structure that protrudes from the bacterial cell surface. Unlike the T5aSS, these adhesins do not possess any enzymatic functions and are not proteolytically cleaved from the cell surface (Leo et al., 2012). The structure of TAAs generally consists of a head, a neck, a stalk (forming the passenger) and an membrane anchor (β -barrel) in the OM of Gram-negative bacteria (Linke et al., 2006). The prototypical member of this group is the *Yersinia* adhesin A (YadA) of *Yersinia enterocolitica* and *Y. pseudotuberculosis* (Bölin et al., 1982; Mühlkamp et al., 2015; Skurnik et al., 1984) which cause a variety of disease ranging from diarrhea to septicemia, mesenteric lymphadenitis and reactive arthritis.

All TAAs have homologous, trimeric membrane anchor at the C-terminus. The anchor forms a 12-stranded β -barrel OM pore, with each protomer contributing 4 strands, through which the remaining parts of the three polypeptide chains are translocated. The characteristic feature of TAAs is their ability to trimerize and connect to the ubiquitous stretches of the trimeric coiled coils and are hence called ‘trimeric’ autotransporters. The extracellular stalk domains of TAAs are highly repetitive fibrous structures that vary in length. The stalk projects the adhesive head domain away from the bacterial cell surface towards its adhering partners. It also protects the bacteria from host defense mechanisms. For example, the stalk confers serum resistance in the case of YadA (Roggenkamp et al., 2003). The head domain consists of a trimer of left-handed β -helices which is connected to the stalk by a short conserved region called the neck. The head domain is C-terminal to the stalk (Linke et al., 2006) but in case of YadA, the head domain is N-terminal. There may be more heads present further down the protein with the stalk in between.

Like T5aSS, the TAA preprotein, synthesized in the cytoplasm, transits the IM via the Sec machinery (Dautin et al., 2007; Linke et al., 2006). Some “pre-TAAs” are modified by

glycosylation in the cytoplasm (Tang et al., 2012). Once the unfolded protein reaches the periplasm, the signal peptide is cleaved off and the passenger begins folding in the periplasm to prepare for OM export. The passenger then translocates through the OM pore in a C-to-N-terminal direction (i.e. via a hairpin intermediate) to protrude from the cell surface by a mechanism that is not fully understood (Chauhan et al., 2019; Qin et al., 2015).

1.2.4 The type Vd secretion system: fused two-partner secretion system (T5dSS)

A novel secreted protein, called PlpD, was discovered in *Pseudomonas aeruginosa* and is the prototypical member of the bacterial lipolytic enzyme family of patatin-like proteins (PLP) (Salacha et al., 2010).

Like most ATs, PlpD is translated as a single polypeptide chain consisting of a secretory domain (passenger) which is fused to its transporter domain (the β -barrel) by a POTRA domain. The N-terminus of the protein has a signal peptide that directs transport across the IM via the Sec machinery. Following the signal peptide is a α/β hydrolase domain, which contains the lipase activity of PlpD. C-terminal to the lipase domain is a presumed periplasmic POTRA domain followed by the 16-stranded β -barrel similar to TpsB of the T5bSS. The C-terminus is inserted into the OM and the passenger is secreted (Salacha et al., 2010). Once the passenger is transported, it is cleaved similar to some lipases exported by the T5aSS (Salacha et al., 2010). Due to the combined functional and structural similarity to T5aSS and T5bSS respectively, PlpD is categorized as a separate class, the type Vd secretion system (Arnold et al., 2010; Casasanta et al., 2017; Leo et al., 2012; Salacha et al., 2010).

1.2.5 The type Ve secretion system: the inverse autotransporter (IAT) system (T5eSS)

The prototypical members of the T5eSS are the closely related adhesins Intimin of EPEC and Invasin of *Yersinia* spp. A topology model for Intimin/Invasin adhesin was published in 2010 (Tsai et al., 2010) showing an N-terminal periplasmic domain assumed to bind peptidoglycan, a β -barrel that resides in the OM, a α -helix that plugs the pore formed by the β -barrel and extracellular Ig domains that is connected to the β -barrel by the α -helix. Although Tsai and colleagues categorized Intimin and Invasin as ‘a novel family of secreted proteins’ (Tsai et al., 2010), bioinformatics and experimental analysis showed that they belonged to the autotransporter family (Oberhettinger et al., 2012).

The structural organization of Intimin/Invasin family is inverted compared to that of the classical autotransporters; hence, they are called inverse autotransporters (IATs). In contrast to T5aSS, the passenger is located C-terminal to the β -barrel. The passenger is exported in the N-to-C-terminal direction i.e. the opposite direction of T5aSS (Leo et al., 2012; Oberhettinger

et al., 2012). The inverted passenger export happens via a hairpin intermediate, which is looped through the β -barrel pore pulling the passenger outside the cell (Oberhettinger et al., 2015). The exported passenger then folds from the N- to C-terminus (Leo et al., 2016). In light of this significant difference, it was suggested to group Intimin, Invasin and related proteins in a new type V subclass named Type Ve secretion (Leo et al., 2012).

Though the Intimin/Invasin family follows an inverted order of passenger secretion, proteins belonging to the T5eSS follow a similar path of OM translocation as T5aSS. The proteins transit the IM via the Sec machinery, which recognizes the signal peptide (Touzé et al., 2004), and enters the periplasm. Once they reach the periplasm, the periplasmic chaperones like SurA and Skp keep the protein unfolded and DegP degrades any misfolded protein (Bodelón et al., 2009a; Oberhettinger et al., 2012). Intimin and Invasin then depend on BamA (of the BAM complex) for insertion into the OM.

1.3 Intimin: an adhesion protein of EPEC

Intimin (94 kDa) is an important virulence factor of attaching and effacing bacteria, such as EPEC, that tightly adheres to the host intestinal epithelial cells inducing the formation of lesions, attaching and effacing lesions (A/E lesions), on the surface of the enterocytes. The lesions are characterized by degeneration of the absorptive brush border microvilli, which results in reorganization of host cell actin cytoskeleton into actin pedestals beneath the surface of the bacterial adhesion. The locus of enterocyte effacement (LEE) of EPEC is important for actin pedestal formation and encodes for Intimin.

1.3.1 Function of Intimin

Intimin is found in many bacterial pathogens, which include enteropathogenic and enterohemorrhagic *Escherichia coli* (EPEC and EHEC), *Citrobacter rodentium* and *Hafnia alvei*, causative agents of diarrhea. These pathogens intimately attach to the intestine forming the A/E lesions with Intimin playing a vital role in this attachment.

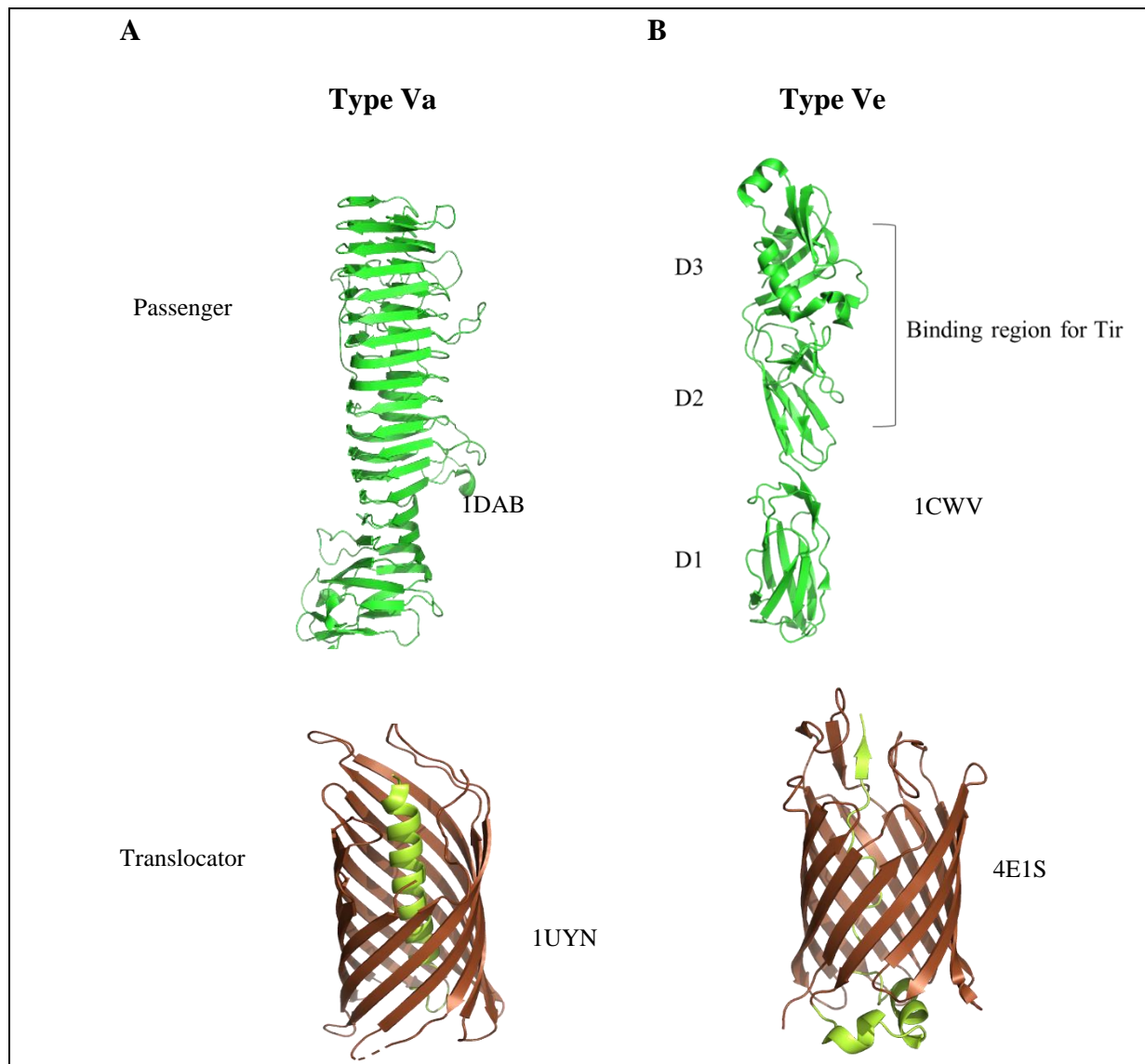
The *eaeA* gene, which codes for Intimin, is present on a horizontally acquired pathogenicity island LEE (Schmidt, 2010). Based on sequence differences, several different alleles of Intimin have been described, α to ϵ , that have similar functions and in many cases can complement each other (Leo et al., 2015c).

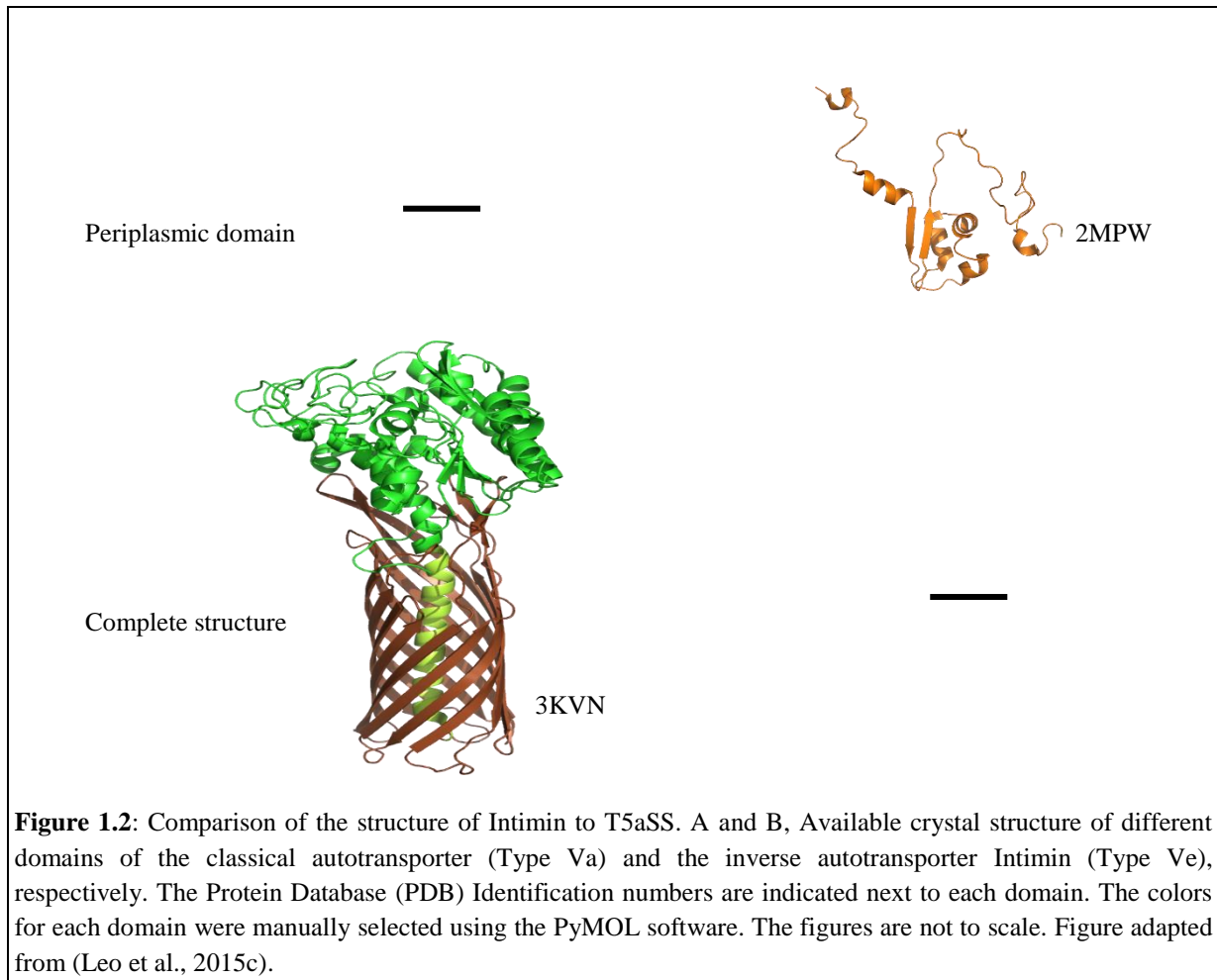
Interestingly, the receptor for Intimin is not found on the host cell but is a protein translocated from the bacterium into the host cell membrane via a T3SS (Kenny et al., 1997) and is called the translocated Intimin receptor (Tir). Tir, also named EspE (Deibel et al., 1998), has an extracellular domain which binds with moderate affinity ($K_d \sim 0.3 \mu\text{M}$) to Intimin, a transmembrane domain, and a cytoplasmic domain. Phosphorylation of Tir triggers the

formation of local actin polymerization thereby resulting in actin-pedestals (Leo et al., 2015c; Luo et al., 2000; Marchès et al., 2000; McKee et al., 1995). There have been debatable reports that Intimin can independently bind to host cells, to β_1 integrins and nucleolin, even in the absence of Tir (Frankel et al., 1996; Hartland et al., 1999; Sinclair and O'Brien, 2002). However, the *in vivo* role of Intimin binding to a secondary receptor is poorly understood (Leo et al., 2015c; Liu et al., 1999; Mallick et al., 2012).

1.3.2 Structure of Intimin

The crystal structures for the passenger, the β -barrel and a part of the periplasmic domain of Intimin is depicted in Figure 1.2. Earlier, only structural information for the passenger of Intimin was available (Hamburger et al., 1999c; Kelly et al., 1999a). Now crystal structures for the passenger (Hamburger et al., 1999b), the β -barrel (Fairman et al., 2012a) and part of the periplasmic domain (Leo et al., 2015a) are available (Figure 1.2).





1.3.2.1 The signal peptide

Like classical autotransporters, Intimin transits the IM via the Sec machinery and enters the periplasm. The N-terminal signal peptide is longer than the usual 16 to 20 amino acid residues of a standard signal peptide and aids in slowing down IM translocation by staying attached to the Sec machinery. Unlike T5aSS, IATs do not have conserved N-terminal extensions or a conserved signal peptide sequence (Leo et al., 2015c; Tsai et al., 2010). Before the N-terminal signal peptide is cleaved, the C-terminal β -barrel inserts into the OM and initiates secretion. As a result, this prevents premature folding of the passenger domain in the periplasm (Szabady et al., 2005).

1.3.2.2 The periplasmic domain

Intimin has a short conserved periplasmic domain, called the α -helices, connected to the C-terminal β -barrel (Leo et al., 2015c; Tsai et al., 2010). Additionally, it has an N-terminal periplasmic domain, a Lysin motif (LysM). Such domains are present in proteins that bind to

peptidoglycan and/or chitin (Buist et al., 2008). The LysM of Intimin binds to peptidoglycan at low pH (Leo et al., 2015b).

The length of the passenger influences the presence or absence of the lysin motif; that is, inverse autotransporters with long passengers are likely to have a LysM (Leo et al., 2015b). Invasin, for instance, does not contain this motif. The presence of LysM may prevent membrane rupture by providing better mechanical anchoring of Intimin in the OM. It has been proposed that this binding also keeps the protein sturdy during autotransport or during receptor binding (Leo et al., 2015b; Martinez-Gil et al., 2017). However, the binding takes place only under acidic conditions. The authors suggested that this low pH requirement for binding may help pathogens resist the acidic environment in the stomach of the host during its passage (Leo et al., 2015b).

1.3.2.3 The translocator: the β -barrel and the linker

The β -barrel is the most conserved region in the IATs and its presence is characteristic of the family (Fairman et al., 2012b; Leo et al., 2015c). Analogous to the classical autotransporters, the structure of the transmembrane domain of Intimin is a 12-stranded β -barrel that forms a hydrophilic pore in the OM (Oberhettinger et al., 2012). The linker, that connects the β -barrel and the passenger (Figure 1.2), is located within the OM pore formed by the β -barrel. Unlike T5aSS, the linker of Intimin and Invasin is in an extended conformation and the N-terminal region of the linker stabilizes the β -barrel in the OM (Fairman et al., 2012b). The linker leans dominantly on to one side of the β -barrel forming a cavity on the periplasmic side, while the extracellular side is mostly covered by an extracellular loop (Fairman et al., 2012b; Leo et al., 2015c).

The C-terminus of the linker forms a small anti-parallel β -sheet with two extracellular loops of the β -barrel. The N-terminus of the linker forms an α -helical turn on the periplasmic side, which is assumed to plug the pore to prevent OM leakage (Fairman et al., 2012b; Leo et al., 2015c).

1.3.2.4 The passenger

The passenger domains of the IAT family are long fibrous structures that usually consist of an array of immunoglobulin (Ig)-like domains (Hamburger et al., 1999a; Nesta et al., 2012; Tsai et al., 2010). The crystal structure of the Intimin passenger (Figure 1.2 B) shows 2 Ig-like domains (D1-2) capped by a C-type lectin domain (D3). D2 and D3 together form the binding region for the receptor protein Tir (Kelly et al., 1999a). Additionally, a third Ig-like domain, D0, is present at the N-terminus of the passenger but absent in the crystal structure. Another domain, D00, at the extreme N-terminus of the passenger has been identified (Fairman et al., 2012a; Leo et al., 2016). For IATs, some passenger domain subtypes contain a repetition of

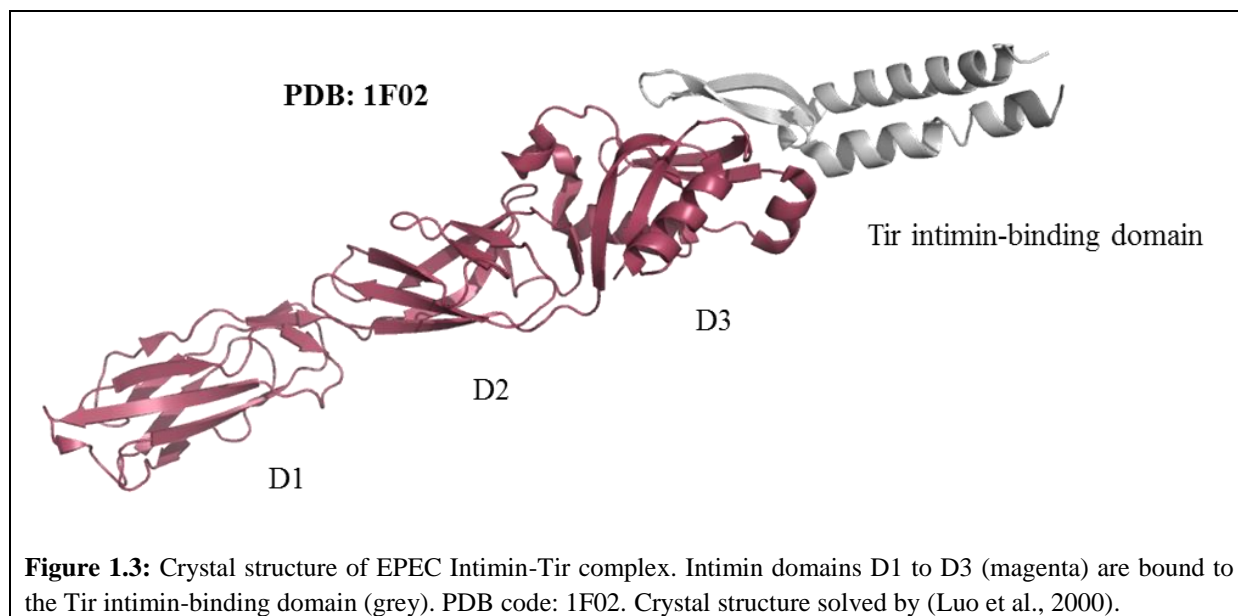
certain type of Ig-like domains, while some subtypes of Ig-like domains located at the C-terminus are present in just one copy, suggesting their importance in specific functional roles (Leo et al., 2015c). Usually, the passengers have a C-type lectin domain at their C-termini (Hamburger et al., 1999a; Kelly et al., 1999b; Leo et al., 2015c). Disulphide bonds with ~70 intervening residues stabilize these C-type lectin domains (Tsai et al., 2010).

The crystal structures of the passengers for Invasin and FdeC show long extended fibrous structures (Hamburger et al., 1999a; Luo et al., 2000; Nesta et al., 2012; Tsai et al., 2010); however, the structure for the C-terminus Intimin passenger shows a kink between the last two Ig-like domains suggesting that there is flexibility between the domains (Kelly et al., 1999b).

1.3.3 Intimin dimerization

The N-terminal periplasmic domain, LysM, of Intimin is vital for Intimin dimerization. Leo *et al.* were able to show that the spacer region connecting LysM to the periplasmic α -helices mediates dimerization (Leo et al., 2015b). However, Touzé *et al.* experimentally demonstrated that a construct containing the translocator domain and the periplasmic α -helices that connect to the β -barrel, formed stable dimers (Touzé et al., 2004), suggesting that the periplasmic α -helices form another site that mediates dimerization. On a different note, it was shown for the *Y. pseudotuberculosis* Invasin protein that multimerization was mediated by the second extracellular Ig-like domain (Dersch and Isberg, 2000; Dersch and Isberg, 1999). In light of these findings, it can be concluded that at least three different regions in the inverse autotransporters can mediate dimerization: through the N-terminal periplasmic domain, the periplasmic α -helices or through an Ig-like domain in the passenger (Leo et al., 2015b; Leo et al., 2015c).

The crystal structure for Intimin-Tir (Figure 1.3), the only structure of an inverse autotransporter bound to its receptor available, shows an Intimin molecule bound to the a side of the Tir jutting out at a low angle (Luo et al., 2000). Along with the finding that Intimin can form dimers itself, it was suggested that when one Intimin dimer binds to two different Tir dimers, each Tir dimer can further recruit a second Intimin dimer and this cycle continues. As a result, the Tir receptors would form clusters leading to actin rearrangements and pedestal formation (Leo et al., 2015c; Touzé et al., 2004).



1.3.4 Findings on the inverse autotransport process of Intimin

Earlier, it was suggested that Intimin and Invasin were analogous to monomeric autotransporters, but no experimental data was provided that supported this hypothesis (Newman and Stathopoulos, 2004). Recently, by sequence analysis and insertion of epitope tags into the loops and turns of the β -barrel, investigators confirmed the inverted topology of Intimin and Invasin compared to T5aSS, and thereby classified them as T5eSS (Fairman et al., 2012a; Oberhettinger et al., 2012).

The mechanism of autotransport for ATs (which is independent of ATP or a membrane potential as energy source (Thanassi et al., 2005)) remains unclear. Although most of the research done to elucidate this process points towards a hairpin model wherein the passenger is translocated C- to N-terminal through the pore of the β -barrel. For the Intimin/Invasin family, since the domain organization is inverted compared to T5aSS, the passenger would be transported with an inverted polarity, the N-to-C terminal. When the investigators replaced a highly conserved glycine residue present in the pore lumen of the β -barrel of Invasin with larger residues of amino acids, it resulted in obstruction of the β -barrel pore and hindered autotransport (Oberhettinger et al., 2012). However, the β -barrel was still correctly inserted into the OM. Based on these results, the authors suggested the hairpin mechanism of autotransport for T5eSS, though there was no evidence yet (Leo et al., 2012; Oberhettinger et al., 2012).

In Intimin, insertion of a double HA tag after amino acid position 453 located in the D00 domain of the extracellular N-terminal passenger, resulted in the formation of a stalled T5eSS intermediate. By performing immunofluorescence staining on this stalled variant and treating the bacteria with Proteinase K, the authors showed that the passenger was stalled in a hairpin conformation. That is, the N-terminal part of the passenger with the HA tag was surface

exposed whereas the C-terminus of the passenger remained in the periplasm (Oberhettinger et al., 2015). This stalled variant also supported the idea that passenger translocation occurs in the opposite direction (N-to-C) compared to classical autotransporters (C-to-N) (Oberhettinger et al., 2012). During their experiments, the authors showed that the β -barrel was fully folded and inserted into the OM suggesting that membrane insertion and passenger export takes place with a fully folded β -barrel (Oberhettinger et al., 2015).

Introduction of an HA-tag in the D00 domain sequence of the Intimin passenger disrupted a predicted β -strand. The authors found that the insertion of this tag in the D00 led to misfolding of the D00 domain and stalled passenger secretion. They also showed that deletion of this domain did not hinder passenger secretion. With AFM experiments, the authors were able to show that the Ig-like domains act as independent folding modules where one domain can fold at the cell surface regardless of whether it is followed by other domains. Additionally, they performed folding experiments to find that the D00 domain folds robustly compared to the HA-tagged D00 variant and the variant where the predicted β -strand was deleted. Based on these findings, Leo and colleagues proposed a model where sequential folding of the Ig-like domains in the passenger energizes passenger secretion at the cell surface (Leo et al., 2016).

1.3.5 Biogenesis of Intimin

To give a summary, Intimin transits the IM via the Sec machinery with its N-terminal signal peptide recognized by the SecYEG translocon. The periplasmic chaperones, like SurA, bind to the protein and keep it unfolded. Experimental results showed that depletion of SurA led to the aggregation of the protein in the periplasm, which in turn resulted in upregulation of the periplasmic quality control protease DegP (Bodelón et al., 2009b; Oberhettinger et al., 2012). DegP degrades any misfolded protein in the periplasm. Skp plays a minor role in this process. Also, the periplasmic oxidoreductase DsbA was shown to facilitate the formation of the C-terminal disulphide bond required for stabilizing the C-type lectin domain, which forms the crown of the passenger (Bodelón et al., 2009b). Once inside the periplasm, the BAM complex aids in folding of the β -barrel domain of the protein and inserts it into the OM (Oberhettinger et al., 2012) while the passenger presumably still interacts with BamA. This suggested that BamA is involved in β -barrel membrane integration and simultaneously takes part in passenger secretion.

2. Aim

2.1 Questions

The β -barrel participates in Intimin passenger secretion (Oberhettinger et al., 2015; Oberhettinger et al., 2012). However, the role of different regions of the β -barrel in the secretion process are not known. The aim of this project was to better understand the molecular details of hairpin formation and passenger secretion by introducing point and deletion mutations in three regions of the Intimin β -barrel.

The three regions of interest in the β -barrel are:

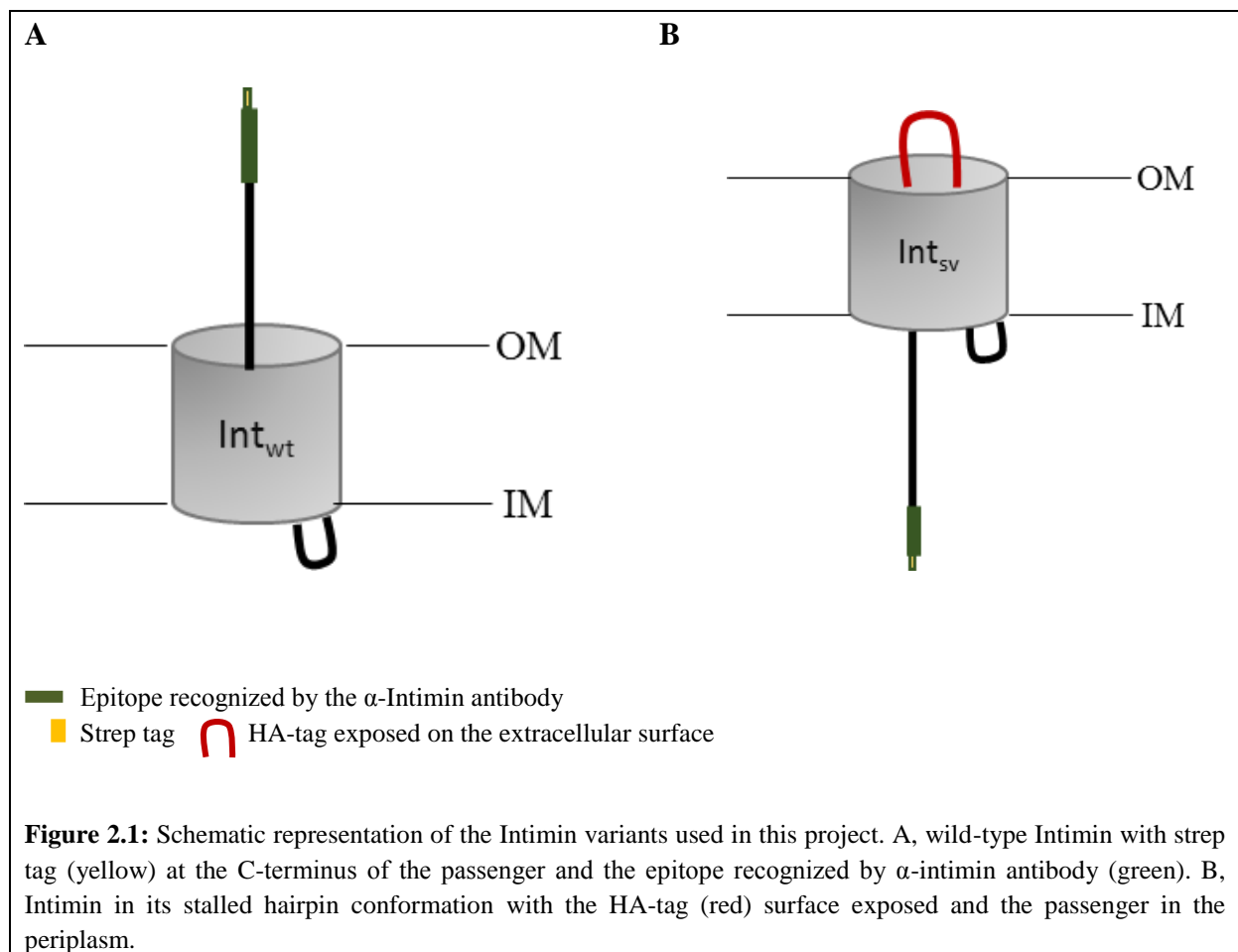
1. The α -helical turn on the periplasmic side of the β -barrel.
2. The linker connecting the β -barrel to the passenger and interacting residues facing the lumen of the β -barrel.
3. The small β -sheet formed between the linker and two loops of the β -barrel on the extracellular surface.

Our aim was to answer the following questions pertaining to the function of the three regions in the β -barrel. This would help refine and give insight into the existing model of the inverse autotransport process.

- 1) What is the role played by the α -helical turn on the periplasmic side of the β -barrel? Is it involved during the process of hairpin formation and passenger secretion? Will introducing mutations in this turn effect the mechanism of autotransport?
- 2) The C-terminal region of the linker, that connects the β -barrel to the passenger, has been shown to stabilize the β -barrel (Fairman et al., 2012b) in the OM. Will introducing mutations in the linker and disrupting its interactions with the lumen of the β -barrel have any effect on the hairpin formation and/or passenger secretion?
- 3) What role does the β -sheet have on the stability of the hairpin and /or the passenger? Will introducing mutations in the β -strand preceding the D00 domain of the passenger hinder passenger export and/or destabilize the hairpin?

2.2 Overall Strategy

Two Intimin variants were used in this project. The wild-type Intimin (Int_{wt}), where the passenger secretion is complete and the stalled Intimin variant (Int_{sv}) (Oberhettinger et al., 2015) where the introduction of an double HA-tag at position 453 resulted in the formation is an Intimin in a stalled secretion intermediate (Figure 2.1). The aim of this project was to introduce the same set of mutations in both these variants to uncouple the effects of the mutations on passenger secretion in the Int_{wt} background and hairpin formation in the Int_{sv} background. The C-terminus of Int_{wt} is targeted by the polyclonal Intimin antibody and the HA-tag is surface exposed and can be detected by an antibody against the HA-tag, but the C-terminus of the passenger is in the cytoplasm.



3. Materials and Methods

3.1 Genetics

3.1.1 Primers

The primers used in this study, unless stated otherwise, were designed manually and produced by Thermo Fisher Scientific. Appendix 2 gives the list of primer sequences.

3.1.2 Plasmids

An overview of the plasmids used in this study is summarized in Table 3.1. The gene coding for Intimin was re-cloned from pASK-IBA2 Int wt-Strep and pASK-IBA2 Int HA453-Strep (Oberhettinger et al., 2012), individually into pET-22b(+) plasmid for convenient auto-induction of protein expression. The use of pET-22b(+) is described in Section 3.3.1.

Table 3.1: Summary of plasmids used in this project

Name	Purpose	Description	Source
pASK-IBA2 Int wt-Strep	Cloning	<i>eeA</i> gene in XbaI-HindIII sites of pASK-IBA2, Amp ^R	(Oberhettinger et al., 2012)
pASK-IBA2 Int HA453-Strep	Cloning	Intimin+HA453 in XbaI-HindIII sites of pASK-IBA2 with a tandem HA tag after residue 453, Amp ^R	(Oberhettinger et al., 2015)
pET-22b(+)	Vector Control	Expression vector with autoinducible T7 promoter, Amp ^R	Novagen
pET22 Int wt-Strep	Introduce mutatio	<i>eeA</i> gene in XbaI-HindIII sites of pET-22b(+) with pelB leader sequence and C-terminal Strep-tag, Amp ^R	This project
pET22 Int HA453-Strep	Introduce mutations	Intimin+HA453 in XbaI-HindIII sites of pET-22b(+) with pelB leader sequence, a tandem HA tag after residue 453 and a C-terminal Strep-tag, Amp ^R	This project

3.1.3 Polymerase chain reaction (PCR)

PCR is used to amplify a specific region of DNA in a given sample. In this procedure, a PCR reaction mixture containing the template DNA, Primers, DNA polymerase and dNTPs are mixed in a buffer in a small reaction tube. This tube is then placed in a thermal cycler that is programmed to start a series of 20-40 repeated cycles of temperature changes where the DNA template, containing the target region to be amplified, is denatured at high temperature creating ssDNA. The primers, complementary to the target region of the DNA, then anneal to the ssDNA template. The dNTPs present in the PCR mixture provide building blocks for the DNA polymerase to create a new strand of DNA by primer extension. This cycle is repeated several times to generate millions of copies of that specific DNA segment. All polymerases, dNTPs and buffers used in the PCR protocols described below were from NEB.

3.1.3.1 PCR using Q5 polymerase

For introducing mutations and amplifying the DNA, Q5[®] High-Fidelity DNA polymerase was used due to its low error rate and high fidelity of performance. The PCR reactions were aliquoted into PCR tubes and placed in the Biometra Personal Thermocycler (from Analytik Jena) for DNA amplification. Table 3.2 gives the composition of the reaction mixture made per reaction and Table 3.3 shows the steps and corresponding temperatures used in the program.

Table 3.2: PCR reaction mixture

Reagent	Amount (μ l) per reaction tube
5x Q5 Reaction Buffer	10
10mM dNTP mix	1
10ng DNA template	0.5
100 μ M Forward primer	0.5
100 μ M Reverse primer	0.5
Distilled H ₂ O	37
Q5 Polymerase	0.5
Total Volume	50

Table 3.3: Program for PCR using Q5 polymerase

Step	Temperature ($^{\circ}$ C)	Time
Initiation	98	30 sec
Denaturation	98	10 sec
Annealing	60	20 sec
Extension	72	20 sec/kb (Return to step 2, 24x)
Final Elongation	72	10 min
Hold	12	∞

To avoid plasmid carryover of template DNA, PCR products were treated with 1 μ l DpnI and incubated at 37 $^{\circ}$ C for 1 hour. DpnI is a restriction enzyme that digests the methylated, non-

mutated parental DNA template. After DpnI treatment, the PCR product was transformed (section 3.2.4) into *E. coli* TOP10 cells (Section 3.2.1). Plasmid from the transformed colonies was isolated (Section 3.1.8) and the samples were sent in for sequencing to Eurofins Genomics (Section 3.1.9).

3.1.4 Cloning by gibson assembly

Gibson assembly is an isothermal, single-reaction method used for the assembly of more than one overlapping DNA molecules (Gibson et al., 2009). In this method, two overlapping DNA fragments are sealed together in a single step when mixed together with the Gibson Assembly Master Mix (Appendix 3Table 1). The T5 exonuclease in the mix removes nucleotides from the 5' ends of the dsDNA creating 3' overhangs. As these overhangs are complementary, they begin to anneal and the Phusion DNA polymerase starts to add nucleotides extending the fragment. *Taq* DNA ligase then seals the nicks. This assembly technique is a very quick and efficient method used in molecular cloning as it does not require primers containing restriction sites, avoids the steps of cutting off the restriction enzyme post alterations and isolation of the modified DNA. This method proceeds directly to ligation and a circular plasmid containing the gene of interest is formed (Figure 3.1).

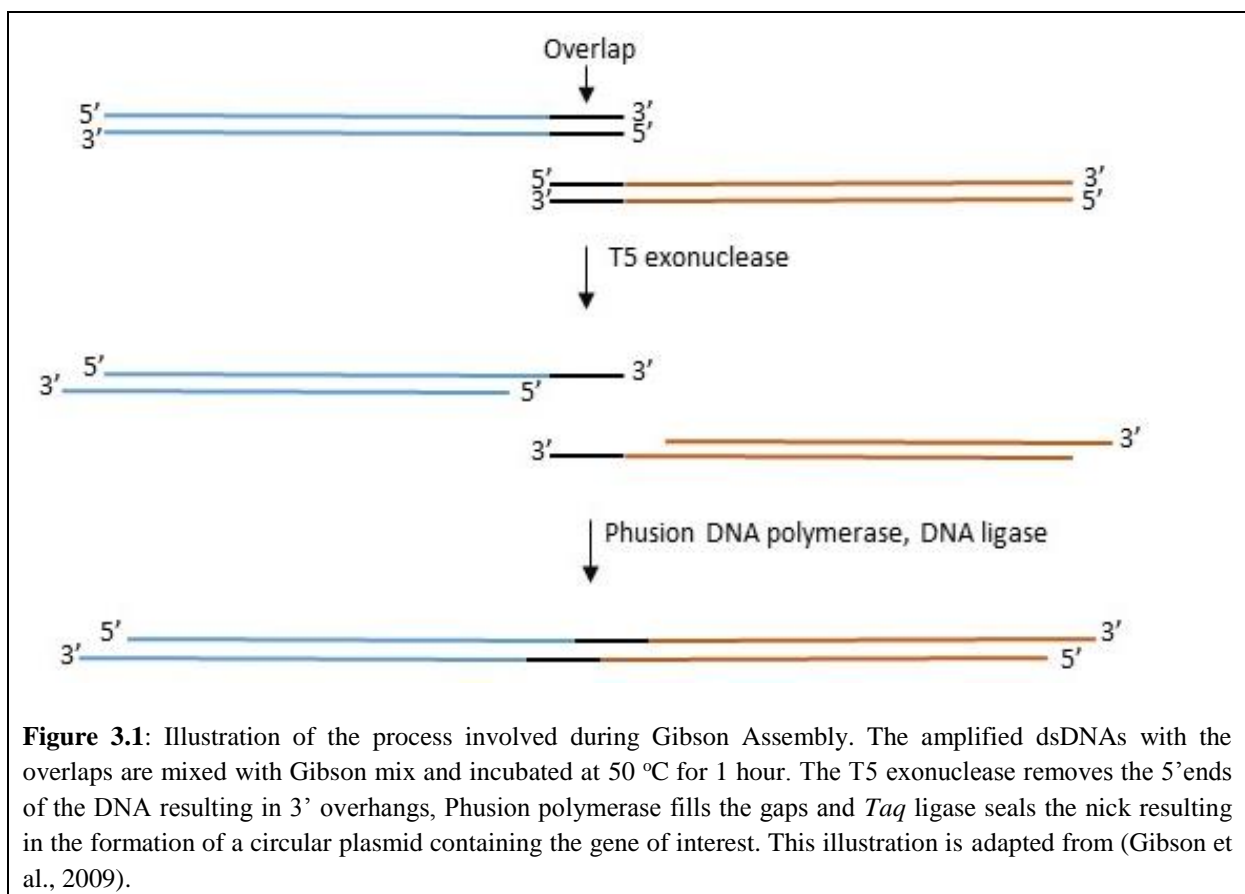


Figure 3.1: Illustration of the process involved during Gibson Assembly. The amplified dsDNAs with the overlaps are mixed with Gibson mix and incubated at 50 °C for 1 hour. The T5 exonuclease removes the 5' ends of the DNA resulting in 3' overhangs, Phusion polymerase fills the gaps and *Taq* ligase seals the nick resulting in the formation of a circular plasmid containing the gene of interest. This illustration is adapted from (Gibson et al., 2009).

In order to re-clone the coding sequence of *eeA* from pASK-IBA2 Int wt-Strep and pASK-IBA2 Int HA453-Strep individually into the pET-22b (+) plasmid, primers with overlapping ends complementary to the insert from the pASK-IBA2 and to the pET-22b (+) plasmid were used to amplify the DNA segments by PCR. After amplification, the PCR products were DpnI treated at 37 °C for 1 hour and then run in agarose gel electrophoresis (Section 3.1.6). The correct bands were cut out of the gel and purified using the Monarch[®] DNA Extraction Kit by NEB. After purification, DNA concentration was measured based on absorbance at 260 nm using the Eppendorf Biophotometer[®]. In a 1.5 ml Eppendorf tube, 200 ng of insert for 100 ng of vector was added and equal volume of 2x Gibson mix (Appendix 3, Table 1) was added. The reactions were prepared on ice. Once the reaction was assembled, it was incubated at 50 °C for 1 hour and then transformed (Section 3.2.4) into chemically competent *E. coli* TOP10 cells. Colony PCR was performed to verify the presence of insert in the pET-22b (+) vector. The list of primers used for PCR is given in Table 3.4.

Table 3.4: A summary of the primers used of amplification of insert and vector.

Constructs that were amplified	Primers for amplification
pASK-IBA2 Intimin	pelB-Int F, pET22-Strep R
pASK-IBA2 Intimin+HA453	pelB-Int F, pET22-Strep R
pET-22b(+)	pET22rec F, pET22rec R

3.1.5 Colony PCR

After cloning, colony PCR was performed to confirm for the presence of insert. As the error rate of the DNA polymerase used in colony PCR is trivial, Taq DNA polymerase is used. Table 3.5 gives the PCR mixture prepared per reaction and Table 3.6 gives the program used for this protocol. After preparation of the reaction mixture, some bacteria from a transformed colony was picked up using a small pipette tip and streaked onto a selection plate. The tip was then dipped into a PCR tube containing the reaction mixture. The PCR tubes were then placed in the Biometra Personal Thermocycler (from Analytik Jena) for DNA amplification. The selection plate was left for incubation and grown overnight.

Table 3.5: PCR mixture

Reagent	Amount (µl) per reaction tube
50x 10mM dNTP mix	0.4
10x Taq Reaction Buffer	2
100 µM Forward primer	0.2
100 µM Reverse primer	0.2
Distilled H ₂ O	17
Taq Polymerase	0.2
Total Volume	20

Table 3.6: Program for Colony PCR

Step	Temperature (°C)	Time
Initiation	94	3 minutes
Denaturation	94	30 sec
Annealing	50	30 sec
Extension	72	1 min/kb (Return to step 2, 24x)
Final Elongation	72	5 min
Hold	12	∞

3.1.6 Agarose gel electrophoresis for DNA separation

To verify the sizes of the PCR products, 1% agarose gels made with agarose (Sigma), 1x TAE buffer and GelGreen® Nucleic Acid Stain for DNA staining were used (Appendix 3, Table 2). The electrophoresis was run using 1x TAE buffer. The DNA samples were mixed with 6x DNA sample buffer (Appendix 3, Table 2) and loaded on to the 1% agarose gels. Quick load 1 kb DNA ladder from NEB were used. The gels were run using VWR 250 V power source at constant voltage of 100 V for approximately 30 to 40 minutes.

3.1.7 Site-directed mutagenesis by PCR

PCR was used to introduce point and deletion mutations into the pET22 Int wt-strep and pET22 Int HA453-Strep (Liu and Naismith, 2008). Primers containing the desired mutations were designed manually (Appendix 2). About 5 µl of PCR product was mixed with 1 µl of 6x DNA sample buffer (Appendix 3, Table 2) and then run in an agarose gel to verify the sizes of the product. Once the sizes were verified, the PCR product was mixed with 1 µl of DpnI and incubated at 37 °C to digest methylated DNA. After DpnI digestion, 8 µl of the digested sample was transformed into *E. coli* TOP10 cells (Section 3.2.1) and grown for about 16 hours overnight at 37 °C. The colony was then inoculated in LB media (Section 3.2.2) and grown overnight for about 16 hours at 37 °C. Plasmid was then isolated from culture (Section 3.1.8) and the samples were sent for sequencing (Section 3.1.9) to verify presence of the mutation. After verification, the plasmids were then transformed into *E. coli* BL21 ΔF cells (Section 3.2.4).

3.1.8 Plasmid extraction

The plasmid miniprep kit used for plasmid extraction was QIAprep® Spin Miniprep Kit from QIAGEN. The protocol was followed as per the manufacturer's instructions.

3.1.9 Sequencing

To verify re-cloning of *eaeA* into pET-22b(+) plasmid and to verify insertion of desired mutations into the pET22 Intimin-Strep and pET22 Intimin+HA453-Strep plasmids, 100 ng of these plasmids extracted and 5 μ M of the sequencing primers in a total volume of 10 μ l was sent to Eurofins Genomics. Eurofins Genomics uses the LighRun™ sequencing services which is based on Sanger sequencing (Sanger and Coulson, 1975) to provide the sequence of the plasmid. Once the sequencing results were given, the ApE program (Davis, 2012) was used for analyzing the sequences.

3.2 Microbiology

3.2.1 Bacterial strains

The bacterial strains used in this project were *E.coli* TOP10 (LifeTechnologies™) for cloning and BL21 Δ F (Meuskens et al., 2017) for expression (Table 3.7). The TOP10 strain is optimized for cloning experiments, BL21 Δ F was optimized for overexpression of Intimin and the EPEC strain was optimized for adhesion assays.

3.2.2 Media and growth conditions for bacterial strains

The liquid media for growth of all *E.coli* TOP10 strains used in this project was Lysogeny Broth (LB) (Bertani, 1951) and the cultures were grown at 37 °C. BL21 Δ F strain requires low salt LB, which is essentially the same as LB instead contains low amount of salt in the media, and grows well at 30°C (Meuskens et al., 2017). See Table 3 of Appendix 3 for composition of LB and low salt LB medium. For growth of the bacterial strains on agar plates, LB agar with the corresponding antibiotic was used (Table 3.7).

Table 3.7: An overview of the strains, the media, antibiotics, temperature requirements and purpose of usage

Strains	Media	Antibiotic	Temperature(°C)	Purpose
E.coli TOP10	LB	Ampicillin	37	Cloning
E.coli BL21 Δ F	Low salt LB	Ampicillin	30	Expression
EPEC E2348/69 Δ <i>eaeA</i>	RPMI 1640 with 10 % Fetal calf serum, 1 % L-glutamine	None	37	Adhesion

3.2.3 Antibiotics

The stock concentration and working concentration of the antibiotics used for selection in the culture growth medium is given in Table 3.8.

Table 3.8: Antibiotics used in this project

Antibiotic	Stock Concentration(mg/ml)	Working Concentration ($\mu\text{g/ml}$)	Company
Ampicillin	100	100	AppliChem

3.2.4 Transformation of chemically competent *E. coli* cells

3.2.4.1 Transformation using CaCl_2 competent cells

E. coli BL21 ΔF and TOP10 cells were made chemically competent first by preparing overnight cultures in 5 ml low salt LB and incubating them at 30 °C and 37 °C, respectively. The overnight cultures were diluted in a 1:100 ratio into 100 ml fresh media and incubated at 30 °C/37 °C until the bacteria reached the mid-log phase of growth, i.e. Optical Density₆₀₀ (OD_{600}) = 0.3 - 0.5. The cells were collected by centrifugation at 6,500 x g for 10 minutes in VWR Micro Star 17R tabletop centrifuge. The cells were resuspended in 1/4 of the original volume of ice-cold 0.1 M CaCl_2 , i.e. 25 ml, and incubated on ice for 30 minutes or longer. During this time the tabletop centrifuge was cooled to 4°C. The cells were pelleted again as above and resuspended in 1/25 of original volume of ice-cold 0.1 M CaCl_2 (Merck), i.e. 4 ml. An equal volume (4 ml) of ice-cold 60% glycerol (VWR AnalaR NORMAPUR) was added and mixed well. 200 μl aliquots were made of these competent cells in 1.5 ml Eppendorf tubes. At this stage the cells could be used directly. Tubes to be used later were flash frozen in liquid nitrogen and stored at – 80 °C (Dagert and Ehrlich, 1979).

For transformation, about 10 ng of the plasmid was added to 100 μl of thawed competent BL21 ΔF cells or TOP10 cells and incubated on ice for 30 minutes or more. The mixture was subjected to heat shock for 45 seconds at 42 °C and left on ice for 2 minutes before plating on LB agar with ampicillin. The plate was incubated overnight at 30 °C or 37 °C depending on the strain used (Section 3.2.1).

3.2.4.2 Transformation using Transformation and storage solution (TSS) competent cells

An alternative, quick and easy, one-step method was also used for preparing competent cells (Chung et al., 1989). In this protocol, an overnight culture of the bacteria were prepared and diluted 1:100 the next until the bacteria reached the mid-log phase, i.e. OD_{600} = 0.3 - 0.5. The cells were then cooled down by placing on ice and pelleted at 6,500 x g for 10 minutes at 4°C in the Beckman Coulter Allegra X-30R centrifuge. The pellet was resuspended in 1/10 of original volume of ice-cold TSS buffer (Appendix 3, Table 5). About 100 μl aliquots were made and either used directly or stored at – 80 °C. For transformation, the same process is followed as described in Section 3.2.4.1.

3.3 Expression and assembly of Intimin mutants

3.3.1 Overexpression of Intimin by auto-induction

For protein production, auto-induction was employed. The media used for auto-induction is the ZYP-5052 (William Studier, 2005) (Appendix 3, Table 6). The name ZYP-5052 was designated by Studier as Z stands for 1% N-Z-amine, Y stands for 0.5 % yeast extract and P stands for the salts composition in ZYP medium and 5052 is 0.5% glycerol, 0.05 % glucose, and 0.2 % lactose (as in ZYP-5052). The plasmid pET-22b(+) contains a T7 promoter that is indirectly activated by lactose provided in the media. First, glucose is utilized by the bacteria as a primary source of carbon avoiding the immediate breakdown and usage of lactose. This allows the cells to grow up to a high level of density before overexpressing Intimin. Once the level of glucose depletes, glycerol and lactose are utilized. Lactose then induces expression of the T7 RNA polymerase on the bacterial chromosome which in turn activates the T7 promoter on the pET-22b(+) plasmid. This activation of the T7 promoter results in the expression of the gene encoding the target protein, in this case Intimin.

E.coli BL21 Δ F strains containing the pET-22b(+) plasmid and *eaeA* variants were first grown to the mid-log phase in low salt LB media at 30 °C and then diluted 1:200 in the ZYP-5052 auto-induction media and grown overnight for about 16 hours at 30 °C. The cells were collected the next day to carry out protein extractions or perform experiments. This method is simple to perform and often yields higher protein content compared to using synthetic inducers like isopropylthiogalactoside.

3.3.2 Outer membrane protein (OMP) isolation

E.coli BL21 Δ F were grown overnight in 200 ml auto-induction medium (Section 3.3.1) at 30°C. Cells corresponding to 200 ml at an $OD_{600} = 1.0$ were collected and resuspended in 10 ml of 10 mM HEPES (Sigma) pH 7.4. After resuspension, $MgCl_2$ (Merc) and $MnCl_2$ (Sigma) were added to 1 mM, lysozyme from chicken egg white (BioChemica BC) to 0.1 mg/ml, Dnase I from bovine pancreas (Sigma) to 10 μ g/ml. The cells were lysed (3 passes) using Heilscher - Ultrasound Technology UP400S sonicator at 50% cycle duty and more than 60 % amplitude. The samples were then centrifuges for 10 min at 4000 x g to remove cell debris. The supernatant was collected in a polycarbonate 29 x 104 mm centrifuge tube (Beckman Coulter®) and the membranes were pelleted by using an Avanti J-26S XP centrifuge (Beckman Coulter) at 22 000 x g for 45 minutes. The pellet was resuspended in 2 ml of 10 mM HEPES pH 7.4 and 2 ml of 2 % N-lauroyl Sarcosine (Sigma) was added to solubilize IMs and incubated at Room Temperature (RT) for 30 minutes with shaking. After incubation, the mixture was centrifuged as before for 45 minutes to pellet the OM. The OM pellet was washed with 1 ml 10 mM HEPES pH 7.4 and centrifuged again as above for 10 minutes. The OM pellet was resuspended again in 1 ml 10 mM HEPES.

3.3.3 Heat modifiability assays

About 60 μ l of the isolated OM suspension was mixed with 20 μ l of 4 x SDS-PAGE sample buffer (Appendix 3, Table 7) half of the OM pellet samples were denatured by heating at 95°C for 10 minutes and the other half of the sample was left at RT for 10 minutes. Samples were then loaded onto an SDS-PAGE gel for analysis (Section 3.4). SDS-PAGE and Western Blotting (Section 3.5) were performed on the OM pellet fractions to analyze heat-modifiability of the protein. A change in migration behavior between the denatured and unheated samples was interpreted as a shift (Oberhettinger et al., 2015).

3.3.4 Membrane integration assays by urea extraction

The remaining OM suspension was centrifuged with the same conditions as above for 10 minutes and resuspended in 1 ml urea extraction buffer (Appendix 3, Table 8). The samples were incubated at 37 °C for 1 hour with shaking. Post incubation, the samples were ultracentrifuged at 170,000 x *g* at 22°C using a Beckman Coulter Optima™ MAX Ultracentrifuge. The entire supernatant (1 ml) was mixed with 4 x SDS-PAGE sample buffer and the pellet was resuspended in 1ml 10 mM HEPES pH 7.4 and mixed with 333 μ l of 4 x SDS-PAGE sample buffer. SDS-PAGE (Section 3.4) and Western Blotting (Section 3.5) were performed on the urea-extracted fractions to analyze membrane insertion of the protein (Oberhettinger et al., 2015).

3.4 SDS-Polyacrylamide gel electrophoresis

Pre-made polyacrylamide gels were used for the separation of OM proteins according to size. The gels were Novex™ WedgeWell™ 4-20 % Tris-Glycine Gel provided by Thermo Fisher Scientific. The protein ladder used was PageRuler Prestained NIR Protein Ladder by Thermo Scientific. Except for heat modifiability assays, all samples were denatured prior to loading by heating for 10 minutes at 95 °C. About 5 μ l of the samples were loaded on to the SDS-PAGE gels and run using 1 x SDS-PAGE running buffer at 225V for 40 to 60 minutes. To avoid overheating particularly during the heat modifiability experiments, the runs were performed in an ice bath.

3.5 Western blotting

After SDS-PAGE electrophoresis, proteins were transferred to a Nitrocellulose Blotting Membrane (Amersham™ Protran™ Supported 0.45 μ m NC, GE Healthcare Life science). Six filter papers and one nitrocellulose (NC) membrane were cut according to the size of the SDS-PAGE gel and soaked in transfer buffer (composition in Appendix 3, Table 9) for 4 to 5

minutes. The transfer sandwich, 3 filter papers - NC membrane - SDS-PAGE gel - 3 filter papers, were stacked on TE70X semi-dry transfer unit and air bubbles were removed. The transfer was run for 55 minutes at 60 mA, a maximum voltage of 30 V for 1 gel and for 55 min at 100 mA, 30V for transfer of 2 gels. After transfer, the membrane was blocked with 10 ml of 2 % skimmed milk powder (Fluka) in 1 x PBS (Appendix 3, Table 9) for 1 hour at RT. The membrane was then probed with purified IgG fraction of polyclonal rabbit anti-EaeA (1:5,000) (Oberhettinger et al., 2015) in blocking buffer (Appendix 3, Table 9) and incubated for 1 hour at RT on shaker. The blot was then washed three times in PBST (Appendix 3, Table 9) for 5 to 10 minutes each wash. The blot was incubated with secondary anti-rabbit antibody (1:10,000) in 2 % skimmed milk powder for 1 hour at RT, following which the membrane was washed three times with PBST. The blots were viewed using the Odyssey® CLx Infrared Imaging System and analyzed using the Image Studio Software.

3.6 Immunofluorescence microscopy

For immunofluorescence staining, cultures were auto-induced (Section 3.3.1) in 5 ml ZYP-5052 (Appendix 3, Table 6) auto-induction medium and grown overnight. About 2×10^7 cells in 1 ml PBS were collected, by measuring OD₆₀₀, on polyethyleneimine-coated 10mm coverslips in a polystyrene 24 well microtitre plate by centrifugation at 4000 x g for 5 min. The coverslips were washed with PBS to remove cells that did not stick to the coverslip. The cells were then fixed with 200 µl of 4 % paraformaldehyde in PBS for 30 min. After fixing, the cells were washed and blocked with 1 % Bovine Serum Albumin (BSA) (from VWR chemicals) in PBS at RT for 1 hour. The primary antibodies rabbit anti-EaeA (1:200) and HA probe-rabbit antibody (1:100) in 1 % BSA were added and incubated for 1 hour at RT. The coverslips were washed again three times with PBST following which the CF488A Goat anti-rabbit antibody (1:200) in 1 % BSA was added and incubated in the dark for 2 hours at RT. The coverslips were then mounted on a glass slide with 10 µl of Biotium's EverBrite™ Mounting Medium with DAPI and sealed around the perimeter with Biotium's CoverGrip™ Coverslip Sealant. The samples were imaged using an UPlanFLN 100x/1.3 oil immersion on an Olympus Fluoview FV1000 Inverted Confocal Microscope. The blue channel (DAPI) was imaged first and then the green channel (CF488A).

3.7 Whole-cell ELISAs

For quantitative analysis of Intimin expression, whole-cell Enzyme Linked Immunosorbent Assays (ELISAs) were performed. Cultures were autoinduced by growing them overnight in 5 ml of ZYP-5052 medium. Bacteria were diluted to an OD₆₀₀ of 0.2 in PBS and 100 µl of cells were added to wells of a polystyrene microtitre plate. The plate was left for 1 hour at RT allowing the bacteria to adhere to the surface of the well. The cells were washed three times with 200 µl PBS + 0.1 % BSA (Appendix 3, Table 10) and blocked for 1 hour at RT with 2 % BSA in PBS (Appendix 3, Table 10). The primary antibodies were rabbit anti-EaeA (1:1000)

for Intimin variants in the wild-type background and anti-HA tag rabbit antibody (1:2000) (Santa Cruz Biotechnology) for stalled Intimin variants diluted in 2 % BSA and 100 μ l of these solutions were added to the wells and incubated for 1 hour at RT. After incubation, the wells were washed three times with 0.1% BSA in PBS and the secondary antibody anti-rabbit-HRP (from Agrisera) diluted 1:2000 in 2 % BSA in PBS was added and incubated at RT for 1 hour. The wells were washed again three times as above and the samples were detected using the colorimetric HRP substrate ABTS (ThermoScientific) as per the manufacturer's instructions. The reactions were stopped with 1 % SDS once color had developed and the absorbance was measured at 410 nm using the Biotek SynergyTM H1 microplate reader with Gen5 software.

3.8 Statistics

Statistical analysis was performed using Microsoft Excel employing ANOVA and t-test in order to look for statistical significance between the mutant proteins and the control background.

3.9 Bioinformatics

To check for conservation of the regions of mutations within β -barrels of IATs, sequence analysis was performed using the programs of the online Max Planck Institute for Developmental Biology bioinformatics toolkit. The domain sequence for Intimin β -barrel was submitted to position-specific iterated BLAST (Altschul and Koonin, 1998) search against the nr_bac70 database with 5 iterations. The resulting sequences were then aligned using Kalign (Lassmann and Sonnhammer, 2005). The alignment was then viewed using the alignment viewer provided by the programs and manually edited in order to show the sequences of the mutations next to each other.

3.10 Adhesion assays with pre-infected HeLa cells

About 1.5×10^5 HeLa cells per well were seeded onto a 24-well plate with 10 mm hydrolytic glass coverslips and grown overnight at 37 °C, 5 % CO₂ in GibcoTM RPMI 1640 Medium (PAA, Pasching, Austria) supplemented with 10 % fetal calf serum (FCS), 1 % L-glutamine and 1 % penicillin/streptomycin (Pen/Strep; Gibco, Darmstadt, Germany). Overnight cultures of EPEC $\Delta eaeA$ strain and *E. coli* BL21 ΔF strains producing the Intimin in the wild-type and stalled-variant background were grown in 8 ml liver medium with respective growth conditions (Table 3.7). Eight ml of liver medium was inoculated with the overnight cultures at a starting OD₆₀₀ of 0.1 and incubated for 2 hours at 30°C (BL21 ΔF) or 37 °C (EPEC $\Delta eaeA$). After 2 hours of incubation, the BL21 ΔF strains were induced with 0.5 mM IPTG and

incubated for 4 hours at 27°C. On the other hand, the EPEC $\Delta eaeA$ cells were washed twice with prewarmed 1 x Dulbecco's Phosphate-Buffered Saline (DPBS) (Gibco) and incubated again for 1 hour at 37 °C, 5 % CO₂ in the RPMI 1640 Medium without Pen/Strep. After incubation, the EPEC $\Delta eaeA$ cells were harvested by centrifugation at 4000 x g for 5 min and washed once with 1 x DPBS. The bacteria were resuspended in half the original culture volume of PBS and 3×10^7 bacteria, collected by measuring the OD₆₀₀, per well were used to preinfect the HeLa cells at an MOI (Multiplicity of Infection) of 100. The medium and bacteria were mixed well and bacteria were brought into close contact with the cells by centrifugation at 300 x g for 2 min. The plate was then incubated for 1 hour at 37 °C, 5 % CO₂. After preinfection, the plate was washed with prewarmed 1 x DPBS four times and the remaining adherent bacteria were killed by incubating the plate in RPMI medium supplemented with gentamicin for 1 hour. After incubation, the plate was washed until no bacteria were left adhering to the HeLa cells and then incubated with RPMI media without antibiotics until the BL21 ΔF strains were ready for adhesion experiments. The induced bacteria were harvested, washed and resuspended in half the original culture volume, as done before for the EPEC strain. The HeLa cells were then infected with the BL21 ΔF strains corresponding to 3×10^7 bacteria per well at an MOI of 100. The medium and bacteria were mixed and bacteria were brought into close contact with the cells by centrifugation at 300 x g for 2 min. The infected cells were incubated for 1 hour at 37 °C, 5 % CO₂. The cells were washed with PBS until the non-adherent control strain showed no adhesion of bacteria to cells based on light microscopy. The PBS was removed and the cells were fixed with 4% PFA (Paraformaldehyde) in PBS and fixed either overnight at 4°C or 1 hour at RT (Oberhettinger et al., 2015).

After fixation, the cells were washed once with PBS and the coverslips with samples were stained with 10 μ l of Fuchsin stain for approximately 30 seconds. The coverslips were then washed with PBS and sterile water and left to air-dry. Once the coverslips dried, they were mounted onto glass slides with the mounting medium Roti®-Histokitt. The slides were then viewed under the Olympus Light microscope at 60 x magnification in oil immersion and the images were taken using the Cell[^]B software. Processing of the image was done using IrfanView.

3.11 Plasmid stability

Few strains with the mutated Intimin that showed major effects on hairpin formation and passenger secretion were tested for stability of the plasmid. In this test, a serial dilution, from 10⁻¹ to 10⁻⁵, of the control and the mutants were performed. Ten μ l of dilutions 10⁻³, 10⁻⁴ and 10⁻⁵ were plated onto selection plates LA low salt + Ampicillin and LA low salt. The plates were then grown overnight for about 16 hours at 37 °C. The plates were then examined for viable count.

4. Results

4.1 Designing mutations in the β -barrel of Intimin

Based on the available crystal of the β -barrel of Intimin (Fairman et al., 2012b), all mutations were designed to disrupt important interactions between residues in the α -helical turn located on the periplasmic side of the β -barrel, the linker and interacting residues in the lumen of the β -barrel and the small β -sheet present on the extracellular side of the β -barrel. The effects of these mutations were analyzed in both the Int_{wt} and Int_{sv} background (Figure 2.1). The name designated to the mutations is based on: the single-letter code (SLC) of the mutated amino acid followed by its position in the sequence and then the SLC of the new amino acid in its position. The mutations were introduced by PCR (Section 3.1.3). The list of primers used to introduce the mutations is shown in Table 4.1 and the primer sequences are listed in Appendix 2.

4.1.1 Mutations in the α -helical turn on the periplasmic side of the β -barrel

Five mutations were introduced in the α -helical turn present on the periplasmic side of the β -barrel of Intimin (Figure 4.1). The mutations are D298A, I382D, P421A, L430A and $\Delta\alpha$ -helix. In mutation D298A, the hydroxyl group present on Aspartic acid at position 298 forms a hydrogen bond with the main chain amino group of leucine located at position 430. Mutating aspartic acid to alanine would disrupt this hydrogen bond formation. In mutation I382D, isoleucine 382 is involved in a hydrophobic interaction with another isoleucine residue situated at position 419. Introducing a charged amino acid like aspartic acid would disrupt this hydrophobic interaction. In mutation P421A, proline at position 421 forms a kink in the α -helical turn. Replacing proline with alanine would disrupt the kink making it less flexible. In mutation L430A, side chain of leucine 430 is involved in a hydrophobic interaction with the side chain of phenylalanine located at position 266. The idea is to disrupt the hydrophobic interaction by replacing leucine with alanine that has a shorter side chain. In mutation Δ 412-430GS, the α -helical turn is entirely replaced with alternating residues of glycine and serine of the same length. This replacement would make the α -helical turn more flexible more flexible.

4.1.2 Mutations in the linker connecting the β -barrel to the passenger and interacting residues facing the lumen of the β -barrel

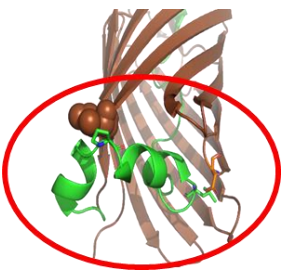
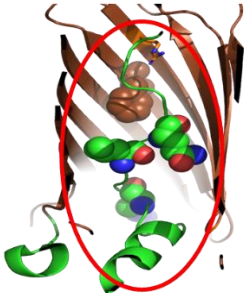
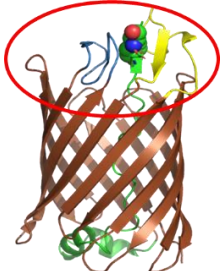
Similarly, six mutations were introduced in the linker connecting the β -barrel to the passenger and interacting residues facing the lumen of the β -barrel (Figure 4.2). The mutations are F277A, R288A, R434A, L437A, Q439A and Δ linker. In mutation F277A, the side chain of

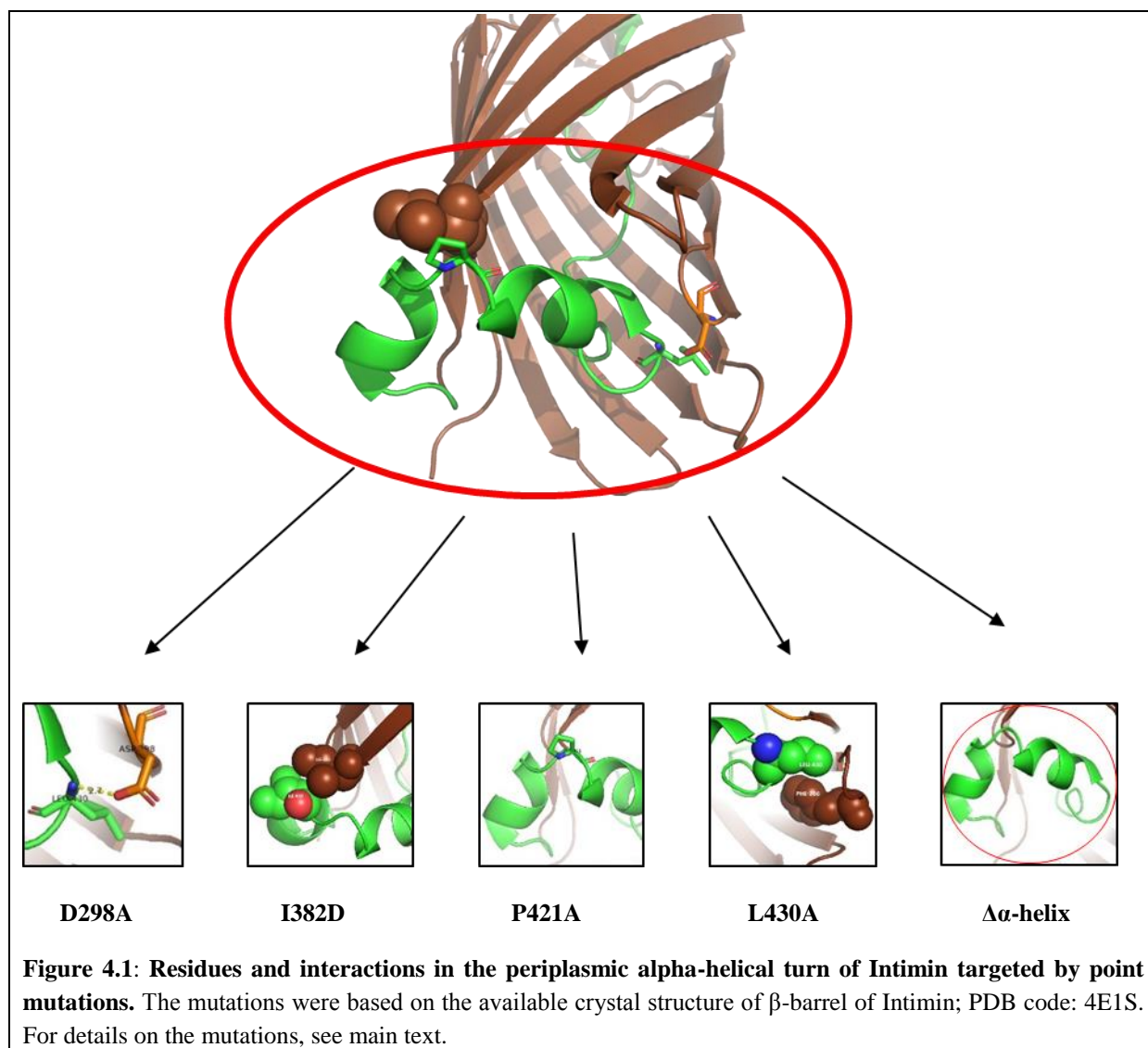
phenylalanine is involved in a hydrophobic interaction with the side chain of valine located at position 438. Replacing phenylalanine with the alanine containing a shorter side chain disrupts the hydrophobic interaction. In mutation R288A, the amino group on the side chain of arginine at position 288 forms a hydrogen bond with the hydroxyl group on the main chain of asparagine located at position 441. Replacing arginine with alanine would disrupt the interaction. In mutation R434A, the amino group on the side chain of arginine forms a hydrogen bond with the hydroxyl group on the main chain of glutamine located at position 236. Replacing arginine with alanine would disrupt the hydrogen bond interaction. In mutation L437A, the side chain of leucine is involved in a hydrophobic interaction with the side chain of glutamine and the side chain of asparagine located at positions 214 and 229 respectively. Replacing leucine with the alanine containing a shorter side chain would disrupt the hydrophobic interaction. In mutation Q439A, the side chain of glutamine is involved in a hydrophobic interaction with the side chain of arginine located at position 333. Shorter side chain containing alanine would disrupt this interaction. In mutation Δ linker, the entire linker is deleted and replaced with alternating residues of glycine and serine of the same length making it more flexible.

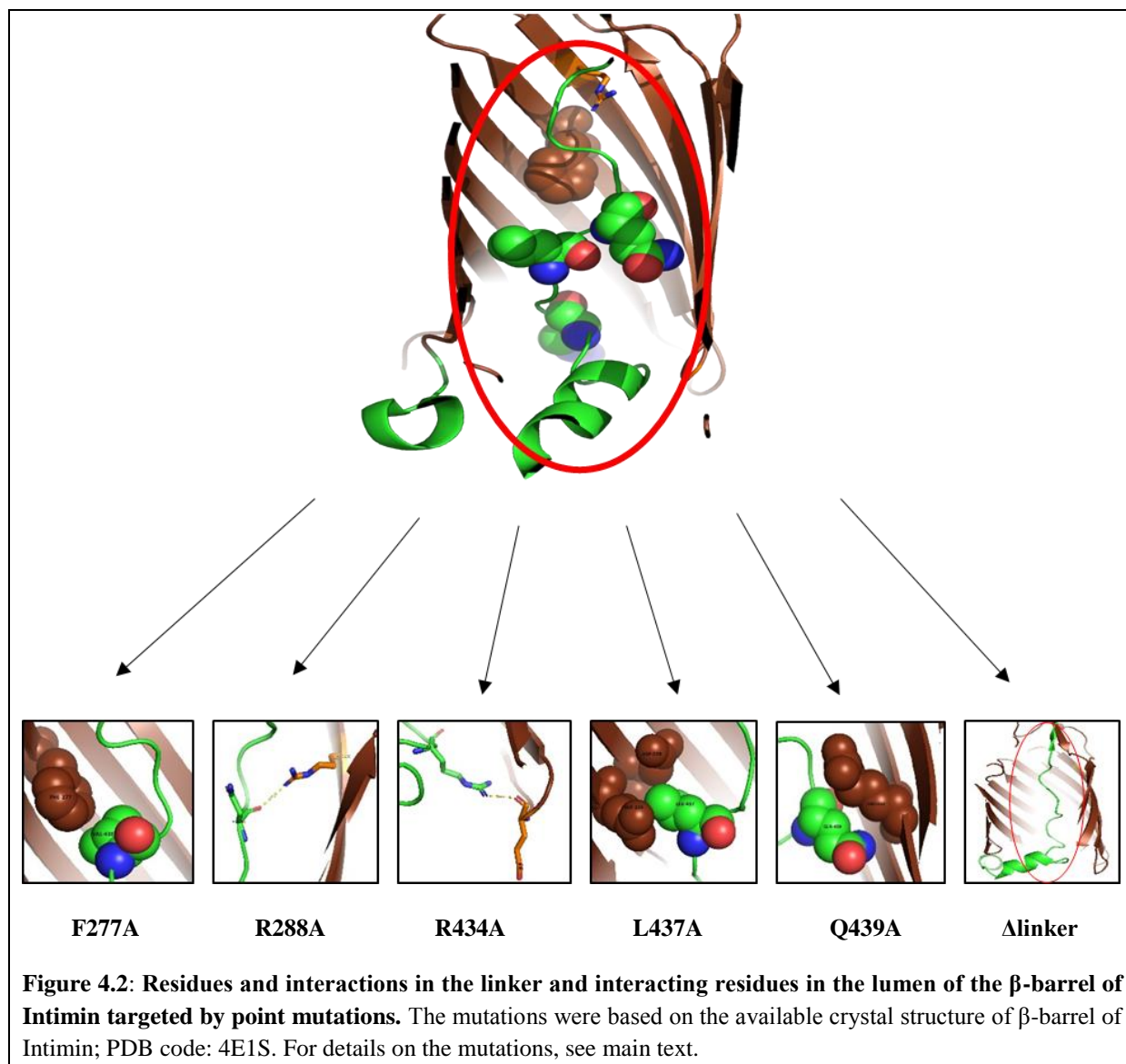
4.1.3 Mutations in the small β -sheet formed between the linker and two loops of the β -barrel on the extracellular surface

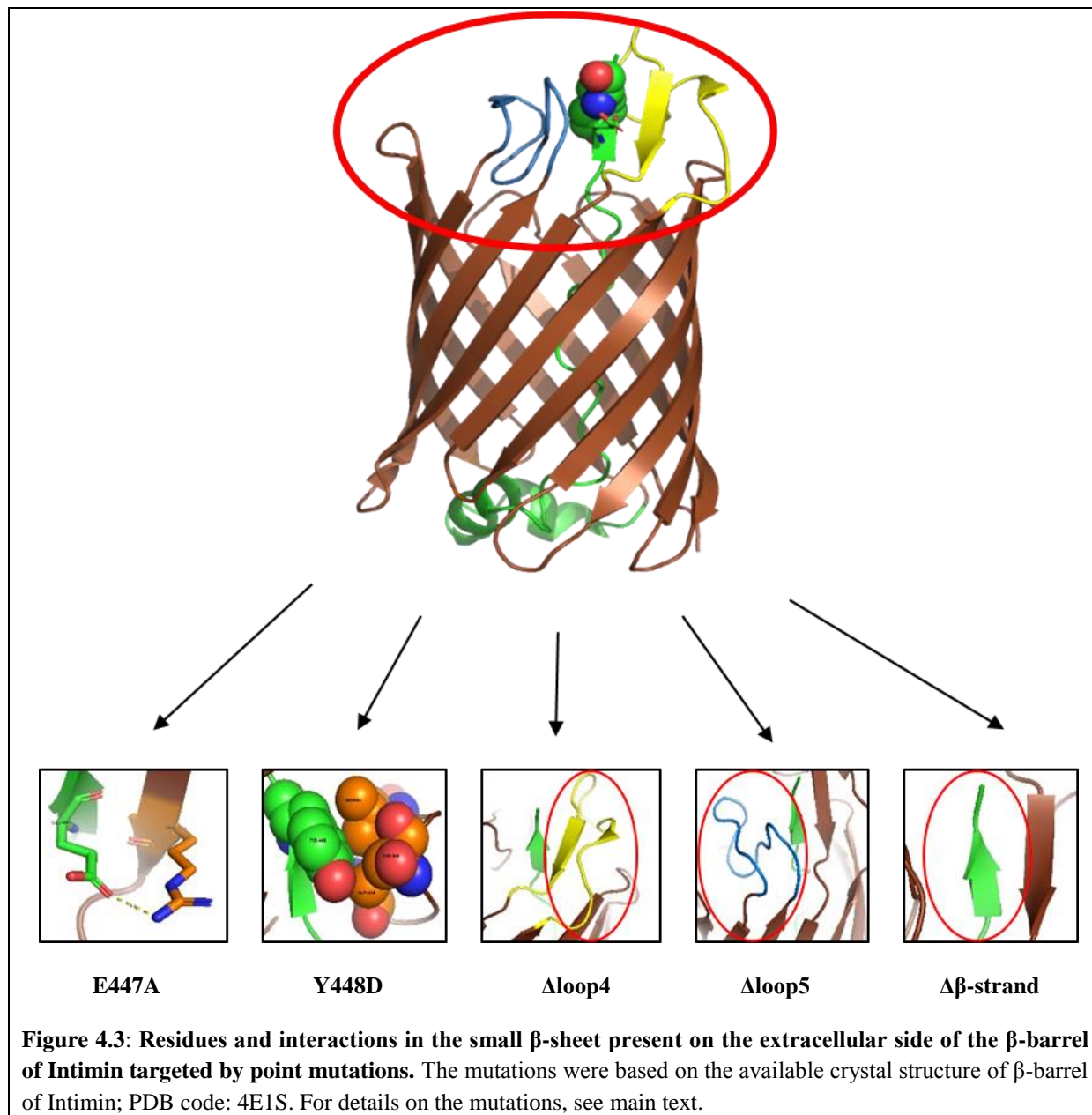
Five mutations were introduced small β -sheet formed between the linker and two loops of the β -barrel on the extracellular surface (Figure 4.3). The mutations are E447A, Y448D, Δ loop4, Δ loop5 and $\Delta\beta$ -strand. In mutation E447A, the hydroxyl group on the side chain of glutamic acid forms a hydrogen bond with an amino group on the side chain of arginine located at position 325. Replacing glutamic acid with alanine will disrupt this interaction as alanine contains only a methyl group as its side chain. In mutation Y448D, the side chain of tyrosine at position 448 is involved in a hydrophobic interaction with the side chains of alanine, serine and leucine located at positions 359, 363 and 366 respectively. Replacing tyrosine with a charged amino acid like glutamine will disrupt the hydrophobic interaction. In mutation Δ loop4, residues from arginine 309 to alanine 327 (shown in yellow) are deleted and replaced with 4 residues of Glycine. The idea is to replace the loop formed on the extracellular space of the β -barrel with a short segment to analyze the effect on the mechanism of inverse autotransport. In mutation Δ loop5, residues from tyrosine 354 to asparagine 369 (shown in blue) are deleted and replaced with 4 residues of glycine. Replacing loop 5 with a shorter segment of glycine may have an effect on the inverse autotransport mechanism. In mutation $\Delta\beta$ -strand, residues from leucine 446 to lysine 449 (shown in green) that form the β -strand on the C-terminus of the linker are deleted and replaced with 4 residues of glycine. This mutation is made to understand the role of this β -strand during the inverse autotransport process.

Table 4.1: Mutations introduced in the α -helical turn on the periplasmic side of the β -barrel, the linker and interacting residues in the lumen of the β -barrel and the small β -sheet on the extracellular side of the β -barrel of Intimin. For description of the mutations see main text.

Region of Mutation	Mutations	Primer
	D298A	IntD298A Fwd; IntD298A Rev
	I382D	IntI382D Fwd; IntI382D Rev
	P421A	IntP421A Fwd; IntP421A Rev
	L430A	IntL430A Fwd; IntL430A Rev
	$\Delta\alpha$ -helix	Int Δ 412-430GS Fwd; Int Δ 412-430GS Rev
	F277A	IntF277A Fwd; IntF277A Rev
	R288A	IntR288A Fwd; IntR288A Rev
	R434A	IntR434A Fwd; IntR434A Rev
	L437A	IntL437A Fwd; IntL437A Rev
	Q439A	IntQ439A Fwd; IntQ439A Rev
	Δ linker	Int Δ linkerGS Fwd; Int Δ linkerGS Rev
	E447A	IntE447A Fwd; IntE447A Rev
	Y448D	IntY448A Fwd; IntY448A Rev
	Δ loop4	IntR309-A327GGGG Fwd; IntR309-A327GGGG Rev
	Δ loop5	IntY354-N369GGGG Fwd; IntY354-N369GGGG Rev
	$\Delta\beta$ -strand	IntL446-K449GGGG Fwd; IntL446-K449GGGG Rev







4.2 Conserved regions within the β -barrels of IATs

To check for conservations between residues targeted for mutagenesis, β -barrel regions of IATs were aligned using the Max Planck Institute for Developmental Biology Bioinformatics toolkit (Section 3.9). All residues targeted for mutations are conserved (Figure 4.4 and Figure 4.6) except for glutamine at position 439 of Intimin (Figure 4.5). The equivalent residue of glutamine (dashed box) in β -barrel of other IATs is either aspartic acid or glutamine (Figure 4.6).

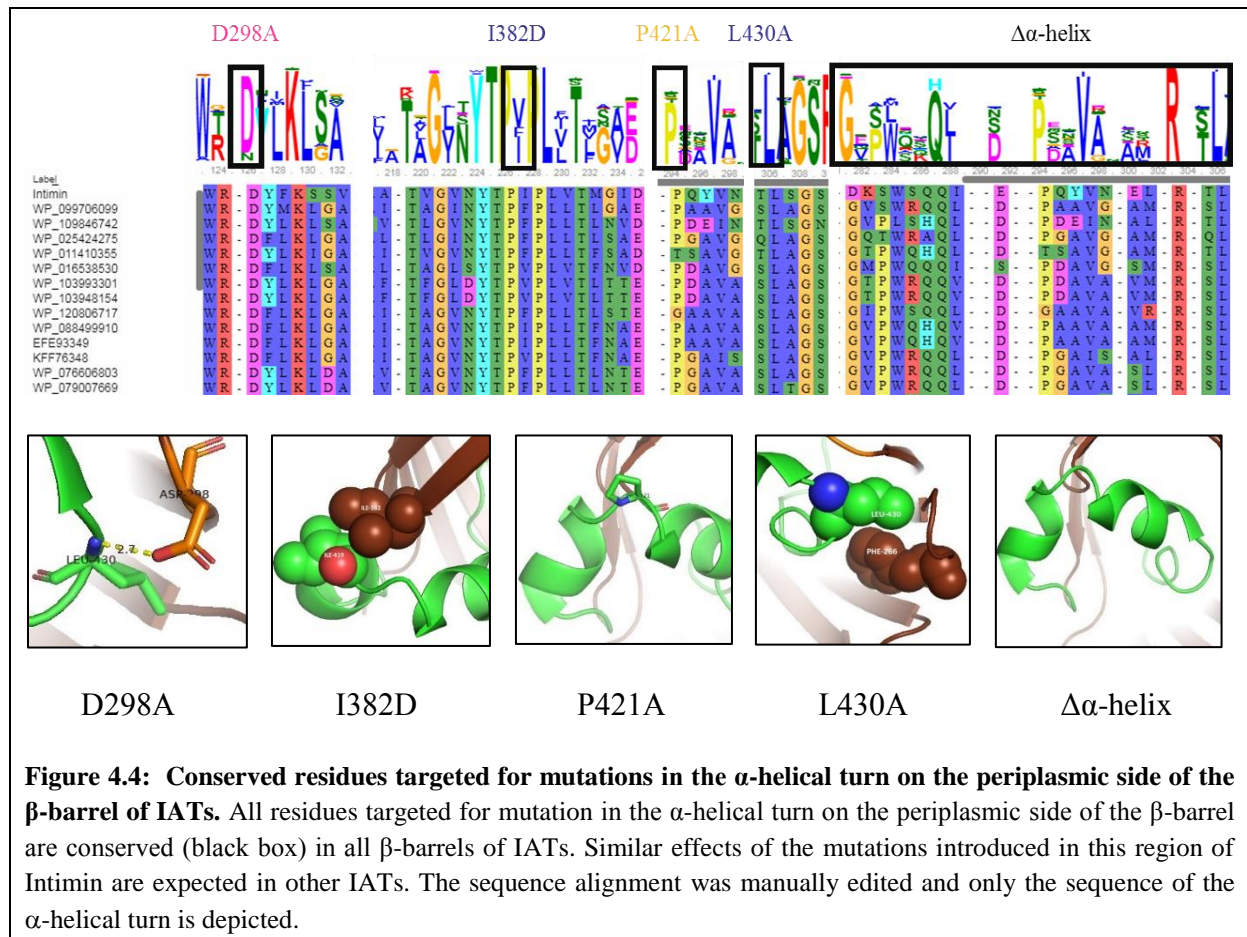


Figure 4.4: Conserved residues targeted for mutations in the α -helical turn on the periplasmic side of the β -barrel of IATs. All residues targeted for mutation in the α -helical turn on the periplasmic side of the β -barrel are conserved (black box) in all β -barrels of IATs. Similar effects of the mutations introduced in this region of Intimin are expected in other IATs. The sequence alignment was manually edited and only the sequence of the α -helical turn is depicted.

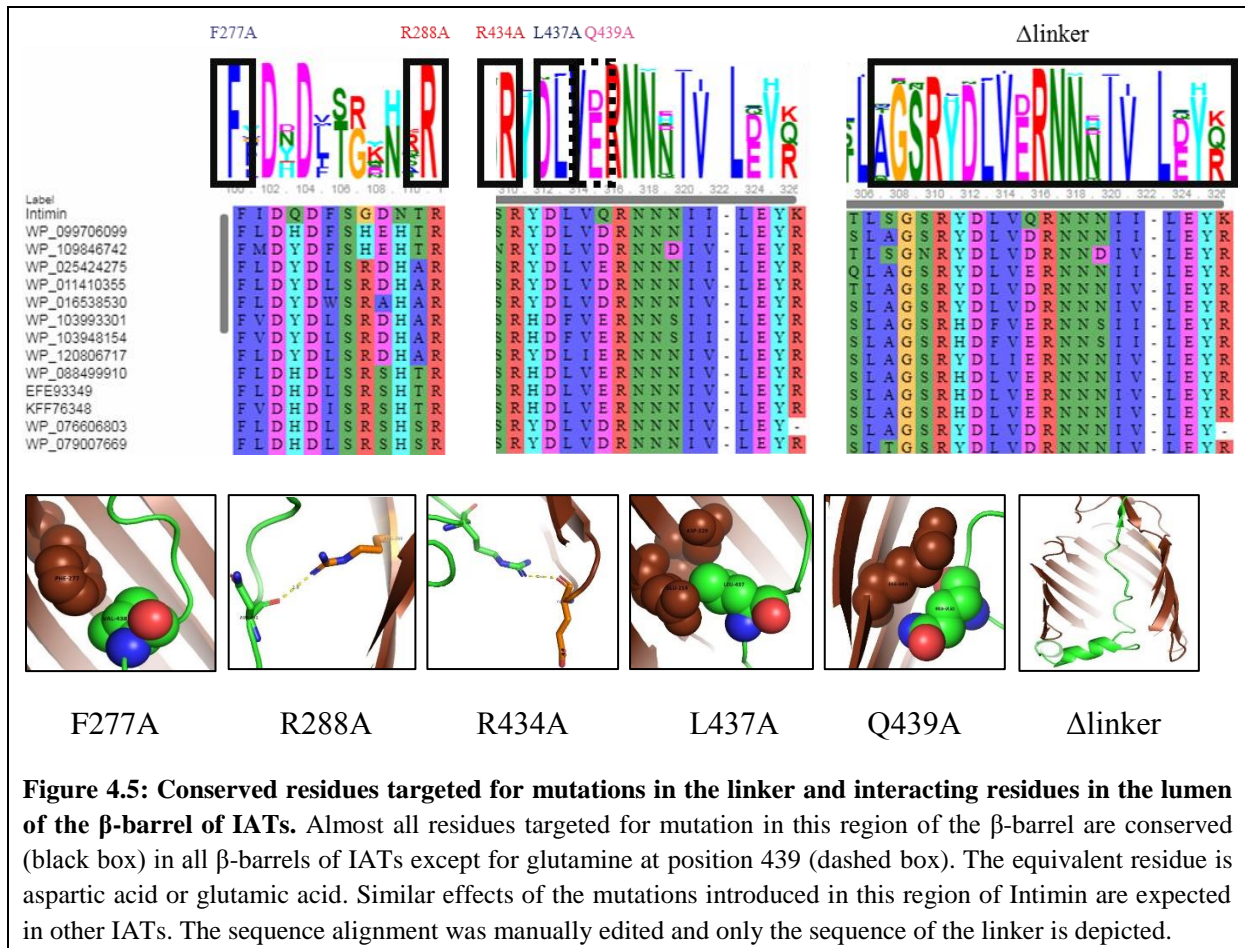
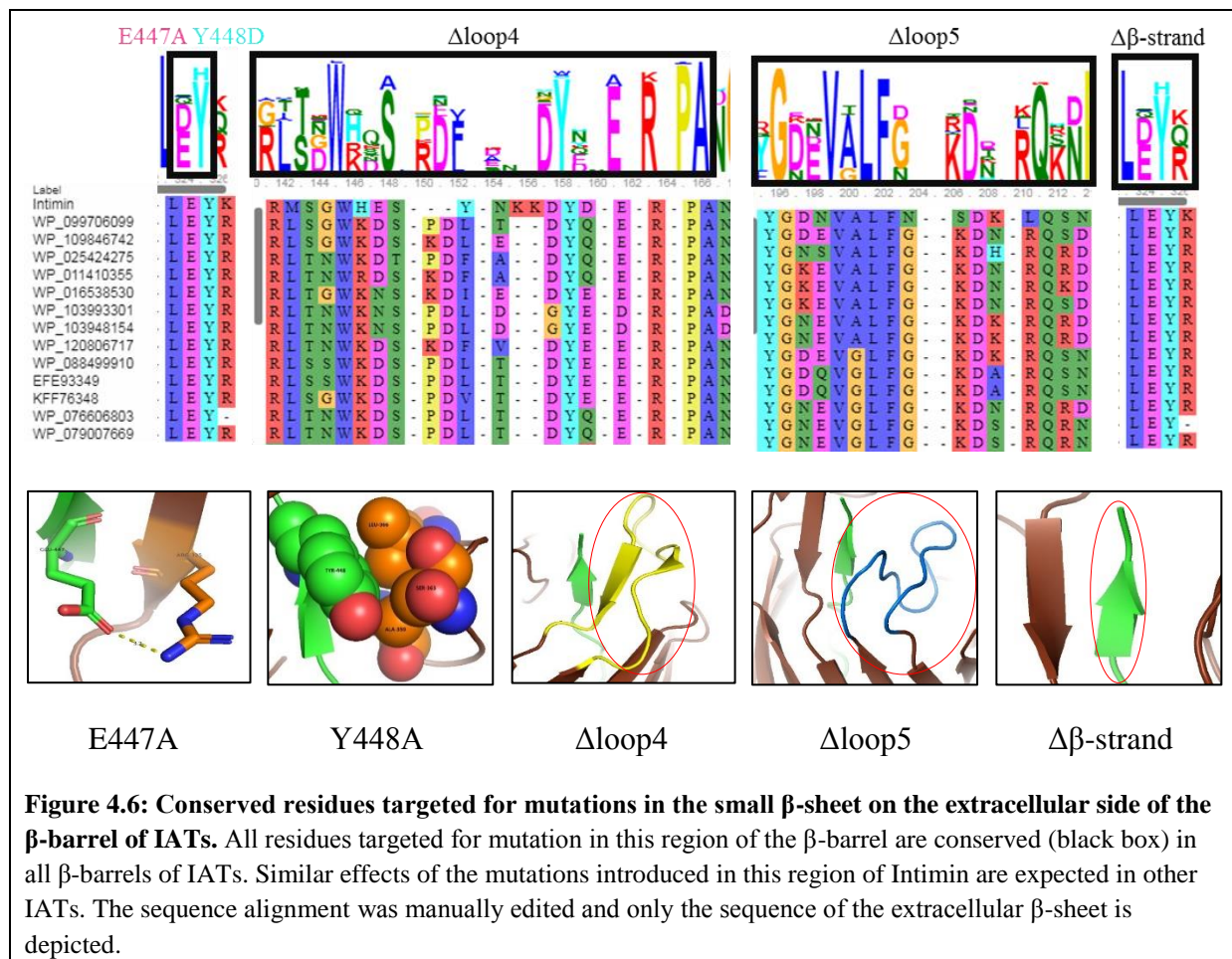


Figure 4.5: Conserved residues targeted for mutations in the linker and interacting residues in the lumen of the β -barrel of IATs. Almost all residues targeted for mutation in this region of the β -barrel are conserved (black box) in all β -barrels of IATs except for glutamine at position 439 (dashed box). The equivalent residue is aspartic acid or glutamic acid. Similar effects of the mutations introduced in this region of Intimin are expected in other IATs. The sequence alignment was manually edited and only the sequence of the linker is depicted.



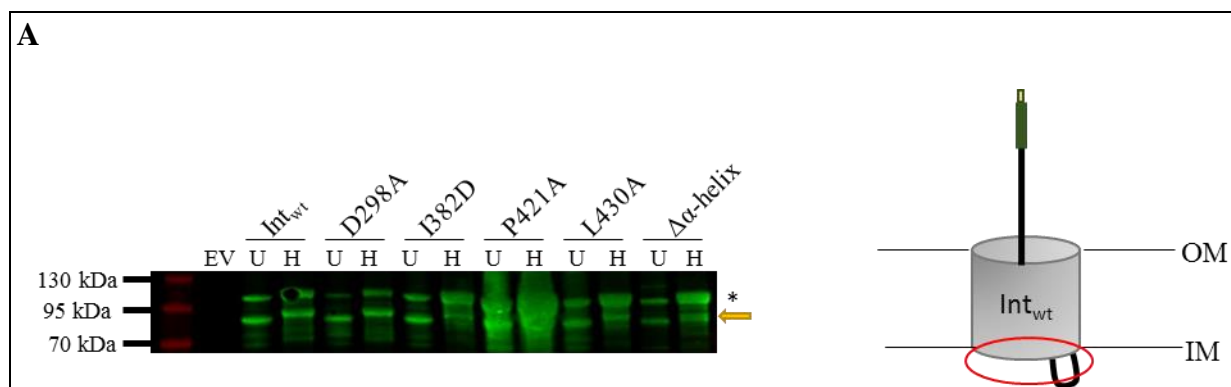
4.3 Expression and assembly of Intimin mutants

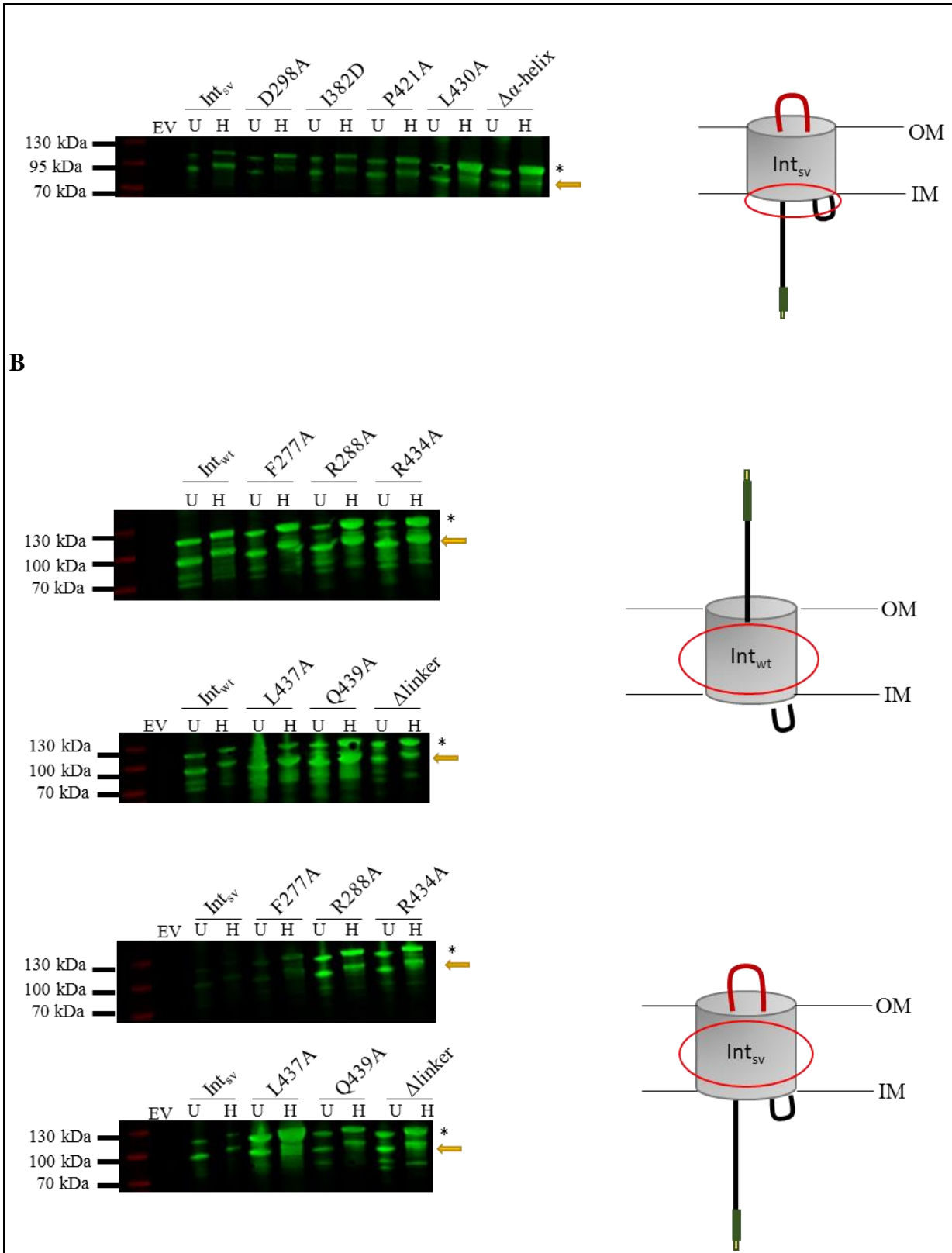
The gene sequence that codes for Int_{wt} and Int_{sv} was cloned into the expression vector pET-22b(+). Mutations were introduced in the two variants using site directed mutagenesis by PCR. The sequence of the PCR products, containing the desired mutation, were verified by sequencing and transformed into *E. coli* BL21 ΔF cells. The cells were then inoculated into autoinduction media for overexpression of Intimin. The samples were then analyzed for interpreting the effects of mutations on Intimin.

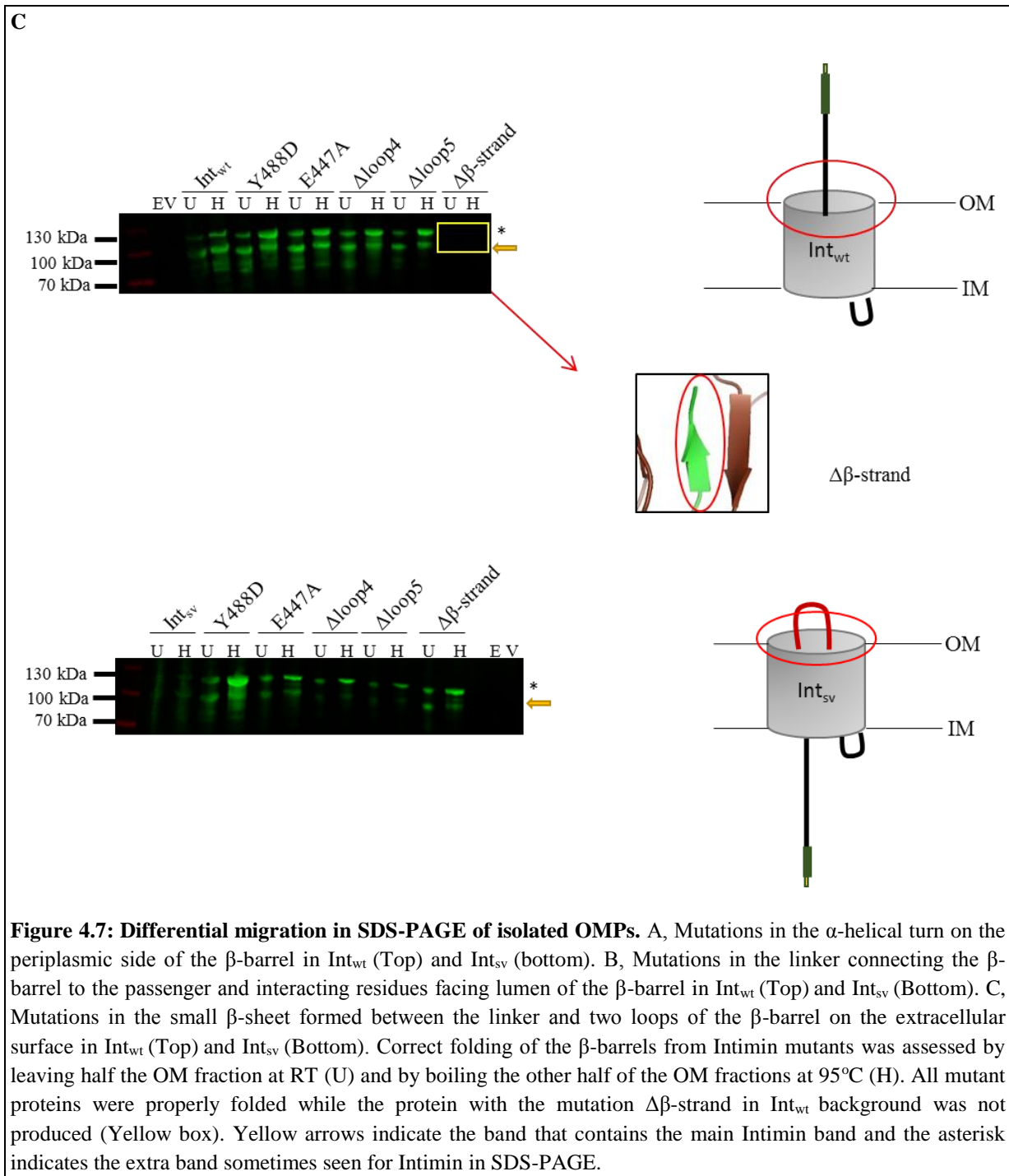
4.3.1 Heat modifiability assays

Heat modifiability assays were done as a preliminary test to assess if the Intimin mutants were localized in the OM and properly folded. Normally, β-barrel proteins unfold upon denaturation i.e., when boiled at 95°C. Proteins that are not denatured travel faster in SDS-PAGE, thereby migrating at an apparently lower molecular weight than the denatured sample. This appears as a shift between the two bands. This unique property of β-barrel proteins helps in interpreting whether they are folded. The proteins were produced in *E. coli* and the OM fractions were isolated. Half of the OM pellet fractions were boiled and the other half was left at RT for 10 minutes. The samples were then loaded onto the gel and heat shifts for almost all variants were observed (Figure 4.7) at the expected size of Intimin (~94 kDa). This implied that the proteins were properly folded. However, no band was observed for the Δβ-strand mutation in either the Int_{wt} or Int_{sv} background (Figure 4.7 C, yellow box). This indicated that Intimin was not produced at all when the β-strand present on the C-terminus of the linker was deleted.

Often, an additional band in Intimin is observed at ~115 kDa (indicated by an asterisk in Figure 4.8) for reasons that are not clear (Heinz et al., 2016; Leo et al., 2016; Oberhettinger et al., 2015). This band was modified by heat.

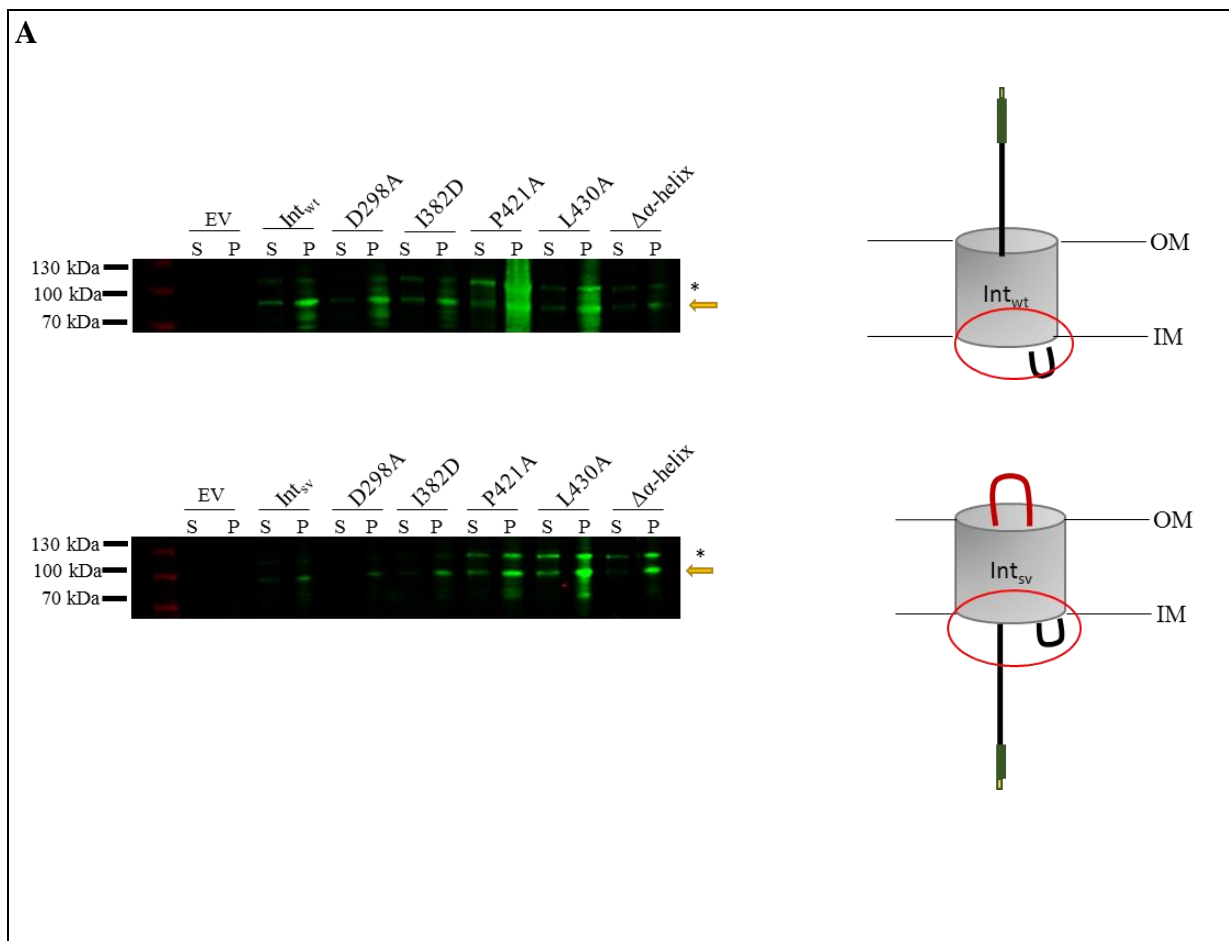


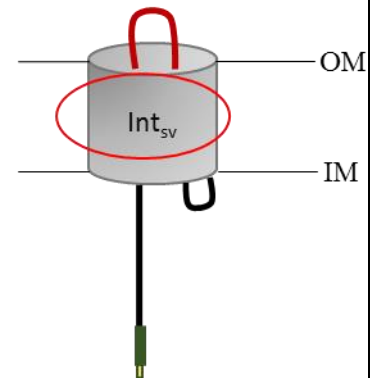
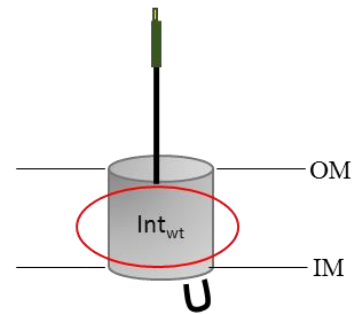
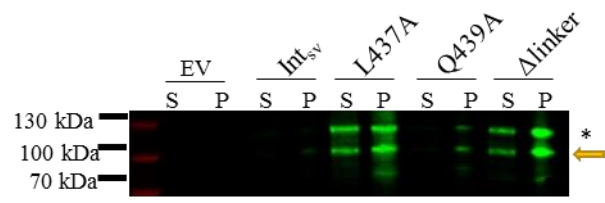
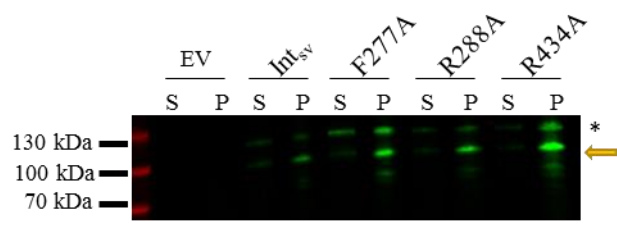
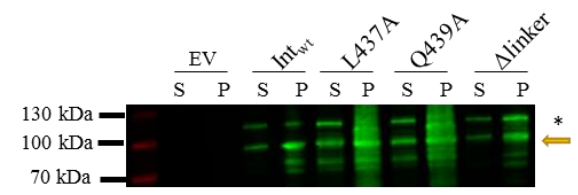
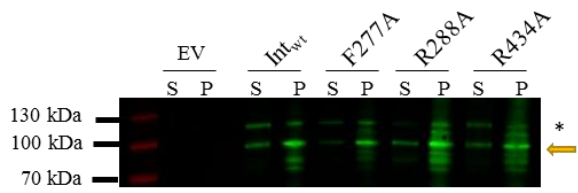
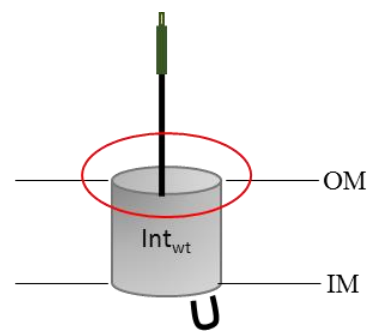
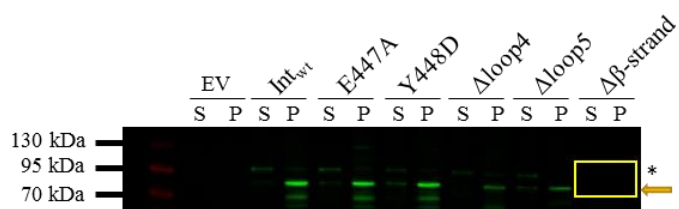


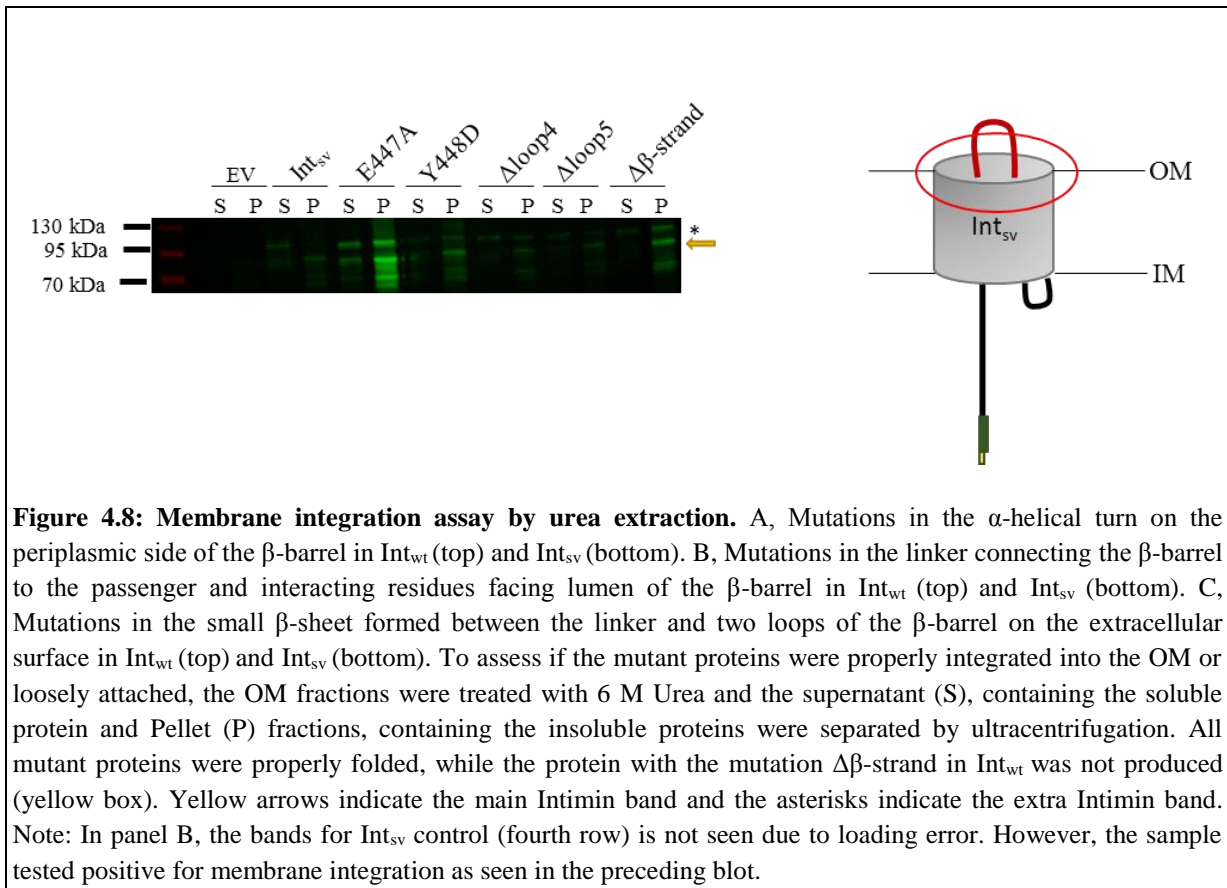


4.3.2 Membrane integration assays

Urea has the ability to destabilize folded proteins. However, proteins that are properly integrated into the OM resist extraction into the supernatant when treated with 6 M urea. In order to assess if the Intimin mutants were properly integrated into the OM or loosely attached by weak hydrophobic interactions, the OM pellet fractions were extracted with 6 M urea (described in detail in material and methods Section 3.3.3) and the pellet, containing the fully integrated protein, and the supernatant, containing the loosely attached proteins, were separated and analyzed by SDS-PAGE and subsequent Western blotting. The pellet fraction showed the presence of Intimin for almost all mutants of Int_{wt} and Int_{sv} except $\Delta\beta$ -strand of the Int_{wt} background (Figure 4.8). This indicated that the proteins were properly integrated in to the OM. Similarly to the heat modifiability assays, the mutation $\Delta\beta$ -strand in the Int_{wt} background did not show any Intimin bands (Figure 4.8 C, Yellow box) which indicated that the protein was not produced. It has been observed before that a small fraction of the protein is found in the supernatant. This may be due to conditions used to overexpress Intimin (Leo et al., 2016; Oberhettinger et al., 2015). However, in all cases where the protein was produced, most of the protein was in the pellet, demonstrating that all Intimin variants were fully integrated into the OM.

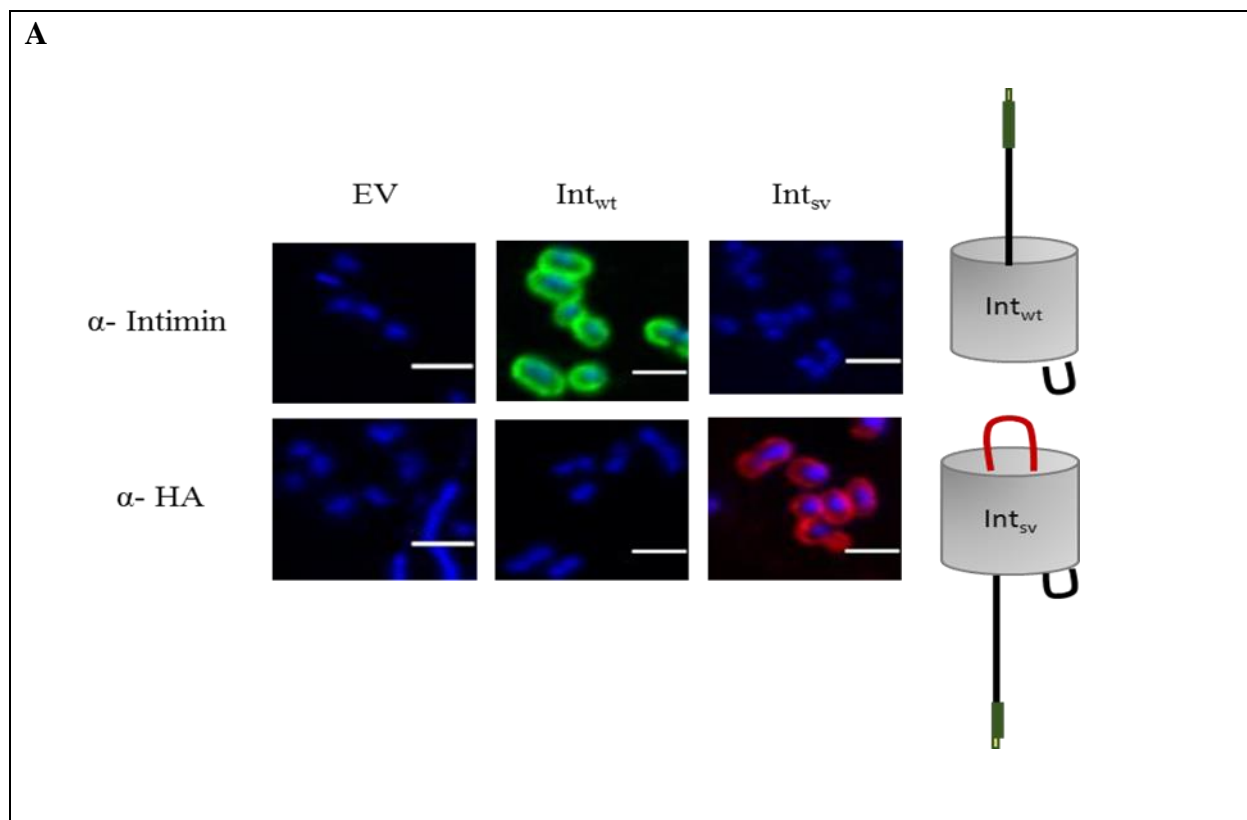


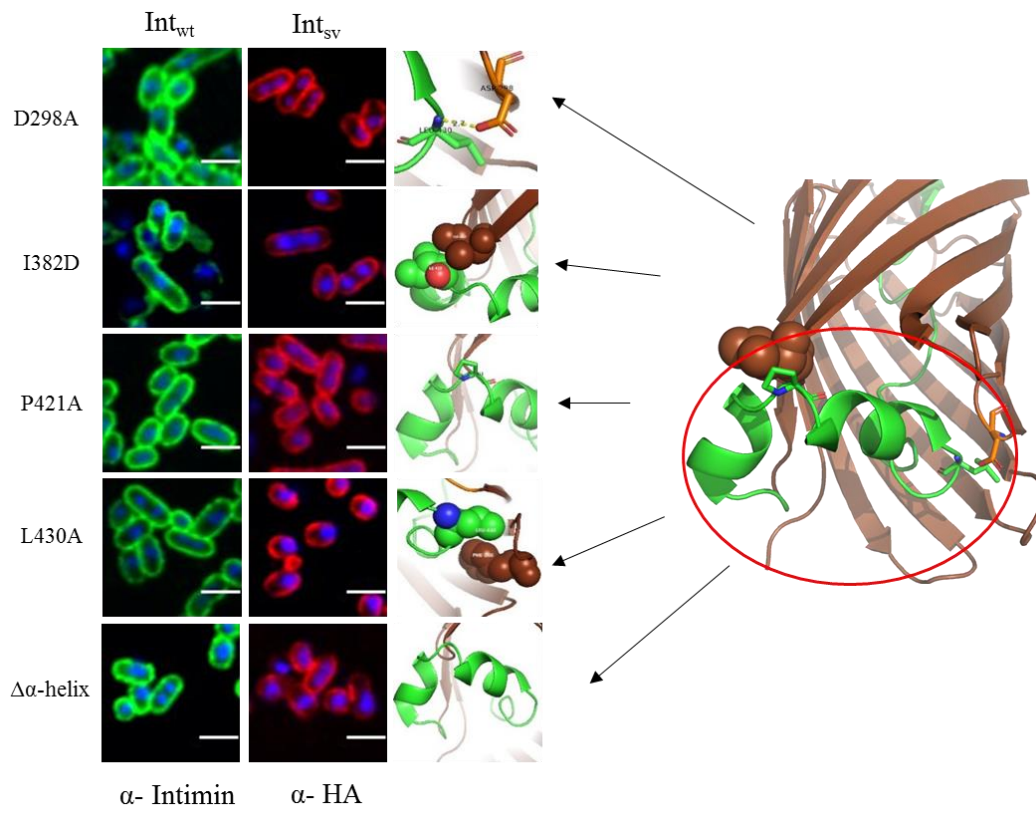
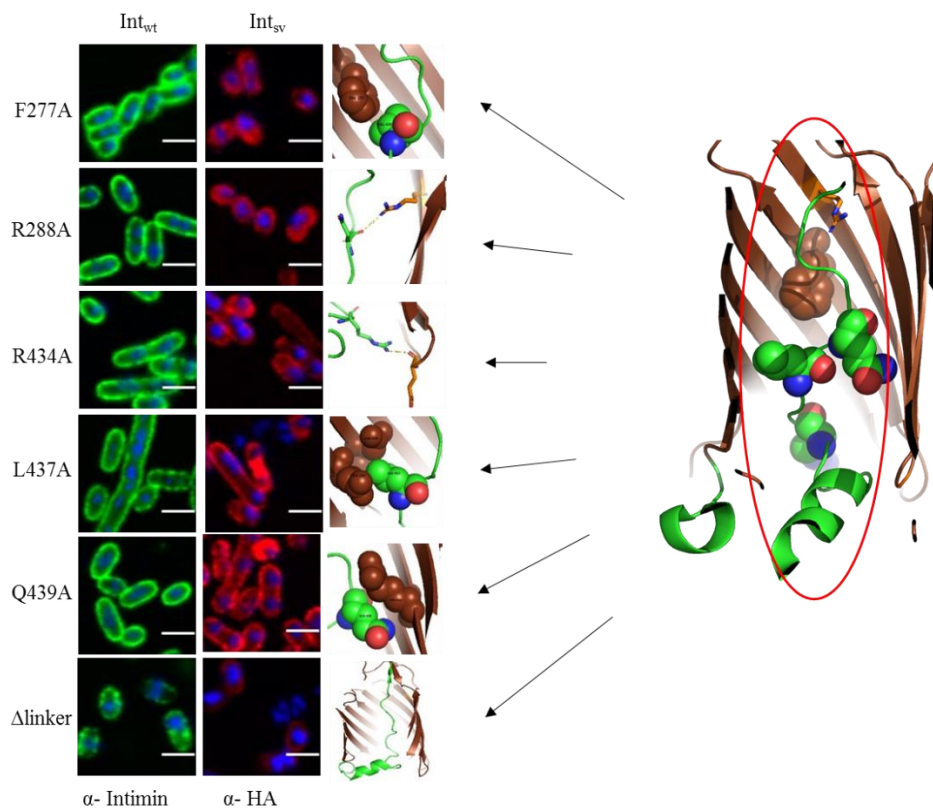
B**C**



4.4 Immunofluorescence microscopy

Immunofluorescence microscopy was performed as a qualitative analysis to assess if the passenger in the Int_{wt} mutant proteins and the hairpin, containing the surface exposed HA-tag (Oberhettinger et al., 2015) in the Int_{sv} mutant proteins, were surface exposed. The passenger of almost all Int_{wt} mutant proteins were surface exposed (Figure 4.10), which is seen as a 'halo' on the bacterial surface when probed with the α -intimin antibody (directed against C-terminus of Intimin). Not surprisingly, the mutation $\Delta\beta$ -strand in the Int_{wt} showed no surface exposure (Figure 4.9 D) when detected with the α -Intimin antibody. The HA tag of majority of the Int_{sv} mutant proteins were surface exposed (Figure 4.9) when α -HA antibody was used and was seen as a halo on the bacterial surface. This demonstrates that the hairpin was formed (Oberhettinger et al., 2015). The $\Delta\beta$ -strand showed no surface exposure in the Int_{sv} background indicating the hairpin was not surface exposed. Since the $\Delta\beta$ -strand mutation did not produce Intimin, as seen in the Western blots of the heat modifiability assays and urea extraction (Figure 4.7 and Figure 4.8 respectively), it was expected that there would be no surface display of the passenger or the hairpin for this variant. Interestingly, Y448D showed surface exposure of the hairpin in the Int_{sv} background although the passenger in the Int_{wt} background was surface exposed. The Δ linker mutation in the Int_{wt} and Int_{sv} background showed mixed populations, where the passenger and hairpin was surface exposed for not all but few bacteria (Supplementary Figure 1).



B**C**

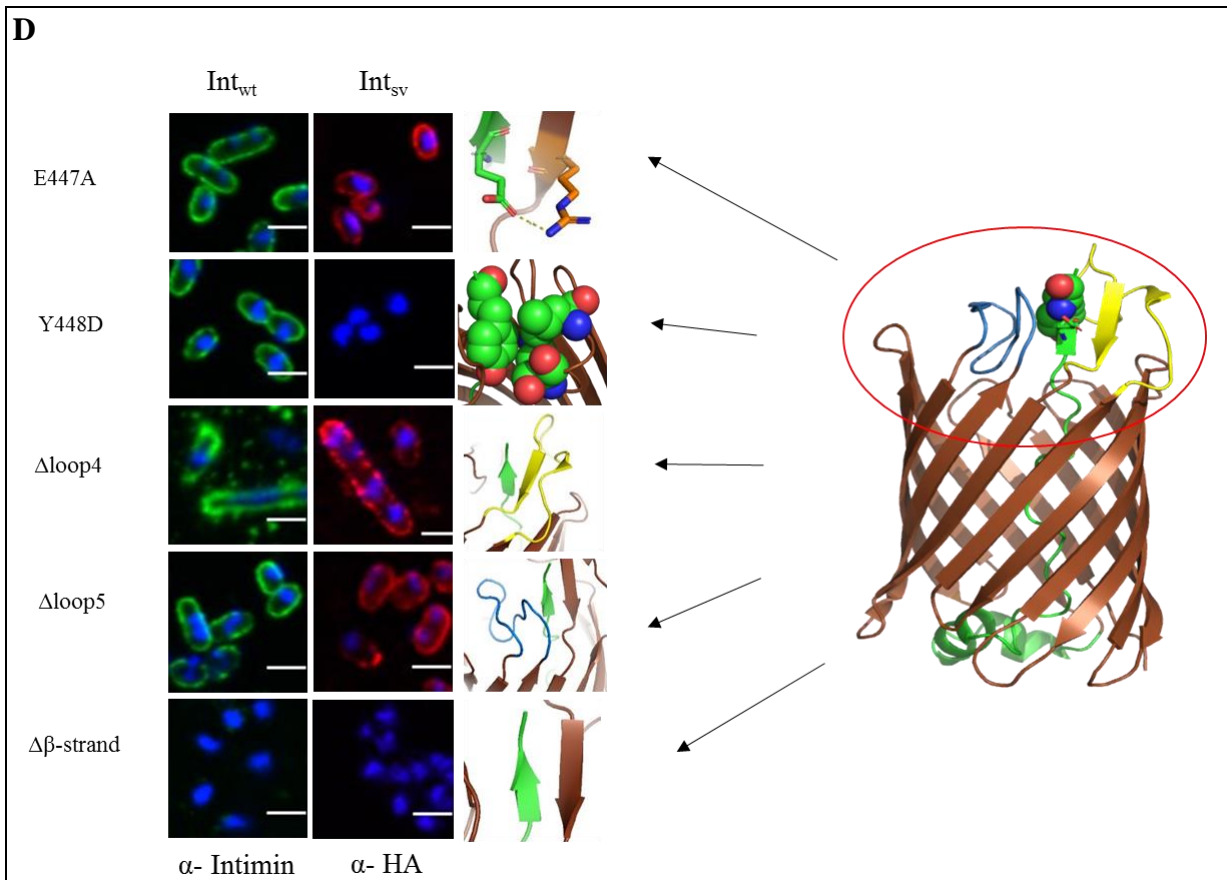
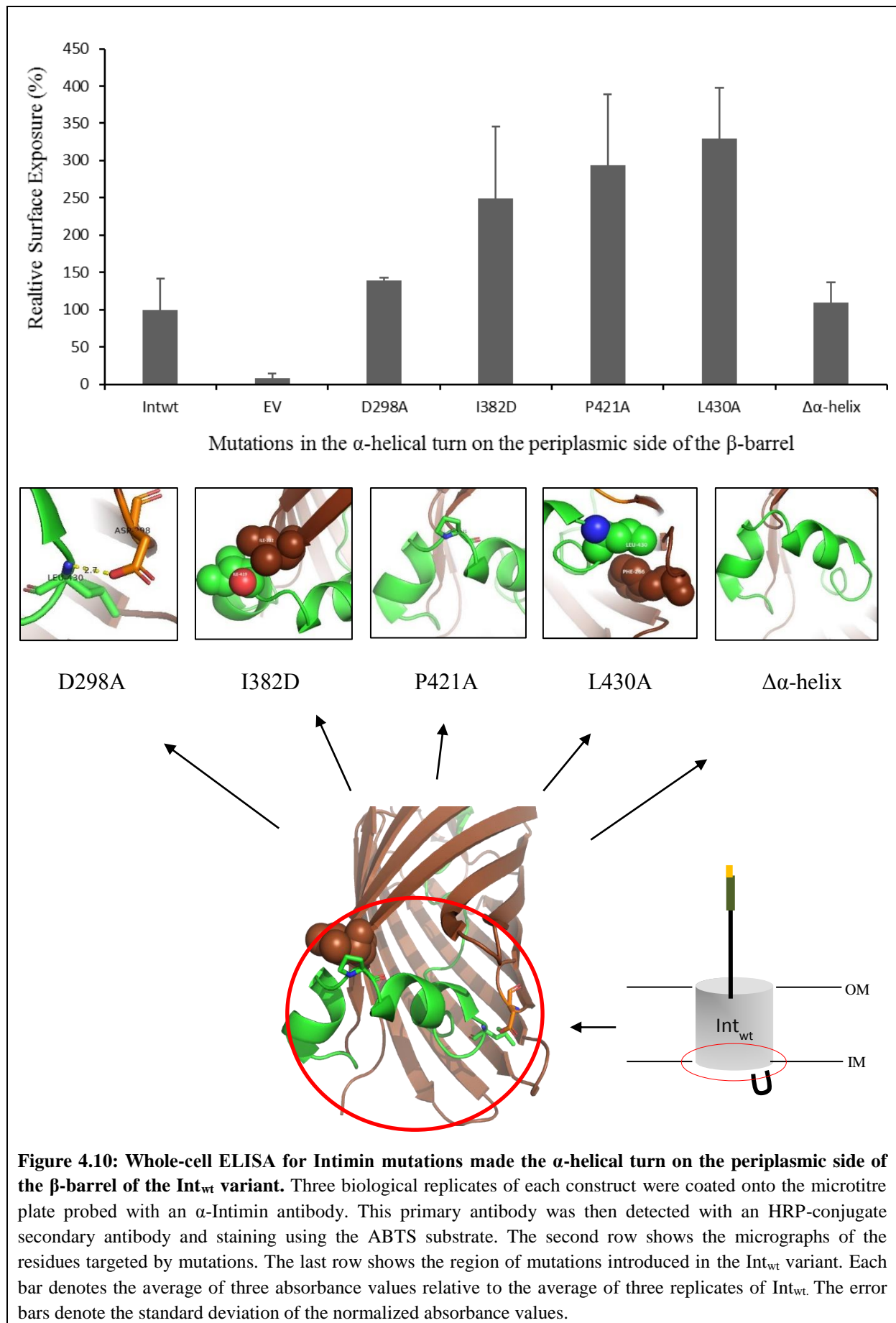


Figure 4.9: Immunofluorescence microscopy of bacteria expressing Intimin variants. The *E. coli* BL21 ΔF cells expressing the Int_{wt} and Int_{sv} mutants were fixed and incubated with α -Intimin antibody, recognizing the C-terminus of Intimin, or α -HA antibody, recognizing the surface exposed HA-tag, respectively. A, empty vector (EV), Int_{wt} and Int_{sv} controls for the mutants proteins were stained and incubated with both α - Intimin and α - HA antibodies. Only the Int_{wt} control and Int_{sv} were expected to stain with α - Intimin and α - HA antibody respectively and they do so. B, Mutations in the α -helical turn on the periplasmic side of the β -barrel in Int_{wt} (left) and Int_{sv} (right). C, Mutations in the linker connecting the β -barrel to the passenger and interacting residues facing lumen of the β -barrel in Int_{wt} (left) and Int_{sv} (right). D, Mutations in the small β -sheet formed between the linker and two loops of the β -barrel on the extracellular surface in Int_{wt} (left) and Int_{sv} (right). Only the CF488A secondary antibody is used, which is seen as green under the confocal microscopy. For easy discrimination purposes, the color for the samples in the Int_{sv} background were changed from green to red using ImageJ. Scale bar, 2 μ m. Note: During sample preparation for Δ loop4 in the Int_{wt} background, the washing steps were not done to optimum levels. Hence, the mage looks spotted in the background (Figure 4.9 D).

4.5 Whole-cell ELISAs

Whole-cell ELISAs were performed as a quantitative measurement of surface display of Intimin variants. For mutations introduced in the α -helical turn on the periplasmic side of the β -barrel, all the Int_{wt} and Int_{sv} variants showed surface exposure of the passenger and hairpin, respectively. Unexpectedly, the mutants of the Int_{wt} variant showed a twice as much surface exposure than the Int_{wt} control (Figure 4.10). Only some mutants of the Int_{sv} variant showed lower surface exposure compared to the control Int_{sv} (Figure 4.11). For mutations introduced between the linker and interacting residues in the lumen of the β -barrel, all mutants of the Int_{wt} and Int_{sv} variants showed surface exposure of the hairpin and passenger. Most mutants of the Int_{wt} variant showed twice as much surface exposure than Int_{wt}, except for the Δ linker mutation, which showed 50 % less surface exposure compared to the Int_{wt} control (Figure 4.12). The mutations in the Int_{sv} showed twice as much surface exposure compared to the Int_{sv} control (Figure 4.13). For mutations in the small β -sheet present on the extracellular side of the β -barrel, all mutants of the Int_{wt} variant showed 50 % or more surface exposure compared to the Int_{wt} control (Figure 4.14). All mutants of the Int_{sv} variant showed 50 % more surface exposure except for the mutations Y448D and $\Delta\beta$ -strand, where the levels of surface exposure were 5-10 % lower than that of the EV control (Figure 4.15). For the results of this assay, the surface exposure of the passenger and hairpin was measured relative to the Int_{wt} and Int_{sv}, respectively, and were plotted on the X-axis as percentages relative to the parent construct (either Int_{wt} or Int_{sv}.)

Statistical analysis was performed in order to look for statistical significance between the mutant proteins. Since the Int_{wt} and Int_{sv} constructs showed surface exposure of Intimin at lower levels than many of the mutant proteins, no statistically significant differences between the control and the mutants were observed.



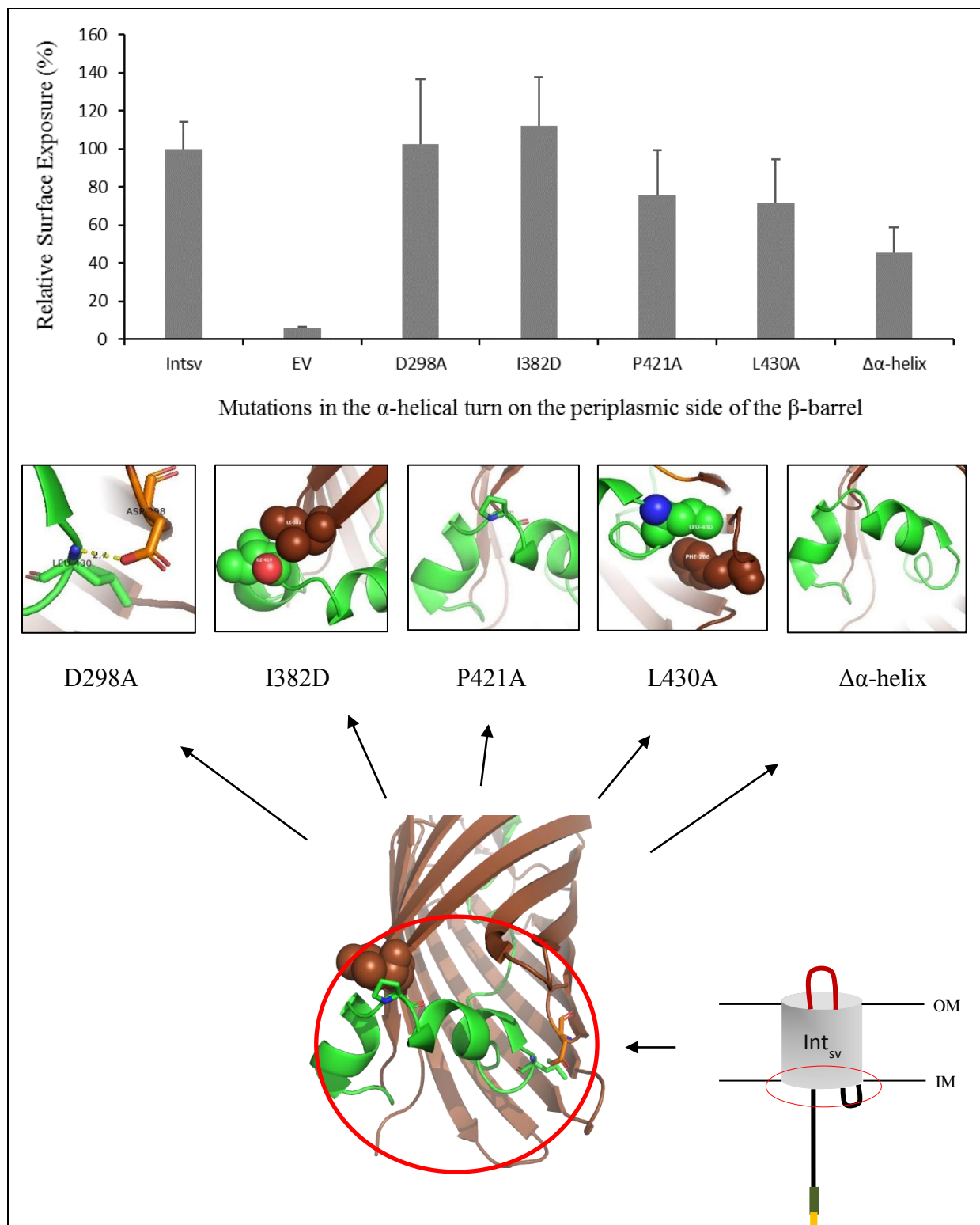
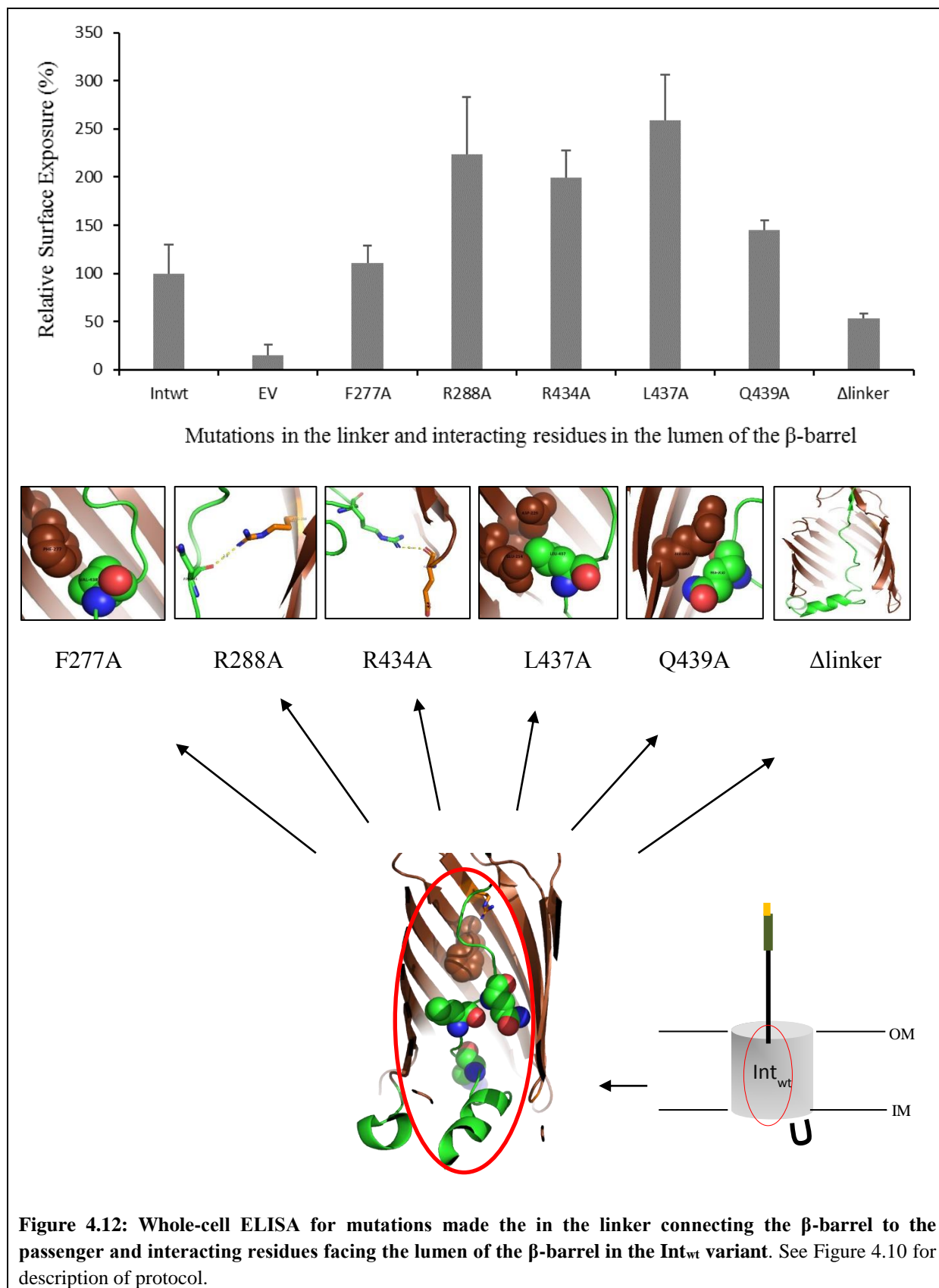


Figure 4.11: Whole-cell ELISA for mutations made in the α -helical turn on the periplasmic side of the β -barrel of the Int_{sv} variant. Three biological replicates of each mutant bacteria were coated onto the microtitre-plate probed with an α -HA antibody. This primary antibody was then detected with an HRP-conjugate secondary antibody and staining using the ABTS substrate. The second row shows the micrographs of the residues targeted by mutations. The last row shows the region of mutations introduced in the Int_{sv} variant. Each bar denotes the average of three absorbance values relative to the average of three replicates of Int_{sv} . The error bars denote the standard deviation of the normalized absorbance values.



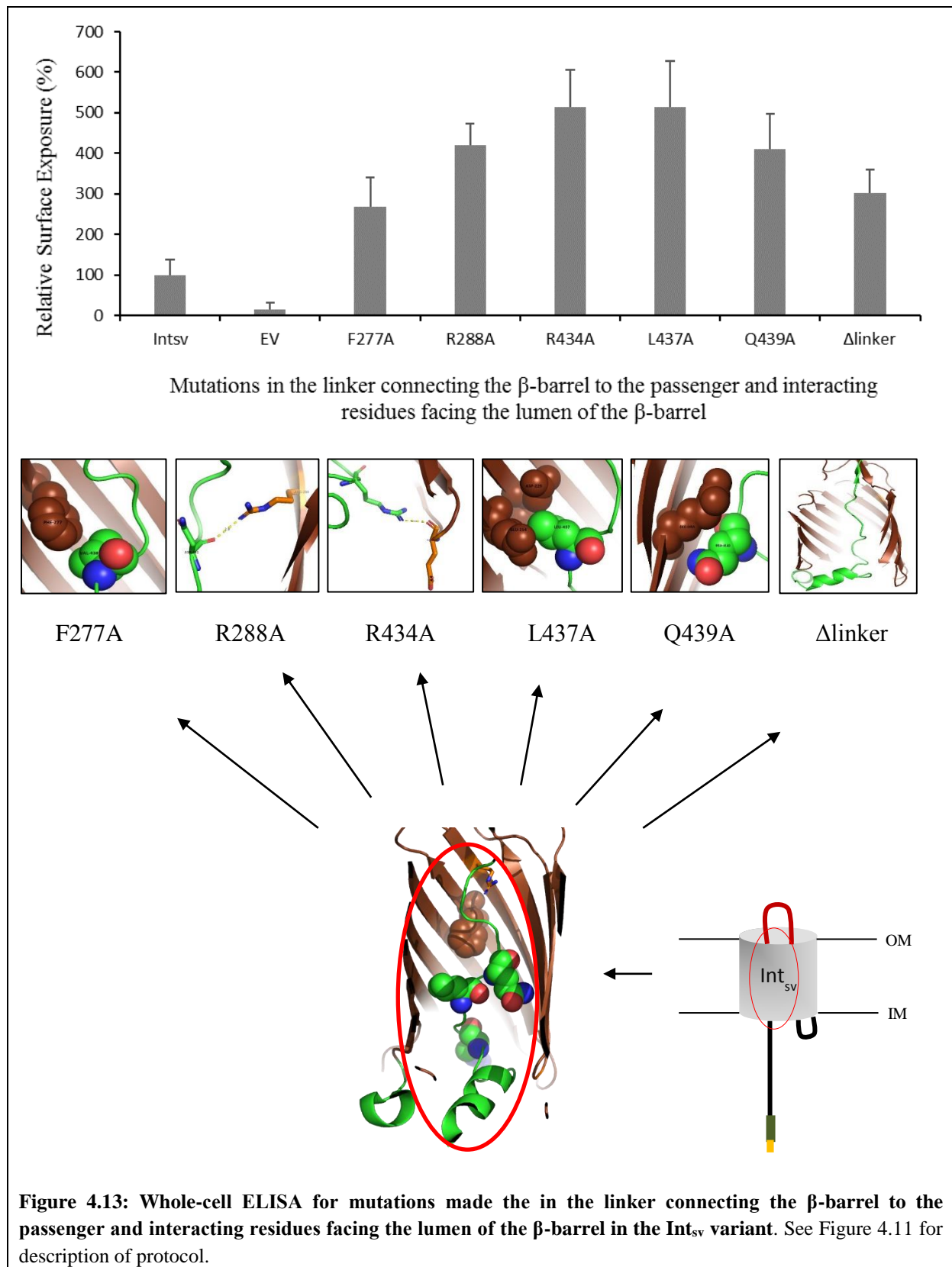
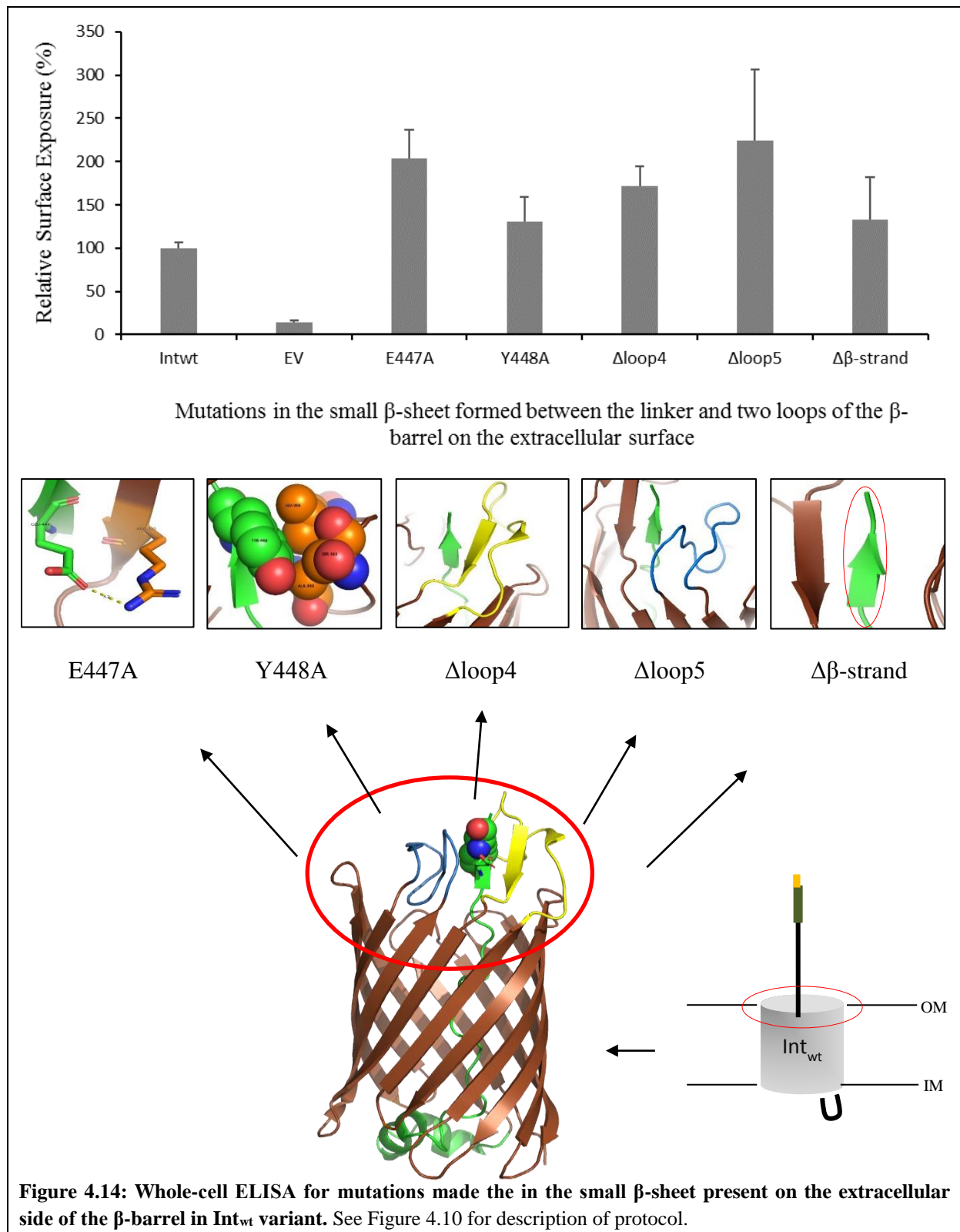


Figure 4.13: Whole-cell ELISA for mutations made the in the linker connecting the β -barrel to the passenger and interacting residues facing the lumen of the β -barrel in the Int_{sv} variant. See Figure 4.11 for description of protocol.



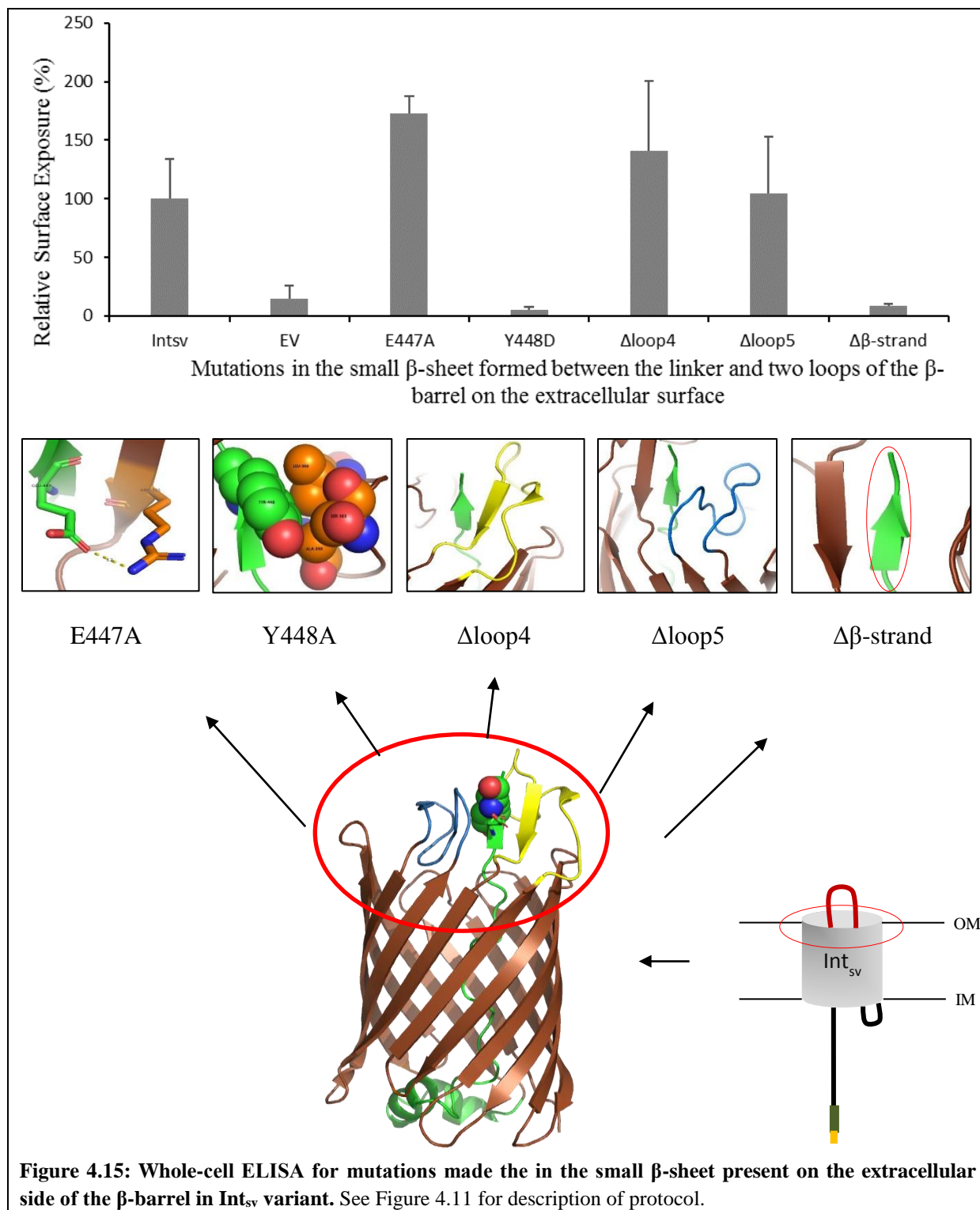
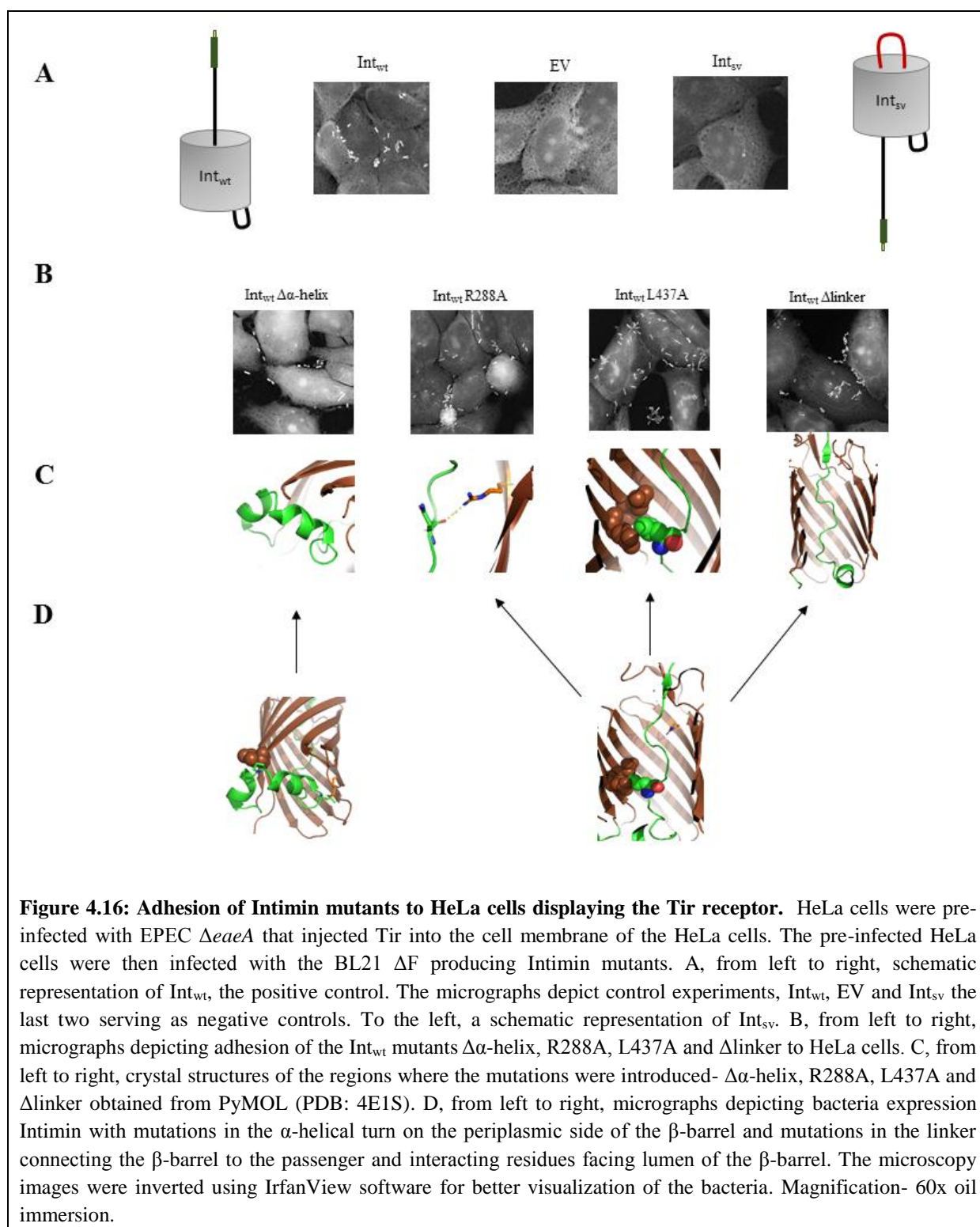


Figure 4.15: Whole-cell ELISA for mutations made the in the small β-sheet present on the extracellular side of the β-barrel in Int_{sv} variant. See Figure 4.11 for description of protocol.

4.6 Adhesion assays

This assay was done to test the adhesive nature of the Int_{wt} mutants. If bacteria with the mutant proteins adhered to the HeLa cells, it would indicate that the passenger was properly folded and the mutation did not affect passenger folding and in turn passenger secretion. The process used was adapted from (Oberhettinger et al., 2012). The Intimin passenger binds specifically to Tir, a receptor translocated to host cells by the bacterium via T3SS, present on the host cells. For this reason, the Int_{sv} mutants cannot adhere to the cells as the passenger is stalled in the hairpin conformation and is not secreted to the cell surface. Therefore, no Int_{sv} variants were used in this assay. In addition, Oberhettinger *et al.* have demonstrated that, a Strep-tag present at the C-terminus of the passenger does not hinder adhesion of Intimin to the HeLa cells, so the Strep tag at the C-terminus of the used constructs was not expected to affect binding to Tir (Oberhettinger et al., 2015). HeLa cells were pre-infected with EPEC lacking Intimin (EPEC $\Delta eaeA$) in order to first allow translocation of Tir to the HeLa cells. The infected cells were then re-infected with the Int_{wt} mutants to see if they could adhere to Tir. Due to time constraints, only few Int_{wt} mutants expected to show differences to Int_{wt} were tested for adhesion. These mutants were Int_{wt} $\Delta\alpha$ -helix, Int_{wt} R288A, Int_{wt} L437A, Int_{wt} Δ linkerGS, Int_{wt} E447A, Int_{wt} Y448D, Int_{wt} Δ loop4, Int_{wt} Δ loop5 and Int_{wt} $\Delta\beta$ -strand. All these mutants except $\Delta\beta$ -strand adhered to the cells (Figure 4.16 and Figure 4.17). The $\Delta\beta$ -strand mutant did not adhere to the HeLa cells, which ties in with the results obtained before, as the protein does not appear to be produced (Figure 4.7 C). Intimin with the mutation Y448D adhered to the HeLa cells normally, even though in the Int_{sv} background it does not seem to form the hairpin. *E. coli* BL21 ΔF containing the pET-22b (+) vector without the *eaeA* gene, was used as a control to monitor efficient removal of the bacteria from HeLa cells during the washing steps. For quantitation, 10 random infected HeLa cells were picked and the average number of bacteria infecting each cell was calculated. Based on the calculations, the mutations Δ loop4 and Δ loop5 adhered to HeLa cells to a lower degree compared to the Int_{wt} control (Table 4.2). The other variants adhered at a similar level as Int_{wt}.

For mutation Y448D in the Int_{wt} and Int_{sv}, there is a correlation between the data obtained from immunofluorescence microscopy, whole-cell ELISAs and quantification of the bacteria adhering to the HeLa cells. However, the mutation $\Delta\beta$ -strand in the Int_{wt} background does not show expected results only during whole-cell ELISA but there is correlation between data obtained during immunofluorescence microscopy and adhesion assays.



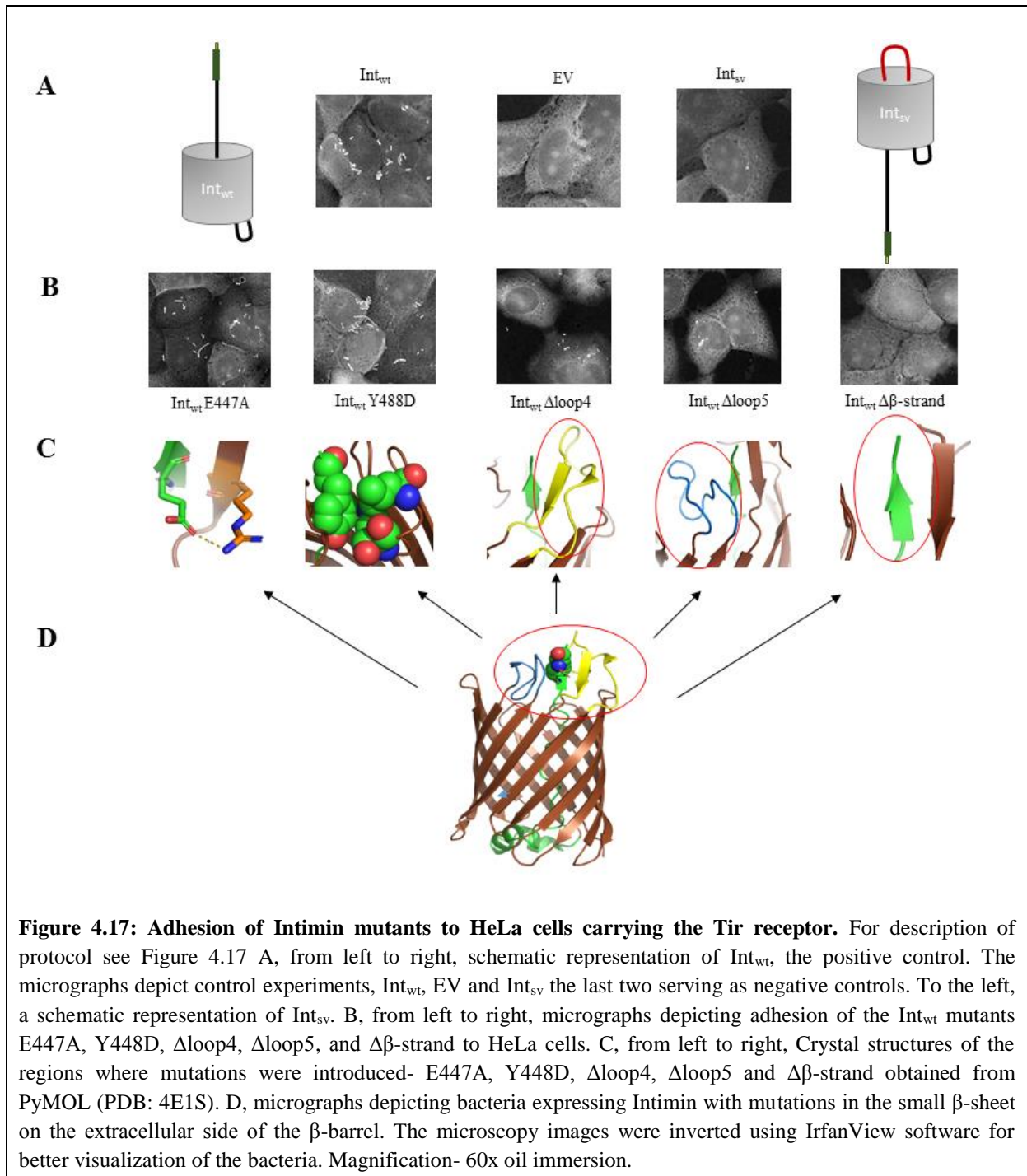
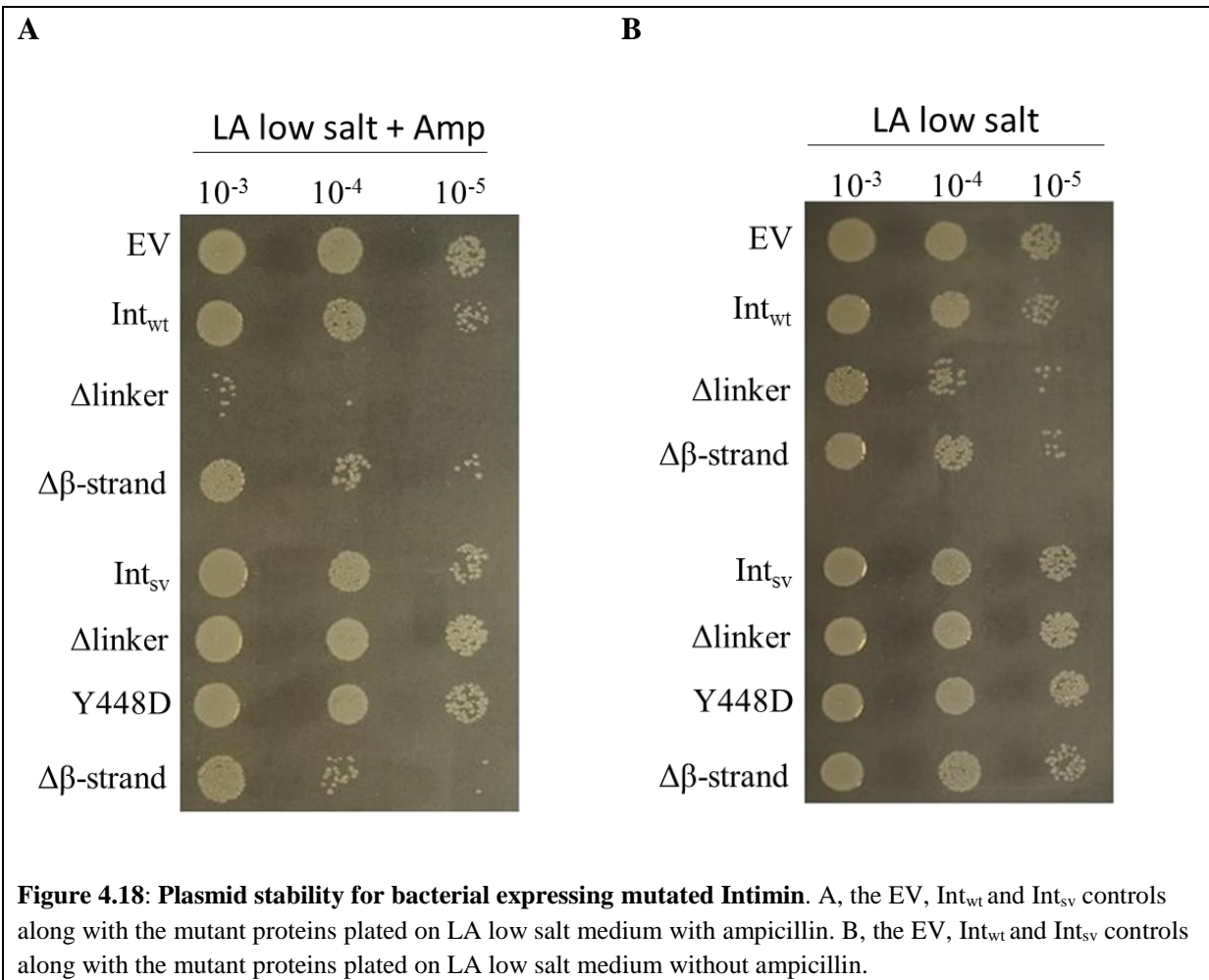


Table 4.2: Average number of bacteria infecting HeLa cells. The number of bacteria infecting 10 cells individually was counted and the average was calculated. The ‘±’ sign denotes the standard deviation for the 10 infected cells.

Bacteria	Number of HeLa cells infected
Int _{wt}	7.8 ± 3.1
EV	0
Int _{sv}	0
Δα-helix	8.1 ± 4.0
R288A	11.2 ± 4.5
L437A	21.4 ± 8.2
Δlinker	12.6 ± 5.1
E447A	15.2 ± 6.2
Y448D	12.6 ± 5.1
Δloop4	3.1 ± 2.4
Δloop5	3.5 ± 3.2
Δβ-strand	0

4.7 Plasmid stability

To analyze if the plasmid was toxic to the cells, viable count assay was performed for the Δlinker and Δβ-strand in the Int_{wt} background and Δlinker, Y448D and Δβ-strand in the Int_{sv} background. Few Intimin mutants were chosen which showed different effects on the hairpin formation and passenger effects compared to the parent Int_{sv} and Int_{wt} respectively. Intimin with mutations Δlinker and Δβ-strand in the Int_{wt} and Int_{sv} background seems to be a burden on the cells when grown on selection plate with ampicillin (Figure 4.18 A) plate compared to when grown on plate without antibiotic (Figure 4.18 B). This indicates that the plasmid is toxic to the cells. When grown on a plate without antibiotic, they survive better as they are not under selection pressure.



5. Discussion

5.1 *E. coli*, Intimin and Pathogenesis

E. coli predominantly colonizes the human intestine as a nonpathogenic facultative anaerobe. Some strains of *E. coli*, like EPEC, have evolved the ability to cause diseases. EPEC, an important cause of acute and chronic pediatric diarrhea, colonizes and forms attaching and effacing (A/E) lesions on the small intestinal epithelium of the host (Moon et al., 1983). The A/E lesions are a characteristic feature of infection which involves intimate adhesion of the bacteria, destruction of brush border microvilli and cytoskeletal rearrangements i.e., actin-rich pedestal formation beneath the surface of attachment (Knutton et al., 1989; Moon et al., 1983). Intimin is an important adhesin of EPEC that mediates intimate attachment to the host epithelial cells causing A/E lesion formation and ultimately, diarrhea. The structure of Intimin is composed of a β -barrel that forms a pore in the OM, a passenger that possesses the functional activity of Intimin and a linker that connects the β -barrel to the passenger. The passenger is exported through the OM via a hairpin intermediate. The details as to how the hairpin is formed and the molecular details of how the passenger is exported is poorly understood. Making mutations in the β -barrel and analyzing the effects of these mutations on hairpin formation and thereby passenger secretion may help in decoding the mechanism of autotransport followed by IATs. Understanding the mechanism followed by IATs would eventually help develop anti-infective strategies to disarm bacteria that contain T5eSS, and prevent them from causing infections.

5.2 The β -strand present at the C-terminus of the linker is important for hairpin formation and passenger secretion

In order to analyze the effects of introducing mutations on the three regions of the β -barrel, heat-modifiability assays, urea extractions, immunofluorescence staining, whole-cell ELISAs and adhesion assays were performed. Heat-modifiability and urea extraction assays were performed as a preliminary test to check if the mutant proteins were properly folded and inserted into the OM. After confirming so, immunofluorescence staining was performed as qualitative analysis of surface exposure of the hairpin and passenger. This technique was previously used by Oberhettinger et al. in order to test for surface exposure of their mutant proteins when trying to understand the inverse autotransport mechanism (Oberhettinger et al., 2012). They could detect the passenger and the HA-tag of the hairpin only if it was exposed on the bacterial surface. For quantitative analysis of the surface exposure, whole-cell ELISAs were performed. While performing these experiments it has come to light that this technique is not ideal to obtain a quantitative measurement of surface exposure of the Intimin mutants. A more sophisticated solution to obtain better results would be to perform fluorescence

activated cell-sorting (FACS) to exactly know how many cells in the population showed surface exposure of Intimin variants and compare it to the control levels. Adhesion assays were performed to analyze if the passenger, after translocation, was properly folded which would then mediate adhesion to the HeLa cells (Oberhettinger et al., 2012). Only few mutants of Int_{wt}, which were assumed to show some differences compared to the Int_{wt} construct, were chosen for adhesion assays due to time constraints.

To understand the role played by the α -helical turn on the periplasmic side of the β -barrel during the inverse autotransport process, mutations were introduced in certain specific positions of the α -helical turn that interact with the periplasmic side of the β -barrel (Section 4.1.1) and the α -helical turn was deleted and replaced with alternating residues of serine and glycine of the same length. As corroborated by data obtained during immunofluorescence microscopy (Figure 4.9 B), whole-cell ELISAs (Figure 4.10 and Figure 4.11) and adhesion assays with the deleted α -helical turn (Figure 4.16), the hairpin and passenger of all mutants were surface exposed and the $\Delta\alpha$ -helix mutant adhered to HeLa cells suggesting that the α -helical turn is not involved during the inverse autotransport process; instead it may be involved in occluding the OM pore, as previously suggested (Fairman et al., 2012b). Based on the crystal structure of the β -barrel of Intimin (Fairman et al., 2012a) (which is shown in its end state), there is not enough space for the α -helical turn to be located near the pore. Hence, it may be positioned away from the pore during the translocation process and later plugs it post passenger translocation. The C-terminus of the linker on other hand was shown to stabilize the β -barrel (Fairman et al., 2012a). The question was, if disrupting interactions between the linker and lumen of β -barrel would somehow hinder hairpin formation and/or passenger secretion. To this extent, mutations were introduced in residues that interacted with the linker and the lumen of the β -barrel that seemed to play an important role in autotransport and the linker was replaced with alternating residues of serine and glycine of the same length (Section 4.1.2). As corroborated by data obtained from immunofluorescence microscopy (Figure 4.9 C), whole-cell ELISAs (Figure 4.14 and Figure 4.15) and adhesion assays with Intimin containing mutations R288A, L437A and Δ linker (Figure 4.16), the hairpin and passenger of all the mutant proteins were surface exposed and the mutants R288A, L437A and Δ linker adhered to HeLa cells. However, cells containing the Δ linker mutations showed mixed populations during immunofluorescence microscopy (Figure 4.9 C and Supplementary Figure 1) and 40 % or less surface exposure compared to the control with whole-cell ELISA (Figure 4.12 and Figure 4.13). This suggests that deleting the linker, to an extent, hinders hairpin formation and passenger secretion. But, the exact number of how many bacteria showed surface exposure should be determined by a more sophisticated technique like FACS.

To understand the role played by the small β -sheet on the extracellular side of the β -barrel and how it effects the hairpin formation and passenger secretion, mutations were introduced to disrupt the interactions between the β -strand of the linker and the β -strand present on loop 5. Additionally, the β -strand present at the very C-terminus of the linker, extracellular loops 4 and 5 was deleted and replaced with only 4 residues of glycine. An interesting effect was observed when the hydrophobic interaction between the β -strand of the linker and loop 5 of the β -barrel was disrupted by introducing a charged amino acid residue (Y448D). In this

mutation, the protein is full length as shown by the western blots (Figure 4.7 C and Figure 4.8 C) but, the hairpin is disrupted with the passenger being surface exposed (Figure 4.9 D). As an explanation for this discrepancy, the interaction between the β -strand and the loops of the β -barrel may have destabilized the hairpin which would result in its backslide into the periplasm; hence, the hairpin cannot be detected on the cell surface. By contrast, even transient formation of the hairpin may have provided enough time for the first domain of the passenger to be exported to the extracellular surface, where it then fold and enables vectorial secretion of the passenger by sequential folding (Leo et al., 2016). Once this has happened, the passenger is prevented from re-entering the periplasm and the protein is locked in this final conformation. Therefore, even transient hairpin formation can lead to secretion for most of the protein (Figure 5.1), as shown by both immunofluorescence and whole-cell ELISA. Replacing the entire β -strand of the linker resulted in no hairpin formation in the Int_{sv} background (Figure 4.9 D) while the protein was seen in the OM fractions (Figure 4.7 C). For this mutant in the Int_{wt} background, no protein was seen in the OM fractions (Figure 4.7 C). Presumably, deleting this β -strand may have either destabilized the β -barrel hindering its integration into the OM and resulting in degradation of the protein in the periplasm by DegP, or may have impaired passenger export post-integration of the β -barrel into the OM. As a result, the β -barrel may have adopted an unfavorable conformation in the OM resulting in its degradation. The latter hypothesis is preferred as the data obtained during heat modifiability assays shows that protein is produced in the Int_{sv} background. The results obtained during whole-cell ELISA for $\Delta\beta$ -strand mutation shows surface exposure of Intimin in the Int_{wt} background while immunofluorescence staining says otherwise. The assumption is that the antibodies targeted against the C-terminus of the passenger enters the pore and somehow binds to the passenger hypothetically located in the periplasm, which is read out as an absorbance. If replacing the β -strand effected the stability of the barrel, the protein would have been degraded in the periplasm before integrating into the OM. This scenario would not support the assumption of the antibodies entering the pore and binding to the C-terminus of the passenger. Also, observing that the mutation Y448D effects the hairpin formation, it is likely that the $\Delta\beta$ -strand effects the hairpin and passenger secretion rather than the stability of the β -barrel.

Based on the aforementioned results, and in comparison to the other regions of the β -barrel, this extracellular β -strand located at the C-terminus of the linker plays an important role in stabilizing the hairpin and promotes passenger secretion through the β -barrel embedded in the OM.

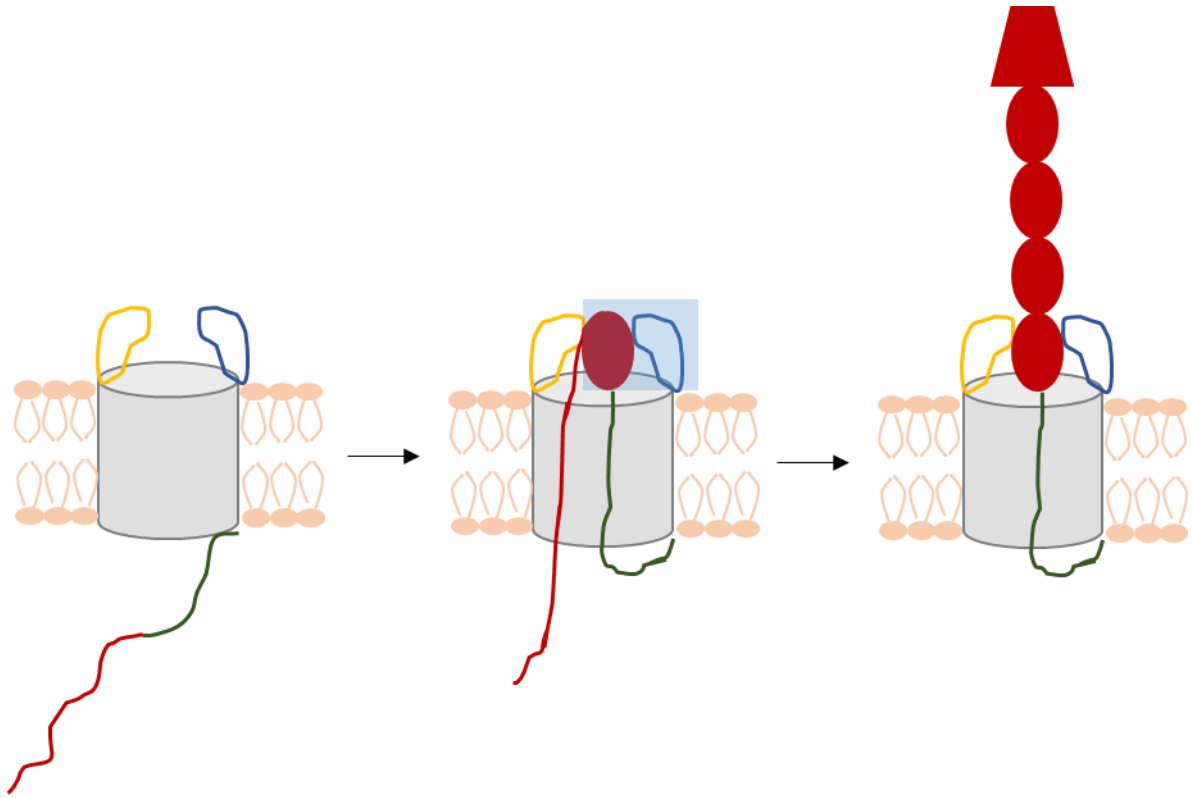
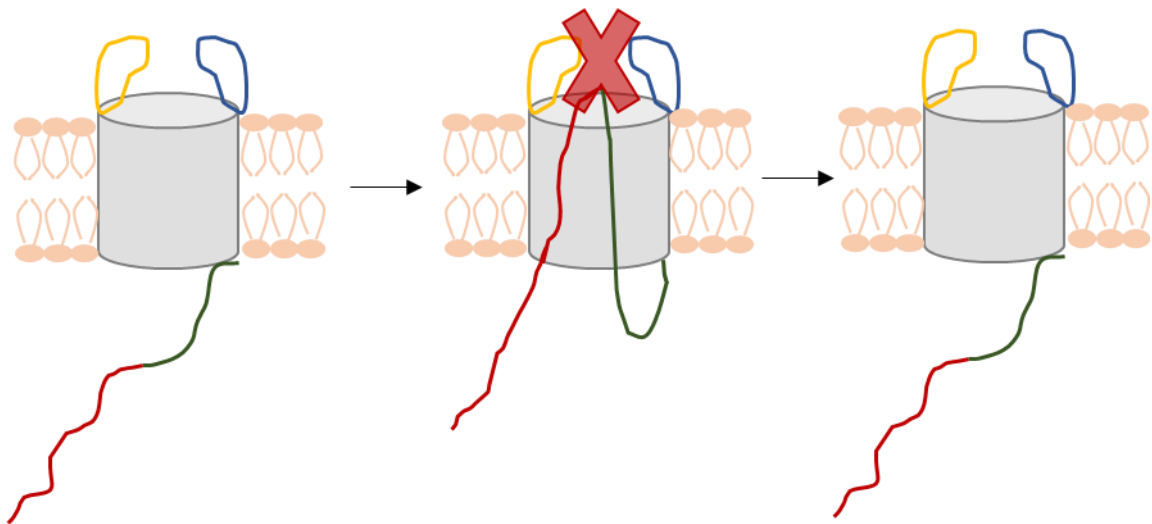
A**B**

Figure 5.1: Possible explanation for the effect seen due to the Y448D mutation in the small β -sheet located on the extracellular side of the β -barrel. A, In the Int_{wt} background, transient interaction (blue box) of the β -strand located in the first domain of the passenger (red circle) allows for passenger translocation. B, In the Int_{sv} background, the interaction between the β -strand destabilizes the hairpin at the extracellular space and results in its backslide into the periplasm. The β -barrel is colored in grey, the linker is shown in green, and the passenger segment is shown as a red line and the domain post secretion is shown as red circles. The yellow and blue lines represent the extracellular loops 4 and 5 respectively.

5.3 Proposed models for the biogenesis of IATs

What is known is, once the β -barrel is inserted into the OM the hairpin is formed and the passenger is then exported by sequential protein folding of individual domains of the passenger. However, how the linker reaches the OM pore formed by the β -barrel and forms the hairpin is unclear. During mutational studies on the small β -sheet present on the extracellular surface, a large hydrophobic interaction formed between the β -strand of the linker and loop 5 of the β -barrel was disrupted which resulted in no surface exposure of the hairpin. Also, deleting the entire β -strand and replacing it by a flexible sequence (4 residues of glycine) resulted in no hairpin formation and hindered passenger export. There are two possible scenarios that explain this result. One, where the β -strand directs the linker into the pore by transient interaction with residues in the lumen of the barrel. After transiently passing through the lumen, the β -barrel forms a stable interaction with the extracellular loops thereby stabilizing the hairpin and promoting passenger secretion. The second scenario is where the β -strand is only needed to stabilize the hairpin at the top of the barrel, in which case something else initiates hairpin formation (Figure 5.2). The possibility that the hairpin is formed in association with BamA of the BAM complex cannot be ruled out. It has been previously shown for T5aSS (Ieva et al., 2011; Jain and Goldberg, 2007; Sauri et al., 2009), T5cSS (Lehr et al., 2010) and T5eSS (Oberhettinger et al., 2012) that the BAM complex is directly involved in the biogenesis of autotransporters. But the exact mechanism as to how and if it is involved in hairpin formation is not known. It has been suggested that the BamA forms a hybrid β -barrel together with the substrate barrel, which is later released in a process called budding (Albrecht et al., 2014; Noinaj et al., 2011; Noinaj et al., 2014; Noinaj et al., 2013). Several scenarios are possible that explain how the hairpin can be formed by interaction of the β -barrel with the BamA of the BAM complex (Figure 5.2) (Oberhettinger et al., 2015).

1. Unlike T5aSS where the β -barrel insertion and hairpin formation are coupled, the β -barrel of IATs is formed with the help of BamA but autotransport is initiated later (Figure 5.3 A).
2. The barrel is formed but the hairpin is inserted during the hybrid stage resulting in two possibilities where, one end stays in the BamA barrel (Figure 5.3 B) or both the ends of the hairpin end up in the intimin β -barrel (Figure 5.3 C).

In all these scenarios the passenger may interact with POTRA domains of the BamA or may also interact with other parts of BamA.

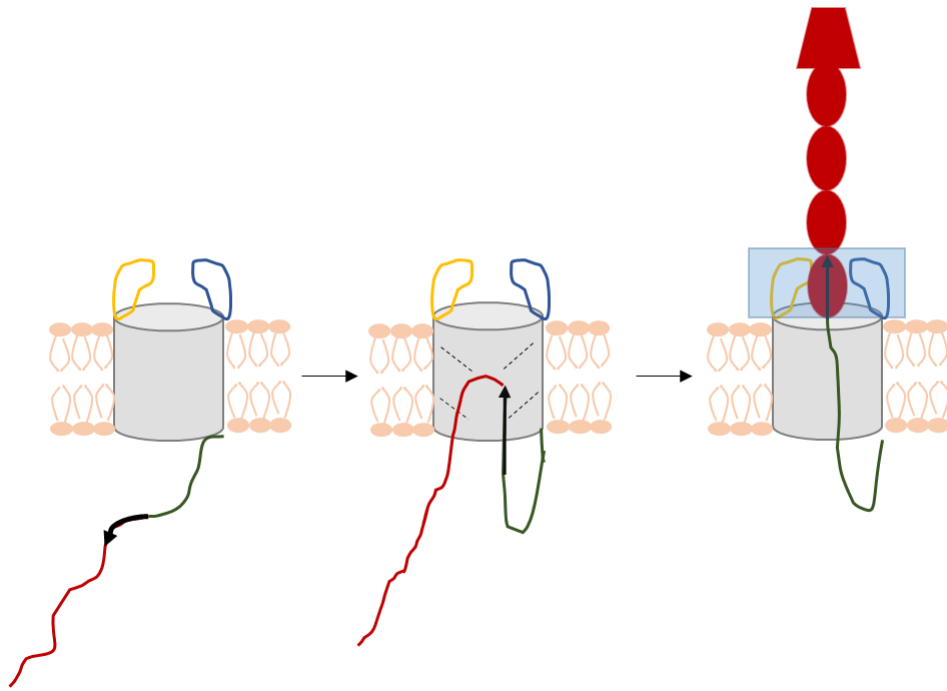
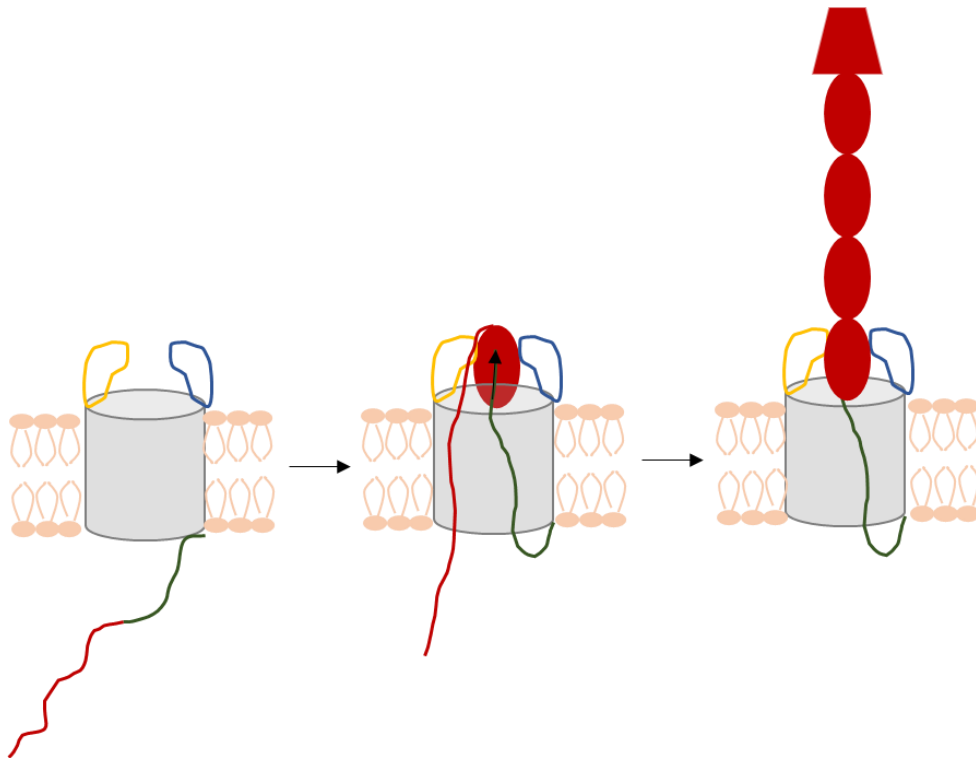
A**B**

Figure 5.2: Proposed models for IATs Biogenesis. A, The β -strand (black arrow) transiently interacts with the lumen of the β -barrel (black dashed lines) and directs the hairpin to the extracellular loop, stabilizing the hairpin and promoting vectorial secretion of the passenger. B, The formation of hairpin is mediated by other means and the β -strand is only involved in stabilizing the hairpin by interacting with the extracellular loops (blue box). Once the hairpin is stabilized, the passenger is secreted in a vectorial manner. For description of color coding see figure 5.1.

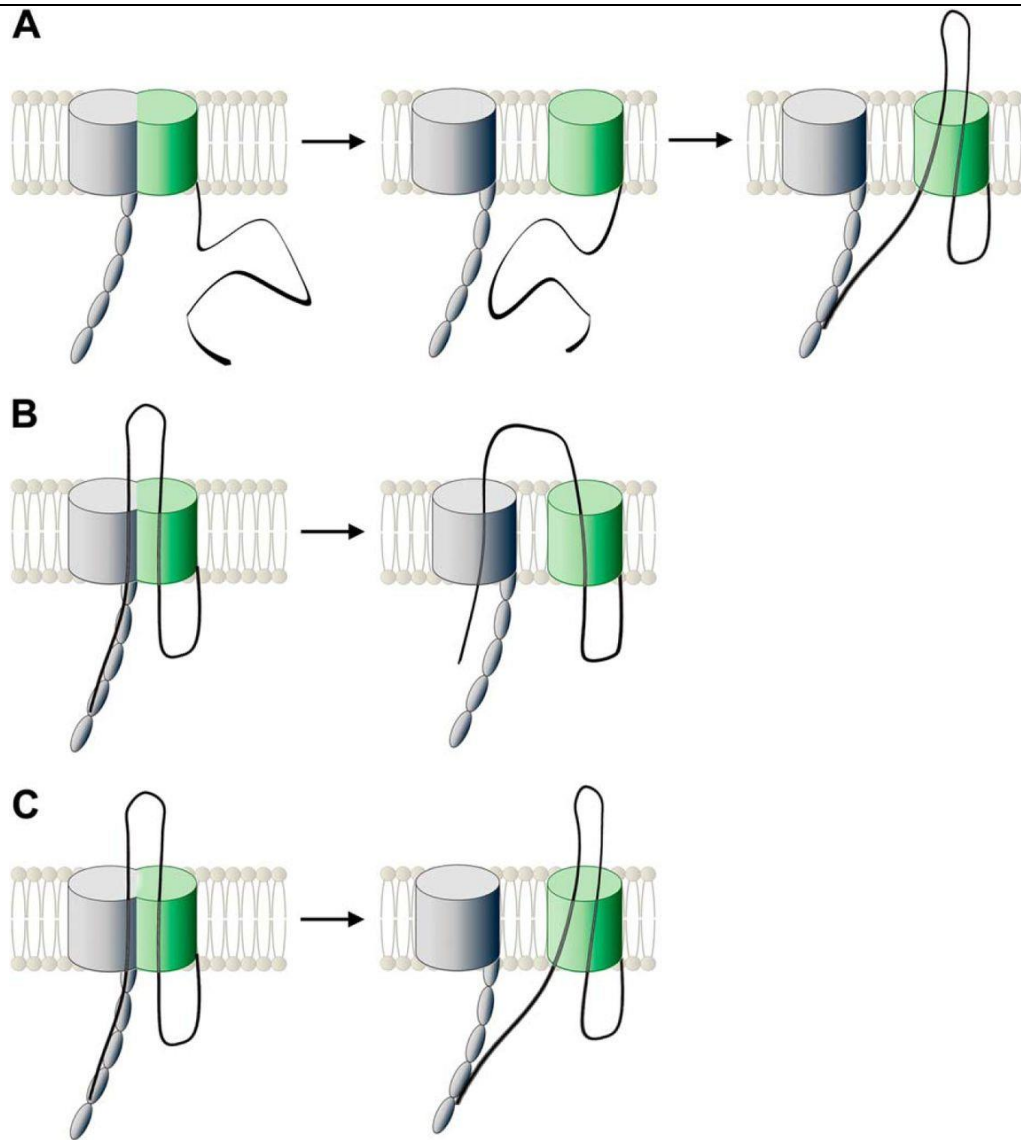


Figure 5.3: Possible Scenarios of hairpin formation. A, Budding of the β -barrel of Intimin from the BamA barrel into the OM and autotransport is initiated later. B, The β -barrel is formed but the hairpin is inserted during the hybrid stage where one end is in the BamA barrel. C, both ends of the hairpin are in the β -barrel. The passenger interacts with the POTRA domain of the BamA in all cases. Figure taken from (Oberhettinger et al., 2015) with permission from the Journal of Biological Chemistry.

Once the hairpin is stabilized, the linker mediates surface exposure of the D00 domain of the passenger enabling the vectorial secretion of the passenger. The mutations introduced in the linker and interacting residues in the lumen of the β -barrel did not have any major effect on hairpin formation or passenger secretion. However, deleting the entire linker and replacing it with alternating residues of serine and glycine resulted in a mixed population of bacteria with and without surface exposure of the hairpin and passenger. This means that the linker does play a role in passenger secretion. But, the exact role is not known. Once the passenger is translocated, the α -helical turn on the periplasmic side of the β -barrel, which is positioned away from the pore to provide space for the hairpin, would then position itself in a manner that occludes the OM pore preventing OM leakage.

6. Conclusion and future goals

The aim of this project was to investigate the role played by the three regions in the β -barrel of Intimin in order to better understand the mechanism of inverse autotransport. During the course of this work, it has come to light that the β -strand present at the C-terminus of the linker is important in stabilizing the hairpin which, presumably, then promotes passenger secretion. The hypotheses are that the β -strand either directs the hairpin into the OM pore, stabilizes the hairpin thereby promoting passenger translocation or, it only stabilizes the hairpin at the top of the β -barrel and the hairpin formation is initiated by other means. In order to test these hypotheses, further experiments like crosslinking would need to be performed to analyze the interactions between the β -strand with different residues of the lumen of the β -barrel during the process of inverse autotransport. Deletion of the β -strand resulted in no surface exposure of both, the hairpin in the Int_{sv} and the passenger in the Int_{wt} background (Figure 4.9 D). However, Intimin seems to be produced in the Int_{sv} background and not in the Int_{wt} background (Figure 4.7 C). The next step would be to knock out the periplasmic protease involved in quality control, DegP, from this mutant protein in the Int_{wt} background and test if this knockout would result in surface exposure of the passenger.

It is still unclear as to how the hairpin is directed into the OM pore formed by the β -barrel or what initiates the formation of hairpin in Intimin. The mechanism of how the BAM complex interacts with the passenger during the inverse autotransport process is still not known. Would deleting the passenger in the Int_{sv} still result in the surface exposure of the hairpin? Answering these questions would shed light on transient interactions that take place within the β -barrel of Intimin and, between the BAM complex and the hairpin of Intimin. Ultimately, this would bring us closer to understanding the mechanism of inverse autotransport and eventually help devise anti-infective strategies that target pathogenic bacteria possessing adhesins of the T5eSS family.

References

- Albrecht, R., Schütz, M., Oberhettinger, P., Faulstich, M., Bermejo, I., Rudel, T., Diederichs, K., and Zeth, K.J.A.C.S.D.B.C. (2014). Structure of BamA, an essential factor in outer membrane protein biogenesis. *70*, 1779-1789.
- Altschul, S.F., and Koonin, E.V. (1998). Iterated profile searches with PSI-BLAST—a tool for discovery in protein databases. *Trends in Biochemical Sciences* *23*, 444-447.
- Aoki, S.K., Diner, E.J., de Roodenbeke, C.T.k., Burgess, B.R., Poole, S.J., Braaten, B.A., Jones, A.M., Webb, J.S., Hayes, C.S., Cotter, P.A., *et al.* (2010). A widespread family of polymorphic contact-dependent toxin delivery systems in bacteria. *Nature* *468*, 439-442.
- Aoki, S.K., Pamma, R., Hernday, A.D., Bickham, J.E., Braaten, B.A., and Low, D.A. (2005). Contact-Dependent Inhibition of Growth in *Escherichia coli*. *Science* *309*, 1245.
- Arnold, T., Zeth, K., and Linke, D. (2010). Omp85 from the thermophilic cyanobacterium *Thermosynechococcus elongatus* differs from proteobacterial Omp85 in structure and domain composition. *The Journal of biological chemistry* *285*, 18003-18015.
- Benz, I., and Schmidt, M.A. (1989). Cloning and expression of an adhesin (AIDA-I) involved in diffuse adherence of enteropathogenic *Escherichia coli*. *Infection and immunity* *57*, 1506-1511.
- Berks, B.C. (2015). The Twin-Arginine Protein Translocation Pathway. *84*, 843-864.
- Bernstein, H. (2019). Type V Secretion in Gram-Negative Bacteria.
- Bertani, G. (1951). Studies on lysogenesis. I. The mode of phage liberation by lysogenic *Escherichia coli*. *Journal of bacteriology* *62*, 293-300.
- Beveridge, T.J. (1999). Structures of gram-negative cell walls and their derived membrane vesicles. *Journal of bacteriology* *181*, 4725-4733.
- Bodelón, G., Marín, E., and Fernández, L.A. (2009a). Role of periplasmic chaperones and BamA (YaeT/Omp85) in folding and secretion of intimin from enteropathogenic *Escherichia coli* strains. *Journal of bacteriology* *191*, 5169-5179.
- Bodelón, G., Marín, E., and Fernández, L.Á. (2009b). Role of Periplasmic Chaperones and BamA (YaeT/Omp85) in Folding and Secretion of Intimin from Enteropathogenic *Escherichia coli* Strains. *Journal of Bacteriology* *191*, 5169.
- Braun, V., Ondraczek, R., and Hobbie, S.J.Z.f.B. (1993). Activation and secretion of *Serratia hemolysin*. *278*, 306-315.
- Buist, G., Steen, A., Kok, J., and Kuipers, O.P. (2008). LysM, a widely distributed protein motif for binding to (peptido)glycans. *Molecular Microbiology* *68*, 838-847.

- Bölin, I., Norlander, L., and Wolf-Watz, H. (1982). Temperature-inducible outer membrane protein of *Yersinia pseudotuberculosis* and *Yersinia enterocolitica* is associated with the virulence plasmid. *Infection and immunity* *37*, 506-512.
- Bönemann, G., Pietrosiuk, A., and Mogk, A. (2010). Tubules and donuts: a type VI secretion story. *76*, 815-821.
- Calvert, M.B., Jumde, V.R., and Titz, A. (2018). Pathoblockers or antivirulence drugs as a new option for the treatment of bacterial infections. *Beilstein J Org Chem* *14*, 2607-2617.
- Casasanta, M.A., Yoo, C.C., Smith, H.B., Duncan, A.J., Cochrane, K., Varano, A.C., Allen-Vercoe, E., and Slade, D.J. (2017). A chemical and biological toolbox for Type Vd secretion: Characterization of the phospholipase A1 autotransporter FplA from *Fusobacterium nucleatum*. *The Journal of biological chemistry* *292*, 20240-20254.
- Chauhan, N., Hatlem, D., Orwick-Rydmark, M., Schneider, K., Floetenmeyer, M., van Rossum, B., Leo, J.C., and Linke, D. (2019). Insights into the autotransport process of a trimeric autotransporter, *Yersinia Adhesin A (YadA)*. *Molecular Microbiology* *111*, 844-862.
- Chevalier, N., Moser, M., Koch, H.G., Schimz, K.L., Willery, E., Loch, C., Jacob-Dubuisson, F., and Müller, M. (2004). Membrane Targeting of a Bacterial Virulence Factor Harboring an Extended Signal Peptide. *Journal of Molecular Microbiology and Biotechnology* *8*, 7-18.
- Christie, P.J., Whitaker, N., and González-Rivera, C. (2014). Mechanism and structure of the bacterial type IV secretion systems. *Biochimica et Biophysica Acta (BBA) - Molecular Cell Research* *1843*, 1578-1591.
- Chung, C.T., Niemela, S.L., and Miller, R.H. (1989). One-step preparation of competent *Escherichia coli*: transformation and storage of bacterial cells in the same solution. *Proceedings of the National Academy of Sciences of the United States of America* *86*, 2172-2175.
- Cianciotto, N.P., and White, R.C. (2017). Expanding Role of Type II Secretion in Bacterial Pathogenesis and Beyond. *Infection and Immunity* *85*, e00014-00017.
- Clantin, B., Delattre, A.-S., Rucktooa, P., Saint, N., Méli, A.C., Loch, C., Jacob-Dubuisson, F., and Villeret, V.J.S. (2007). Structure of the membrane protein FhaC: a member of the Omp85-TpsB transporter superfamily. *317*, 957-961.
- Costa, T.R.D., Felisberto-Rodrigues, C., Meir, A., Prevost, M.S., Redzej, A., Trokter, M., and Waksman, G. (2015). Secretion systems in Gram-negative bacteria: structural and mechanistic insights. *Nature Reviews Microbiology* *13*, 343.
- Dagert, M., and Ehrlich, S.D. (1979). Prolonged incubation in calcium chloride improves the competence of *Escherichia coli* cells. *Gene* *6*, 23-28.
- Dalbey, R.E., Wang, P., and Kuhn, A. (2011). Assembly of Bacterial Inner Membrane Proteins. *Annual Review of Biochemistry* *80*, 161-187.

Dautin, N., Barnard, T.J., Anderson, D.E., and Bernstein, H.D. (2007). Cleavage of a bacterial autotransporter by an evolutionarily convergent autocatalytic mechanism. *The EMBO journal* *26*, 1942-1952.

Dautin, N., and Bernstein, H.D. (2007). Protein Secretion in Gram-Negative Bacteria via the Autotransporter Pathway. *Annual Review of Microbiology* *61*, 89-112.

Davis, M. (2012). ApE: a plasmid editor.

Deibel, C., Krämer, S., Chakraborty, T., and Ebel, F. (1998). EspE, a novel secreted protein of attaching and effacing bacteria, is directly translocated into infected host cells, where it appears as a tyrosine-phosphorylated 90 kDa protein. *Molecular Microbiology* *28*, 463-474.

Deng, W., Marshall, N.C., Rowland, J.L., McCoy, J.M., Worrall, L.J., Santos, A.S., Strynadka, N.C.J., and Finlay, B.B. (2017). Assembly, structure, function and regulation of type III secretion systems. *Nature Reviews Microbiology* *15*, 323.

Dersch, P., and Isberg, R.R. (2000). An Immunoglobulin Superfamily-Like Domain Unique to the *Yersinia pseudotuberculosis* Invasin Protein Is Required for Stimulation of Bacterial Uptake via Integrin Receptors. *Infection and Immunity* *68*, 2930.

Dersch, P., and Isberg, R.R.J.T.E.J. (1999). A region of the *Yersinia pseudotuberculosis* invasin protein enhances integrin-mediated uptake into mammalian cells and promotes self-association. *18*, 1199-1213.

Evans, M.L., and Chapman, M.R. (2014). Curli biogenesis: order out of disorder. *Biochimica et biophysica acta* *1843*, 1551-1558.

Fairman, J.W., Dautin, N., Wojtowicz, D., Liu, W., Noinaj, N., Barnard, T.J., Udho, E., Przytycka, T.M., Cherezov, V., and Buchanan, S.K. (2012a). Crystal structures of the outer membrane domain of intimin and invasin from enterohemorrhagic *E. coli* and enteropathogenic *Y. pseudotuberculosis*. *Structure* *20*, 1233-1243.

Fairman, J.W., Dautin, N., Wojtowicz, D., Liu, W., Noinaj, N., Barnard, T.J., Udho, E., Przytycka, T.M., Cherezov, V., and Buchanan, S.K. (2012b). Crystal Structures of the Outer Membrane Domain of Intimin and Invasin from Enterohemorrhagic *Escherichia coli* and Enteropathogenic *Yersinia pseudotuberculosis*. *Structure(London, England:1993)* *20*, 1233-1243.

Fleming, P.J., Patel, D.S., Wu, E.L., Qi, Y., Yeom, M.S., Sousa, M.C., Fleming, K.G., and Im, W. (2016). BamA POTRA Domain Interacts with a Native Lipid Membrane Surface. *Biophys J* *110*, 2698-2709.

Frankel, G., Lider, O., HersHKoviz, R., Mould, A.P., Kachalsky, S.G., Candy, D.C., Cahalon, L., Humphries, M.J., and Dougan, G.J.J.o.B.C. (1996). The cell-binding domain of intimin from enteropathogenic *Escherichia coli* binds to β 1 integrins. *271*, 20359-20364.

Freudl, R. (2013). Leaving home ain't easy: protein export systems in Gram-positive bacteria. *Research in Microbiology* *164*, 664-674.

Gallique, M., Bouteiller, M., and Merieau, A. (2017). The Type VI Secretion System: A Dynamic System for Bacterial Communication? *8*.

- Gibson, D.G., Young, L., Chuang, R.-Y., Venter, J.C., Hutchison Iii, C.A., and Smith, H.O. (2009). Enzymatic assembly of DNA molecules up to several hundred kilobases. *Nature Methods* 6, 343.
- Green, E.R., and Meccas, J. (2016). Bacterial Secretion Systems: An Overview. *Microbiology spectrum* 4, 10.1128/microbiolspec.VMBF-0012-2015.
- Guérin, J., Bigot, S., Schneider, R., Buchanan, S.K., and Jacob-Dubuisson, F. (2017). Two-Partner Secretion: Combining Efficiency and Simplicity in the Secretion of Large Proteins for Bacteria-Host and Bacteria-Bacteria Interactions. *Frontiers in cellular and infection microbiology* 7, 148-148.
- Hamburger, Z.A., Brown, M.S., Isberg, R.R., and Bjorkman, P.J. (1999a). Crystal Structure of Invasin: A Bacterial Integrin-Binding Protein. *Science* 286, 291.
- Hamburger, Z.A., Brown, M.S., Isberg, R.R., and Bjorkman, P.J. (1999b). Crystal structure of invasins: a bacterial integrin-binding protein. *Science* 286, 291-295.
- Hamburger, Z.A., Brown, M.S., Isberg, R.R., and Bjorkman, P.J.J.S. (1999c). Crystal structure of invasins: a bacterial integrin-binding protein. 286, 291-295.
- Hartland, E.L., Batchelor, M., Delahay, R.M., Hale, C., Matthews, S., Dougan, G., Knutton, S., Connerton, I., and Frankel, G. (1999). Binding of intimin from enteropathogenic *Escherichia coli* to Tir and to host cells. *Molecular Microbiology* 32, 151-158.
- Heinz, E., Stubenrauch, C.J., Grinter, R., Croft, N.P., Purcell, A.W., Strugnell, R.A., Dougan, G., and Lithgow, T. (2016). Conserved Features in the Structure, Mechanism, and Biogenesis of the Inverse Autotransporter Protein Family. *Genome biology and evolution* 8, 1690-1705.
- Hussain, S., and Bernstein, H.D. (2018). The Bam complex catalyzes efficient insertion of bacterial outer membrane proteins into membrane vesicles of variable lipid composition. *The Journal of biological chemistry* 293, 2959-2973.
- Ieva, R., and Bernstein, H.D. (2009). Interaction of an autotransporter passenger domain with BamA during its translocation across the bacterial outer membrane. *Proceedings of the National Academy of Sciences of the United States of America* 106, 19120-19125.
- Ieva, R., Skillman, K.M., and Bernstein, H.D. (2008). Incorporation of a polypeptide segment into the β -domain pore during the assembly of a bacterial autotransporter. *Molecular Microbiology* 67, 188-201.
- Ieva, R., Tian, P., Peterson, J.H., and Bernstein, H.D. (2011). Sequential and spatially restricted interactions of assembly factors with an autotransporter beta domain. *Proceedings of the National Academy of Sciences of the United States of America* 108, E383-E391.
- Jacob-Dubuisson, F., Fernandez, R., and Coutte, L. (2004). Protein secretion through autotransporter and two-partner pathways. *Biochimica et Biophysica Acta (BBA) - Molecular Cell Research* 1694, 235-257.
- Jacob-Dubuisson, F., Guérin, J., Baelen, S., and Clantin, B. (2013). Two-partner secretion: as simple as it sounds? *Research in Microbiology* 164, 583-595.

- Jacob-Dubuisson, F., Locht, C., and Antoine, R. (2001). Two-partner secretion in Gram-negative bacteria: a thrifty, specific pathway for large virulence proteins. *Molecular Microbiology* *40*, 306-313.
- Jain, S., and Goldberg, M.B. (2007). Requirement for YaeT in the outer membrane assembly of autotransporter proteins. *Journal of bacteriology* *189*, 5393-5398.
- Jong, W.S.P., ten Hagen-Jongman, C.M., Ruijter, E., Orru, R.V.A., Genevaux, P., and Luirink, J. (2010). YidC is involved in the biogenesis of the secreted autotransporter hemoglobin protease. *The Journal of biological chemistry* *285*, 39682-39690.
- Julio, S.M., and Cotter, P.A. (2005). Characterization of the filamentous hemagglutinin-like protein FhaS in *Bordetella bronchiseptica*. *Infection and immunity* *73*, 4960-4971.
- Junker, M., Besingi, R.N., and Clark, P.L. (2009). Vectorial transport and folding of an autotransporter virulence protein during outer membrane secretion. *Molecular Microbiology* *71*, 1323-1332.
- Kelly, G., Prasannan, S., Daniell, S., Fleming, K., Frankel, G., Dougan, G., Connerton, I., and Matthews, S. (1999a). Structure of the cell-adhesion fragment of intimin from enteropathogenic *Escherichia coli*. *Nature Structural Biology* *6*, 313-318.
- Kelly, G., Prasannan, S., Daniell, S., Fleming, K., Frankel, G., Dougan, G., Connerton, I., Matthews, S.J.N.S., and Biology, M. (1999b). Structure of the cell-adhesion fragment of intimin from enteropathogenic *Escherichia coli*. *6*, 313.
- Kenny, B., DeVinney, R., Stein, M., Reinscheid, D.J., Frey, E.A., and Finlay, B.B. (1997). Enteropathogenic *E. coli* (EPEC) Transfers Its Receptor for Intimate Adherence into Mammalian Cells. *Cell* *91*, 511-520.
- Knutton, S., Baldwin, T., Williams, P.H., and McNeish, A.S. (1989). Actin accumulation at sites of bacterial adhesion to tissue culture cells: basis of a new diagnostic test for enteropathogenic and enterohemorrhagic *Escherichia coli*. *Infection and immunity* *57*, 1290-1298.
- Koch, H.G., Moser, M., and Müller, M. (2003). Signal recognition particle-dependent protein targeting, universal to all kingdoms of life. In *Reviews of Physiology, Biochemistry and Pharmacology* (Berlin, Heidelberg: Springer Berlin Heidelberg), pp. 55-94.
- Konieczny, M.P., Benz, I., Hollinderbäumer, B., Beinke, C., Niederweis, M., and Schmidt, M.A.J.A.v.l. (2001). Modular organization of the AIDA autotransporter translocator: the N-terminal β 1-domain is surface-exposed and stabilizes the transmembrane β 2-domain. *80*, 19-34.
- Kudva, R., Denks, K., Kuhn, P., Vogt, A., Müller, M., and Koch, H.-G. (2013). Protein translocation across the inner membrane of Gram-negative bacteria: the Sec and Tat dependent protein transport pathways. *Research in Microbiology* *164*, 505-534.
- Lasica, A.M., Ksiazek, M., Madej, M., and Potempa, J. (2017). The Type IX Secretion System (T9SS): Highlights and Recent Insights into Its Structure and Function. *7*.
- Lassmann, T., and Sonnhammer, E.L.L. (2005). Kalign--an accurate and fast multiple sequence alignment algorithm. *BMC Bioinformatics* *6*, 298-298.

- Lehr, U., Schütz, M., Oberhettinger, P., Ruiz-Perez, F., Donald, J.W., Palmer, T., Linke, D., Henderson, I.R., and Autenrieth, I.B. (2010). C-terminal amino acid residues of the trimeric autotransporter adhesin YadA of *Yersinia enterocolitica* are decisive for its recognition and assembly by BamA. *Molecular Microbiology* 78, 932-946.
- Leininger, E., Roberts, M., Kenimer, J.G., Charles, I.G., Fairweather, N., Novotny, P., and Brennan, M.J. (1991). Pertactin, an Arg-Gly-Asp-containing *Bordetella pertussis* surface protein that promotes adherence of mammalian cells. *Proceedings of the National Academy of Sciences of the United States of America* 88, 345-349.
- Leo, J.C., Grin, I., and Linke, D. (2012). Type V secretion: mechanism(s) of autotransport through the bacterial outer membrane. *Philosophical Transactions of the Royal Society B: Biological Sciences* 367, 1088-1101.
- Leo, J.C., Oberhettinger, P., Chaubey, M., Schutz, M., Kuhner, D., Bertsche, U., Schwarz, H., Gotz, F., Autenrieth, I.B., Coles, M., *et al.* (2015a). The Intimin periplasmic domain mediates dimerisation and binding to peptidoglycan. *Mol Microbiol* 95, 80-100.
- Leo, J.C., Oberhettinger, P., Chaubey, M., Schütz, M., Kühner, D., Bertsche, U., Schwarz, H., Götz, F., Autenrieth, I.B., Coles, M., *et al.* (2015b). The Intimin periplasmic domain mediates dimerisation and binding to peptidoglycan. *Molecular Microbiology* 95, 80-100.
- Leo, J.C., Oberhettinger, P., Schütz, M., and Linke, D. (2015c). The inverse autotransporter family: Intimin, invasin and related proteins. *International Journal of Medical Microbiology* 305, 276-282.
- Leo, J.C., Oberhettinger, P., Yoshimoto, S., Udatha, D.B.R.K.G., Morth, J.P., Schütz, M., Hori, K., and Linke, D. (2016). Secretion of the Intimin Passenger Domain Is Driven by Protein Folding. *The Journal of Biological Chemistry* 291, 20096-20112.
- Linke, D., Riess, T., Autenrieth, I.B., Lupas, A., and Kempf, V.A.J. (2006). Trimeric autotransporter adhesins: variable structure, common function. *Trends in Microbiology* 14, 264-270.
- Liu, H., Magoun, L., Leong, J.M.J.I., and immunity (1999). β 1-Chain Integrins Are Not Essential for Intimin-Mediated Host Cell Attachment and Enteropathogenic *Escherichia coli*-Induced Actin Condensation. 67, 2045-2049.
- Liu, H., and Naismith, J.H. (2008). An efficient one-step site-directed deletion, insertion, single and multiple-site plasmid mutagenesis protocol. *BMC Biotechnology* 8, 91.
- Luo, Y., Frey, E.A., Pfuetzner, R.A., Creagh, A.L., Knoechel, D.G., Haynes, C.A., Finlay, B.B., and Strynadka, N.C.J. (2000). Crystal structure of enteropathogenic *Escherichia coli* intimin-receptor complex. *Nature* 405, 1073-1077.
- Lycklama A Nijeholt, J.A., and Driessen, A.J.M. (2012). The bacterial Sec-translocase: structure and mechanism. *Philosophical transactions of the Royal Society of London Series B, Biological sciences* 367, 1016-1028.

- Mallick, E.M., Brady, M.J., Luperchio, S.A., Vanguri, V., Magoun, L., Liu, H., Sheppard, B.J., Mukherjee, J., Donohue-Rolfe, A., and Tzipori, S.J.F.i.m. (2012). Allele- and tir-independent functions of intimin in diverse animal infection models. *3*, 11.
- Marchès, O., Nougayrède, J.-P., Boullier, S., Mainil, J., Charlier, G., Raymond, I., Pohl, P., Boury, M., De Rycke, J., Milon, A., *et al.* (2000). Role of Tir and Intimin in the Virulence of Rabbit Enteropathogenic &Escherichia coli Serotype O103:H2. *Infection and Immunity* *68*, 2171.
- Martinez-Gil, M., Goh, K.G.K., Rackaityte, E., Sakamoto, C., Audrain, B., Moriel, D.G., Totsika, M., Ghigo, J.-M., Schembri, M.A., and Beloin, C. (2017). YeeJ is an inverse autotransporter from *Escherichia coli* that binds to peptidoglycan and promotes biofilm formation. *Scientific Reports* *7*, 11326.
- McKee, M.L., Melton-Celsa, A.R., Moxley, R.A., Francis, D.H., and Brien, A.D. (1995). Enterohemorrhagic *Escherichia coli* O157:H7 requires intimin to colonize the gnotobiotic pig intestine and to adhere to HEP-2 cells. *Infection and Immunity* *63*, 3739.
- Meuskens, I., Michalik, M., Chauhan, N., Linke, D., and Leo, J.C. (2017). A New Strain Collection for Improved Expression of Outer Membrane Proteins. *Frontiers in cellular and infection microbiology* *7*, 464-464.
- Meuskens, I., Saragliadis, A., Leo, J.C., and Linke, D.J.F.i.M. (2019). Type V secretion systems: An Overview of Passenger Domain Functions. *10*, 1163.
- Miller, S.I., and Salama, N.R. (2018). The gram-negative bacterial periplasm: Size matters. *PLoS Biol* *16*, e2004935-e2004935.
- Moon, H.W., Whipp, S.C., Argenzio, R.A., Levine, M.M., and Giannella, R.A. (1983). Attaching and effacing activities of rabbit and human enteropathogenic *Escherichia coli* in pig and rabbit intestines. *Infection and immunity* *41*, 1340-1351.
- Morgan, J.L.W., Acheson, J.F., and Zimmer, J. (2017). Structure of a Type-1 Secretion System ABC Transporter. *Structure* *25*, 522-529.
- Mühlenkamp, M., Oberhettinger, P., Leo, J.C., Linke, D., and Schütz, M.S. (2015). Yersinia adhesin A (YadA) – Beauty & beast. *International Journal of Medical Microbiology* *305*, 252-258.
- Nesta, B., Spraggon, G., Alteri, C., Moriel, D.G., Rosini, R., Veggi, D., Smith, S., Bertoldi, I., Pastorello, I., and Ferlenghi, I.J.M. (2012). FdeC, a novel broadly conserved *Escherichia coli* adhesin eliciting protection against urinary tract infections. *3*, e00010-00012.
- Newman, C.L., and Stathopoulos, C.J.C.r.i.m. (2004). Autotransporter and two-partner secretion: delivery of large-size virulence factors by gram-negative bacterial pathogens. *30*, 275-286.
- Noinaj, N., Fairman, J.W., and Buchanan, S.K. (2011). The crystal structure of BamB suggests interactions with BamA and its role within the BAM complex. *Journal of molecular biology* *407*, 248-260.

- Noinaj, N., Kuszak, A.J., Balusek, C., Gumbart, J.C., and Buchanan, S.K. (2014). Lateral opening and exit pore formation are required for BamA function. *Structure (London, England : 1993)* *22*, 1055-1062.
- Noinaj, N., Kuszak, A.J., Gumbart, J.C., Lukacik, P., Chang, H., Easley, N.C., Lithgow, T., and Buchanan, S.K. (2013). Structural insight into the biogenesis of β -barrel membrane proteins. *Nature* *501*, 385-390.
- Oberhettinger, P., Leo, J.C., Linke, D., Autenrieth, I.B., and Schütz, M.S. (2015). The inverse autotransporter intimin exports its passenger domain via a hairpin intermediate. *The Journal of biological chemistry* *290*, 1837-1849.
- Oberhettinger, P., Schütz, M., Leo, J.C., Heinz, N., Berger, J., Autenrieth, I.B., and Linke, D. (2012). Intimin and Invasin Export Their C-Terminus to the Bacterial Cell Surface Using an Inverse Mechanism Compared to Classical Autotransport. *PLOS ONE* *7*, e47069.
- Oomen, C.J., van Ulsen, P., van Gelder, P., Feijen, M., Tommassen, J., and Gros, P. (2004). Structure of the translocator domain of a bacterial autotransporter. *The EMBO journal* *23*, 1257-1266.
- Palmer, T., and Berks, B.C. (2012). The twin-arginine translocation (Tat) protein export pathway. *Nature Reviews Microbiology* *10*, 483.
- Pavlova, O., Peterson, J.H., Ieva, R., and Bernstein, H.D. (2013). Mechanistic link between β barrel assembly and the initiation of autotransporter secretion. *Proceedings of the National Academy of Sciences of the United States of America* *110*, E938-E947.
- Peterson, J.H., Hussain, S., and Bernstein, H.D. (2018). Identification of a novel post-insertion step in the assembly of a bacterial outer membrane protein. *Molecular Microbiology* *110*, 143-159.
- Peterson, J.H., Tian, P., Ieva, R., Dautin, N., and Bernstein, H.D. (2010). Secretion of a bacterial virulence factor is driven by the folding of a C-terminal segment. *Proceedings of the National Academy of Sciences of the United States of America* *107*, 17739-17744.
- Petriman, N.-A., Jauß, B., Hufnagel, A., Franz, L., Sachelaru, I., Drepper, F., Warscheid, B., and Koch, H.-G.J.S.r. (2018). The interaction network of the YidC insertase with the SecYEG translocon, SRP and the SRP receptor FtsY. *8*, 578.
- Pohlner, J., Halter, R., Beyreuther, K., and Meyer, T.F. (1987a). Gene structure and extracellular secretion of *Neisseria gonorrhoeae* IgA protease. *Nature* *325*, 458-462.
- Pohlner, J., Halter, R., Beyreuther, K., and Meyer, T.F. (1987b). Gene structure and extracellular secretion of *Neisseria gonorrhoeae* IgA protease. *Nature* *325*, 458.
- Provence, D.L., and Curtiss, R., 3rd (1994). Isolation and characterization of a gene involved in hemagglutination by an avian pathogenic *Escherichia coli* strain. *Infection and immunity* *62*, 1369-1380.
- Qin, W., Wang, L., and Lei, L. (2015). New findings on the function and potential applications of the trimeric autotransporter adhesin. *Antonie van Leeuwenhoek* *108*, 1-14.

- Renn, J.P., Junker, M., Besingi, R.N., Braselmann, E., and Clark, P.L. (2012). ATP-independent control of autotransporter virulence protein transport via the folding properties of the secreted protein. *Chemistry & biology* *19*, 287-296.
- Roggenkamp, A., Ackermann, N., Jacobi, C.A., Truelzsch, K., Hoffmann, H., and Heesemann, J. (2003). Molecular analysis of transport and oligomerization of the *Yersinia enterocolitica* adhesin YadA. *Journal of bacteriology* *185*, 3735-3744.
- Ruiz-Perez, F., Henderson, I.R., Leyton, D.L., Rossiter, A.E., Zhang, Y., and Nataro, J.P. (2009). Roles of periplasmic chaperone proteins in the biogenesis of serine protease autotransporters of Enterobacteriaceae. *Journal of bacteriology* *191*, 6571-6583.
- Ruiz-Perez, F., Henderson, I.R., and Nataro, J.P. (2010). Interaction of FkpA, a peptidyl-prolyl cis/trans isomerase with EspP autotransporter protein. *Gut microbes* *1*, 339-344.
- Salacha, R., Kovačić, F., Brochier-Armanet, C., Wilhelm, S., Tommassen, J., Filloux, A., Voulhoux, R., and Blevès, S. (2010). The *Pseudomonas aeruginosa* patatin-like protein PlpD is the archetype of a novel Type V secretion system. *Environmental Microbiology* *12*, 1498-1512.
- Samuelson, J.C., Chen, M., Jiang, F., Möller, I., Wiedmann, M., Kuhn, A., Phillips, G.J., and Dalbey, R.E. (2000). YidC mediates membrane protein insertion in bacteria. *Nature* *406*, 637.
- Sanger, F., and Coulson, A.R. (1975). A rapid method for determining sequences in DNA by primed synthesis with DNA polymerase. *Journal of Molecular Biology* *94*, 441-448.
- Saurí, A., Oreshkova, N., Soprova, Z., Jong, W.S.P., Sani, M., Peters, P.J., Luirink, J., and van Ulsen, P. (2011). Autotransporter β -Domains Have a Specific Function in Protein Secretion beyond Outer-Membrane Targeting. *Journal of Molecular Biology* *412*, 553-567.
- Sauri, A., Soprova, Z., Wickström, D., de Gier, J.-W., Van der Schors, R.C., Smit, A.B., Jong, W.S.P., and Luirink, J. (2009). The Bam (Omp85) complex is involved in secretion of the autotransporter haemoglobin protease. *155*, 3982-3991.
- Schmidt, M.A. (2010). LEEways: tales of EPEC, ATEC and EHEC. *Cellular Microbiology* *12*, 1544-1552.
- Sijbrandi, R., Urbanus, M., Hagen-Jongman, C., Bernstein, H., Oudega, B., Otto, B., and Luirink, J. (2003). Signal Recognition Particle (SRP)-mediated Targeting and Sec-dependent Translocation of an Extracellular *Escherichia coli* Protein, Vol 278.
- Sinclair, J.F., and O'Brien, A.D.J.J.o.B.C. (2002). Cell Surface-localized Nucleolin Is a Eukaryotic Receptor for the Adhesin Intimin- γ of Enterohemorrhagic *Escherichia coli*O157: H7. *277*, 2876-2885.
- Sinnige, T., Weingarh, M., Renault, M., Baker, L., Tommassen, J., and Baldus, M. (2014). Solid-state NMR studies of full-length BamA in lipid bilayers suggest limited overall POTRA mobility. *Journal of molecular biology* *426*, 2009-2021.
- Skurnik, M., Bölin, I., Heikkinen, H., Piha, S., and Wolf-Watz, H. (1984). Virulence plasmid-associated autoagglutination in *Yersinia* spp. *Journal of bacteriology* *158*, 1033-1036.

- Soprova, Z., Sauri, A., van Ulsen, P., Tame, J.R.H., den Blaauwen, T., Jong, W.S.P., and Luirink, J. (2010). A conserved aromatic residue in the autochaperone domain of the autotransporter Hbp is critical for initiation of outer membrane translocation. *The Journal of biological chemistry* 285, 38224-38233.
- St. Geme, J.W., and Yeo, H.-J. (2009). A prototype two-partner secretion pathway: the *Haemophilus influenzae* HMW1 and HMW2 adhesin systems. *Trends in Microbiology* 17, 355-360.
- Szabady, R.L., Peterson, J.H., Skillman, K.M., and Bernstein, H.D. (2005). An unusual signal peptide facilitates late steps in the biogenesis of a bacterial autotransporter. *Proceedings of the National Academy of Sciences of the United States of America* 102, 221-226.
- Tang, G., Ruiz, T., and Mintz, K.P. (2012). O-polysaccharide glycosylation is required for stability and function of the collagen adhesin EmaA of *Aggregatibacter actinomycetemcomitans*. *Infection and immunity* 80, 2868-2877.
- Thanassi, D.G., Stathopoulos, C., Karkal, A., and Li, H.J.M.m.b. (2005). Protein secretion in the absence of ATP: the autotransporter, two-partner secretion and chaperone/usher pathways of gram-negative bacteria. 22, 63-72.
- Touzé, T., Hayward, R.D., Eswaran, J., Leong, J.M., and Koronakis, V. (2004). Self-association of EPEC intimin mediated by the β -barrel-containing anchor domain: a role in clustering of the Tir receptor. *Molecular Microbiology* 51, 73-87.
- Tsai, J.C., Yen, M.-R., Castillo, R., Leyton, D.L., Henderson, I.R., and Saier, M.H., Jr. (2010). The Bacterial Intimins and Invasins: A Large and Novel Family of Secreted Proteins. *PLOS ONE* 5, e14403.
- Willems, R.J.L., Geuijen, C., van der Heide, H.G.J., Renauld, G., Berlin, P., van den Akker, W.M.R., Locht, C., and Mooi, F.R. (1994). Mutational analysis of the *Bordetella pertussis* fim/fha gene cluster: identification of a gene with sequence similarities to haemolysin accessory genes involved in export of FHA. *Molecular Microbiology* 11, 337-347.
- Willett, J.L.E., Ruhe, Z.C., Goulding, C.W., Low, D.A., and Hayes, C.S. (2015). Contact-Dependent Growth Inhibition (CDI) and CdiB/CdiA Two-Partner Secretion Proteins. *Journal of molecular biology* 427, 3754-3765.
- William Studier, F. (2005). Studier, F.W. Protein production by auto-induction in high density shaking cultures. *Protein Expr. Purif.* 41, 207-234, Vol 41.
- Zhang, X.C., and Han, L. (2016). How does a β -barrel integral membrane protein insert into the membrane? *Protein & cell* 7, 471-477.

Appendix 1 Abbreviations

All abbreviations used in the thesis are mentioned below in alphabetical order.

<u>Abbreviation</u>	<u>Full form</u>
ΔF	$\Delta ompF$
ABC	ATP-binding cassette
ABTS	2,2'-azino-bis(3-ethylbenzothiazoline-6-sulphonic acid)
AIDA	Adhesin involved in diffuse adherence
ATP	Adenosine triphosphate
BAM	β -barrel assembly machinery
BSA	Bovine serum albumin
CU	Chaperone-usher
CaCl ₂	Calcium chloride
DNA	Deoxyribonucleic acid
dNTP	Deoxyribose nucleoside phosphate
dsDNA	Double stranded deoxyribonucleic acid
<i>E. coli</i>	<i>Escherichia coli</i>
EDTA	Ethylenediaminetetraacetic acid
EHEC	Enterohemorrhagic <i>E. coli</i>
EPEC	Enteropathogenic <i>E. coli</i>
EV	Empty vector
FCS	Fetal calf serum
HA	Hemagglutinin
Hbp	Hemoglobin protease
HEPES	4-(2-hydroxyethyl)-1-piperazineethanesulfonic acid

HRP	Horseradish peroxidase
IgA	Immunoglobulin A
IM	Inner-membrane
Int _{wt}	Intimin wild-type
Int _{sv}	Intimin stalled variant
LB	Lysogeny broth
LEE	Locus of enterocyte effacement
LPS	Lipopolysaccharide
LysM	Lysin motif
MOI	Multiplicity of infection
MgCl ₂	Magnesium chloride
MnCl ₂	Manganese chloride
NIR	Near - infrared
OM	Outer-membrane
OMP	Outer membrane protein
PCR	Polymerase chain reaction
PBS	Phosphate-buffered saline
PBST	Phosphate-buffered saline with Tween 20
PFA	Paraformaldehyde
PLP	Patatin-like proteins
PlpD	Patatin-like protein D
PMF	Proton motive force
POTRA	Polypeptide transport-associated
RT	Room temperature

SDS – PAGE	Sodium dodecyl sulfate – polyacrylamide gel electrophoresis
Sec	General secretion
SRP	Signal recognition particle
ssDNA	Single stranded deoxyribonucleic acid
SV	Stalled variant
T5aSS	Type Va secretion system
T5bSS	Type Vb secretion system
T5cSS	Type Vc secretion system
T5dSS	Type Vd secretion system
T5eSS	Type Ve secretion system
TAA	Trimeric autotransporter adhesins
TAE	Tris-acetate-EDTA
Tat	Twin arginine translocase
Tir	Translocated intimin receptor
TPS	Two-partner secretion
TSS	Transformation and storage solution
WT	Wild-type
YadA	Yersinia adhesin A

Appendix 2 Primer Sequences

All primers were designed manually and produced by Eurofins Genomics unless stated otherwise.

Cloning of eaeA into pET-22b(+)

<u>Primer Name</u>	<u>Sequence (5'→3')</u>
pelB-Int Fwd	GCCCAGCCGGCGATGGCCAATGGTGAAAATTATTTTAAATTGGGTTC
pET22-Strep Rev	GTTAGCAGCCGGATCTCATTATTTTTCGAACTGCGGGTGG
pET22rec Fwd	TGAGATCCGGCTGCTAACAAAG
pET22rec Rev	GGCCATCGCCGGCTGG

Introducing mutations in the α -helical turn on the periplasmic side of the β -barrel of Intimin

<u>Primer Name</u>	<u>Sequence (5'→3')</u>
IntD298A Fwd	AATACTGGCGAGCTTATTTCAAAGTAGTGTTAACGGCTA
IntD298A Rev	AGCTCGCCAGTATTCGCCACCAATACCTAAACGG
IntI382D Fwd	AACTATACTCCGGATCCTCTGGTGACGATGGGG
IntI382D Rev	ATCCGGAGTATAGTTTACACCAACGGTCGCCGC
IntP421A Fwd	CAGCAAATTGAGGCTCAATATGTTAACGAGTTAAGAACATTAT
IntP421A Rev	AGCCTCAATTTGCTGGGACCACGGTTTATCAAACCTGAT
IntL430A Fwd	GAGTTAAGAACAGCTTCAGGCAGCCGTTACGATCT
IntL430A Rev	AGCTGTTCTTAACTCGTTAACATATTGTGGCTCAATTTGC
Δ 412-430GS Fwd	TTTTCTGGTTCTGGTTCAGGCAGCCGTTACGATCT
Δ 412-430GS Rev	ACCAGAACCAGAAAACCTGATAACGGAACTGCATTGAGT

The linker connecting the β -barrel to the passenger and interacting residues facing the lumen of the β -barrel.

<u>Primer Name</u>	<u>Sequence (5' \rightarrow 3')</u>
IntF276A Fwd	GCTATAACGTCGCCATTGATCAGGATTTTCTGGTGATAAT
IntF276A Rev	GGCGACGTTATAGCCCAACATATTTTCAGGAAGGAAAAAA
IntR288A Fwd	GGTGATAATACCGCGTTAGGTATTGGTGGCGAATACTG
IntR288A Rev	CGC GGT ATT ATC ACC AGA AAA ATC CTG ATC AAT GAA GAC G
IntR434A Fwd	TCAGGCAGCGCTTACGATCTGGTTCAGCGTAATAA
IntR434A Rev	AGCGCTGCCTGATAATGTTCTTAACTCGTTAACATATTGT
IntL437A Fwd	GCCGTTACGATGCTGTTACAGCGTAATAACAATATTATTCTG
IntL437A Rev	AGCATCGTAACGGCTGCCTGATAATGTTCTTAACTCGTT
IntQ439A Fwd	ACGATCTGGTTGCTCGTAATAACAATATTATTCTGGAGTAC
IntQ439A Rev	AGCAACCAGATCGTAACGGCTGCCTGATAATGTTCTT
Δ linkerGS Fwd	AGTGGGTCTGGCTCCGGTAGCATTCTGGAGTACAAAAAGCAGGATA
Δ linkerGS Rev	GCCAGACCCACTACCGCTGCCACGGCTGCCTGATAATGTTCTT

The small β -sheet formed between the linker and two loops of the β -barrel on the extracellular surface.

<u>Primer Name</u>	<u>Sequence (5' \rightarrow 3')</u>
IntE447A Fwd	ACAATATTATTCTGGCGTACAAAAAGCAGGATATTCTTTCTC
IntE447A Rev	CGCCAGAATAATATTGTTATTACGCTGAACCAGATCGTAA
IntY448D Fwd	ATTATTCTGGAGGACAAAAAGCAGGATATTCTTTCTCTGA
IntY448D Rev	GTCCTCCAGAATAATATTGTTATTACGCTGAACCAGATC
Δ R309-A327GGGG Fwd	GGTGGGGGTGGGAATGGCTTCGATATCCGTTTTAAT
Δ R309-A327GGGG Rev	CCCACCCCAACCGAAATAGCCGTTAACTACT TTT G
Δ Y354-N369GGGG Fwd	GGTGGACCTGGTGC GGCGACCGTTGGTGTA

ΔY354-N369GGGG Rev

ACCAGGTCCACCTCCACCATACTGCTCATACATCA

ΔL446-K449GGGG Fwd

GGTGGGGGTGGGAAGCAGGATATTCTTTCTCTGAATATT

ΔL446-K449GGGG Rev

CCCACCCACCAATAATATTGTTATTACGCTGAACCAG

Appendix 3 Buffers and Chemicals

Tables containing the composition of the buffer solutions and chemicals used in this project and mentioned in Section 3 are given below.

Cloning by Gibson Assembly

The composition of the Gibson Master mix during Gibson assembly is given in Table 1.

Table 1: Composition of 2 x Gibson Master Mix

Reagent	Amount (µl)
Isothermal Start Mix	405
1M DTT	25
25mM dNTPs	20
NAD ⁺	50
T5 Exonuclease	1
Phusion [®] High-Fidelity DNA Polymerase	31.25
<i>Taq</i> Ligase	250
Distilled H ₂ O	467.7
Total Volume	1249.95
This mixture was gently mixed and 100 µl aliquots were made.	

Isothermal Start Mix	
Reagent	Amount
PEG 8000	1.5 g
1M Tris-HCl, pH 8.0	3 ml
2M MgCl ₂	150 µl
Mixed in tube rotator until PEG was dissolved in solution.	

Agarose Gels and Buffers used

The composition and the chemicals and their company name is given in table 2

Table 2: Composition of the gels and buffers used in Agarose Gel Electrophoresis

Solution	Components	Company
50 x TAE buffer	242 g Trisma	VWR BDH Chemicals
VWR BDH	20.81 g EDTA	VWR BDH Chemicals
	57.1 ml glacial acetic acid	Sigma
	Water to 1 L	
Agarose	SeaKem®LE Agarose	Lonza
GelGreen® Nucleic acid stain		Biotium
6 x DNA sample buffer	3.5 ml 99.5 % glycerol	VWR AnalaR Normapur
	35 µl 3 m Tris-HCl, pH 8.0	Angus
	20 µl 0.5 M EDTA, pH 8.0	AppliChem
	25 mg Bromophenol blue sodium salt	Sigma
	Water to 10 ml	

Lysogeny Broth and Agar plates

Table 3 gives the composition of LB and low salt LB used for the growth of cultures in this project. Table 4 gives the composition of LB agar used in petriplates for growth of the cultures.

Table 3: Composition of Lysogeny Broth (LB) and low salt LB medium.

Media	Components	Company
LB	10 g NaCl	AnalaR
	10 g Tryptone enzymatic digest from casein	Fluka
	5 g Yeast	VWR
Low salt LB	5 g NaCl	AnalaR
	10 g Tryptone enzymatic digest from casein	Fluka
	5 g Yeast	VWR

Table 4: Composition of LB agar in petriplates for growth of cultures

Media	Components	Company
LB agar	25 g LB broth	BD
	10 g Bactopor agar	BD
	Water to 1 L	

Buffers used for making competent cells

Table 5 gives the composition of TSS buffer used for making chemically competent cells.

Table 5: Composition of TSS buffer in making BL21 or TOP10 competent cells

Solution	Component	Company
TSS buffer	25 ml LB medium	
	2.5 g PEG 8k	Sigma
	1.23 ml DMSO	Sigma Aldrich
	0.75 ml 1M MgCl ₂	Merc

Auto-induction Media

Table 6 gives the composition of the auto-induction media used to induce overexpression of Intimin.

Table 6: The ZYP-5052 media used for the overexpression of Intimin by BL21 Δ F cells containing the pET-22b(+) plasmid.

Media	Components	Company
ZY	10 g Tryptone enzymatic digest of casein	Fluka
	5 g Yeast extract	VWR chemicals
	Water to 925 ml	
50 x 5052	25 ml Glycerol bidistilled	VWR chemicals
	2.5 g D(+)-glucose-monohydrate	VWR chemicals
	10 g Lactose monohydrate	VWR chemicals
	Water to 73 ml	
20 x NPS	66 g $(\text{NH}_4)_2\text{SO}_4$	Merc
	136 g KH_2PO_4	Merc
	142 g Na_2HPO_4	VWR chemicals
ZYP-5052	930 ml ZY medium	
	1 ml MgSO_4	Merc
	50 ml 20 x NPS	
	20 ml 50 x 5052	

Buffers used in SDS-PAGE

Table 7 gives the composition of the sample buffer and running buffers used in SDS-PAGE

Table 7: Composition of 4 x SDS-PAGE sample buffer and 10 x running buffer

Solution	Component	Company
4 x SDS-PAGE sample buffer	40 ml 20 % SDS	AppliChem
	0.04 g bromophenol blue sodium salt	Sigma
	6.6 ml 3M Tris pH 7.5	Angus
	40 % glycerol bidistilled	VWR chemicals
	0.4 ml 0.5M EDTA	AppliChem
	Water to 100 ml	
10 x SDS-PAGE running buffer	30 g Tris	Angus
	144 g glycine	VWR chemicals
	10 g SDS	AppliChem
	Water to 1 L	

Buffers used in Urea extractions

Table 8 gives the composition of the Urea extraction Buffer used after extraction the OM pellet.

Table 8: Composition of the Urea Extraction Buffer

Buffer	Components	Company
Urea Extraction buffer	15 mM HEPES pH 7.4	Sigma
	100 mM glycine	Sigma
	6 M urea	Merc

Buffers used in Western Blotting

Table 9 gives the composition of the transfer buffer and blocking buffer used in western blotting.

Table 9: Composition of the transfer buffer and blocking buffer used in western blotting

Solution	Components	Company
Transfer buffer	25 mM Tris	Angus
	150 mM glycine	Sigma
	10% isopropanol	VWR chemicals
10 x PBS	1.3 M NaCl	Merck
	70 mM Na ₂ HPO ₄	Sigma
	30 mM NaH ₂ PO ₄	Sigma
PBST	0.05 % tween 20	Sigma
	1 x PBS	
Blocking buffer	2 % Skimmed milk powder	Fluka
	1 x PBS	

Buffers used in Whole-cell ELISA

Table 10 gives the composition of the washing buffer and blocking buffer used in Whole-cell ELISA

Table 10: Composition of the washing and blocking buffer used in whole-cell ELISA

Solution	Components	Company
Washing buffer	0.1 % BSA	VWR chemicals
	1 x PBS	
Blocking buffer	2 % BSA	VWR chemicals
	1 x PBS	

Supplementary

